ISSN 1949-8470 (online)

World Journal of *Radiology*

World J Radiol 2011 April 28; 3(4): 85-124

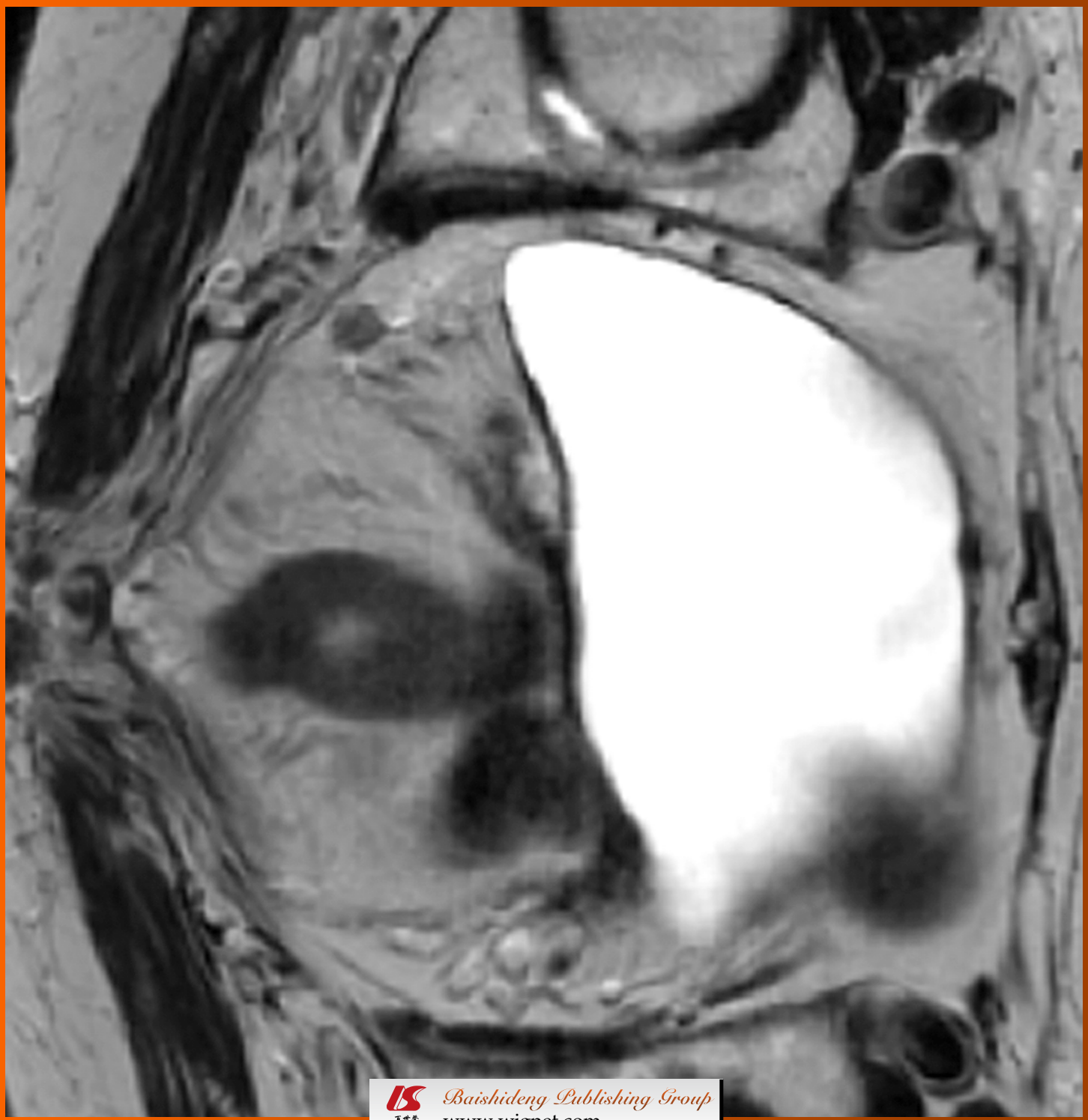

Baishideng Publishing Group
www.wjgnet.com

WJR World Journal of Radiology

A peer-reviewed, online, open-access journal of Radiology

Editorial Board

2009-2013

The *World Journal of Radiology* Editorial Board consists of 319 members, representing a team of worldwide experts in radiology. They are from 40 countries, including Australia (3), Austria (4), Belgium (5), Brazil (3), Canada (9), Chile (1), China (25), Czech (1), Denmark (1), Egypt (4), Estonia (1), Finland (1), France (6), Germany (17), Greece (8), Hungary (1), India (9), Iran (5), Ireland (1), Israel (4), Italy (28), Japan (14), Lebanon (1), Libya (1), Malaysia (2), Mexico (1), Netherlands (4), New Zealand (1), Norway (1), Saudi Arabia (3), Serbia (1), Singapore (2), Slovakia (1), South Korea (16), Spain (8), Switzerland (5), Thailand (1), Turkey (20), United Kingdom (16), and United States (82).

France

Alain Chapel, *Fontenay-Aux-Roses*
Nathalie Lassau, *Villejuif*
Youlia M Kirova, *Paris*
Géraldine Le Duc, *Grenoble Cedex*
Laurent Pierot, *Reims*
Frank Pilleul, *Lyon*
Pascal Pommier, *Lyon*

Germany

Ambros J Beer, *München*
Thomas Deserno, *Aachen*
Frederik L Giesel, *Heidelberg*
Ulf Jensen, *Kiel*
Markus Sebastian Juchems, *Ulm*
Kai U Juergens, *Bremen*
Melanie Kettering, *Jena*
Jennifer Linn, *Munich*
Christian Lohrmann, *Freiburg*
David Maintz, *Münster*
Henrik J Michaely, *Mannheim*
Oliver Micke, *Bielefeld*
Thoralf Niendorf, *Berlin-Buch*
Silvia Obenauer, *Duesseldorf*
Steffen Rickes, *Halberstadt*
Lars V Baron von Engelhardt, *Bochum*
Goetz H Welsch, *Erlangen*

Greece

Panagiotis Antoniou, *Alexandroupolis*
George C Kagadis, *Rion*
Dimitris Karacostas, *Thessaloniki*
George Panayiotakis, *Patras*
Alexander D Rapidis, *Athens*
C Triantopoulou, *Athens*
Ioannis Tsalafoutas, *Athens*
Virginia Tsapaki, *Anixi*
Ioannis Valais, *Athens*

Hungary

Peter Laszlo Lakatos, *Budapest*

India

Anil Kumar Anand, *New Delhi*
Surendra Babu, *Tamilnadu*
Sandip Basu, *Bombay*
Kundan Singh Chufal, *New Delhi*
Shivanand Gamanagatti, *New Delhi*
Vimoj J Nair, *Haryana*
R Prabhakar, *New Delhi*
Sanjeeb Kumar Sahoo, *Orissa*

Iran

Vahid Reza Dabbagh Kakhki, *Mashhad*
Mehran Karimi, *Shiraz*
Farideh Nejat, *Tehran*
Alireza Shirazi, *Tehran*
Hadi Rokni Yazdi, *Tehran*

Ireland

Joseph Simon Butler, *Dublin*

Israel

Amit Gefen, *Tel Aviv*
Eyal Sheiner, *Be'er-Sheva*
Jacob Sosna, *Jerusalem*
Simcha Yagel, *Jerusalem*

Italy

Mohssen Ansarin, *Milan*
Stefano Arcangeli, *Rome*
Tommaso Bartalena, *Imola*
Filippo Cademartiri, *Parma*
Sergio Casciaro, *Lecce*
Laura Crocetti, *Pisa*
Alberto Cuocolo, *Napoli*
Mirko D'Onofrio, *Verona*
Massimo Filippi, *Milan*
Claudio Fiorino, *Milano*
Alessandro Franchello, *Turin*
Roberto Grassi, *Naples*
Stefano Guerriero, *Cagliari*
Francesco Lassandro, *Napoli*
Nicola Limbucci, *L'Aquila*
Raffaele Lodi, *Bologna*
Francesca Maccioni, *Rome*
Laura Martincich, *Candiolo*
Mario Mascalchi, *Florence*
Roberto Miraglia, *Palermo*
Eugenio Picano, *Pisa*
Antonio Pinto, *Naples*
Stefania Romano, *Naples*
Luca Saba, *Cagliari*
Sergio Sartori, *Ferrara*
Mariano Scaglione, *Castel Volturno*
Lidia Strigari, *Rome*
Vincenzo Valentini, *Rome*

Japan

Shigeru Ehara, *Morioka*
Nobuyuki Hamada, *Chiba*
Takao Hiraki, *Okayama*
Akio Hiwatashi, *Fukuoka*
Masahiro Jinzaki, *Tokyo*
Hiroshi Matsuda, *Saitama*
Yasunori Minami, *Osaka*
Jun-Ichi Nishizawa, *Tokyo*
Tetsu Niwa, *Yokohama*
Kazushi Numata, *Kanagawa*
Kazuhiko Ogawa, *Okinawa*
Hitoshi Shibuya, *Tokyo*
Akira Uchino, *Saitama*
Haiquan Yang, *Kanagawa*

Lebanon

Aghiad Al-Kutoubi, *Beirut*

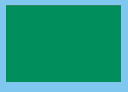

Libya

Anuj Mishra, *Tripoli*

Malaysia

R Logeswaran, *Cyberjaya*
Kwan-Hoong Ng, *Kuala Lumpur*

Mexico

Heriberto Medina-Franco, *Mexico City*

Netherlands

Jurgen J Fütterer, *Nijmegen*
Raffaella Rossin, *Eindhoven*
Paul E Sijens, *Groningen*
Willem Jan van Rooij, *Tilburg*

New Zealand

W Howell Round, *Hamilton*

Norway

Arne Sigmund Borthne, *Lørenskog*

Saudi Arabia

Mohammed Al-Omran, *Riyadh*
Ragab Hani Donkol, *Abha*
Volker Rudat, *Al Khobar*

Serbia

Djordjije Saranovic, *Belgrade*

Singapore

Uei Pua, *Singapore*
Lim CC Tchoyoson, *Singapore*

Slovakia

František Dubecký, *Bratislava*

South Korea

Bo-Young Choe, *Seoul*
Joon Koo Han, *Seoul*
Seung Jae Huh, *Seoul*
Chan Kyo Kim, *Seoul*
Myeong-Jin Kim, *Seoul*
Seung Hyup Kim, *Seoul*
Kyoung Ho Lee, *Gyeonggi-do*
Won-Jin Moon, *Seoul*
Wazir Muhammad, *Daegu*
Jai Soung Park, *Bucheon*
Noh Hyuck Park, *Kyunggi*
Sang-Hyun Park, *Daejeon*
Joon Beom Seo, *Seoul*
Ji-Hoon Shin, *Seoul*
Jin-Suck Suh, *Seoul*
Hong-Gyun Wu, *Seoul*

Spain

Eduardo J Aguilar, *Valencia*
Miguel Alcaraz, *Murcia*
Juan Luis Alcazar, *Pamplona*
Gorka Bastarrika, *Pamplona*
Rafael Martínez-Monge, *Pamplona*
Alberto Muñoz, *Madrid*
Joan C Vilanova, *Girona*

Switzerland

Nicolau Beckmann, *Basel*
Silke Grabherr, *Lausanne*
Karl-Olof Lövblad, *Geneva*
Tilo Niemann, *Basel*
Martin A Walter, *Basel*

Thailand

Sudsriluk Sampatchalit, *Bangkok*

Turkey

Olus Api, *Istanbul*
Kubilay Aydin, *İstanbul*
Işıl Bilgen, *Izmir*
Zulkif Bozgeyik, *Elazig*
Barbaros E Çil, *Ankara*
Gulgun Engin, *Istanbul*
M Fatih Evcimik, *Malatya*
Ahmet Kaan Gündüz, *Ankara*
Tayfun Hakan, *Istanbul*
Adnan Kabaalioglu, *Antalya*
Fehmi Kaçmaz, *Ankara*
Musturay Karcaaltincaba, *Ankara*
Osman Kizilkilic, *Istanbul*
Zafer Koc, *Adana*
Cem Onal, *Adana*
Yahya Paksoy, *Konya*
Bunyamin Sahin, *Samsun*
Ercument Unlu, *Edirne*
Ahmet Tuncay Turgut, *Ankara*
Ender Uysal, *Istanbul*

United Kingdom

K Faulkner, *Wallsend*
Peter Gaines, *Sheffield*
Balaji Ganeshan, *Brighton*
Nagy Habib, *London*
Alan Jackson, *Manchester*
Pradesh Kumar, *Portsmouth*
Tarik F Massoud, *Cambridge*
Igor Meglinski, *Bedfordshire*
Robert Morgan, *London*
Ian Negus, *Bristol*
Georgios A Plataniotis, *Aberdeen*
N J Raine-Fenning, *Nottingham*
Manuchehr Soleimani, *Bath*
MY Tseng, *Nottingham*
Edwin JR van Beek, *Edinburgh*
Feng Wu, *Oxford*

United States

Athanassios Argiris, *Pittsburgh*
Stephen R Baker, *Newark*
Lia Bartella, *New York*
Charles Bellows, *New Orleans*
Walter L Biffl, *Denver*
Homer S Black, *Houston*
Wessam Bou-Assaly, *Ann Arbor*
Owen Carmichael, *Davis*
Shelton D Caruthers, *St Louis*
Yuhchyau Chen, *Rochester*
Melvin E Clouse, *Boston*
Ezra Eddy Wyssam Cohen, *Chicago*
Aaron Cohen-Gadol, *Indianapolis*
Patrick M Colletti, *Los Angeles*
Kassa Darge, *Philadelphia*
Abhijit P Datir, *Miami*
Delia C DeBuc, *Miami*
Russell L Deter, *Houston*
Adam P Dicker, *Phil*
Khaled M Elsayes, *Ann Arbor*
Steven Feigenberg, *Baltimore*
Christopher G Filippi, *Burlington*
Victor Frenkel, *Bethesda*
Thomas J George Jr, *Gainesville*
Patrick K Ha, *Baltimore*
Robert I Haddad, *Boston*
Walter A Hall, *Syracuse*
Mary S Hammes, *Chicago*
John Hart Jr, *Dallas*
Randall T Higashida, *San Francisco*
Juebin Huang, *Jackson*
Andrei Iagaru, *Stanford*
Craig Johnson, *Milwaukee*
Ella F Jones, *San Francisco*
Csaba Juhasz, *Detroit*
Riyad Karmy-Jones, *Vancouver*
Daniel J Kelley, *Madison*
Amir Khan, *Longview*
Euishin Edmund Kim, *Houston*
Vikas Kundra, *Houston*
Kennith F Layton, *Dallas*
Rui Liao, *Princeton*
CM Charlie Ma, *Philadelphia*
Nina A Mayr, *Columbus*
Thomas J Meade, *Evanston*
Steven R Messé, *Philadelphia*
Nathan Olivier Mewton, *Baltimore*
Feroze B Mohamed, *Philadelphia*
Koenraad J Mortele, *Boston*
Mohan Natarajan, *San Antonio*
John L Nosher, *New Brunswick*
Chong-Xian Pan, *Sacramento*
Dipanjan Pan, *St Louis*
Martin R Prince, *New York*
Reza Rahbar, *Boston*
Carlos S Restrepo, *San Antonio*
Veronica Rooks, *Honolulu*
Maythem Saeed, *San Francisco*
Edgar A Samaniego, *Palo Alto*
Kohkan Shamsi, *Doylestown*
Jason P Sheehan, *Charlottesville*
William P Sheehan, *Willmar*
Charles Jeffrey Smith, *Columbia*
Monvadi B Srichai-Parsia, *New York*
Dan Stoianovici, *Baltimore*
Janio Szklaruk, *Houston*
Dian Wang, *Milwaukee*
Jian Z Wang, *Columbus*
Liang Wang, *New York*
Shougang Wang, *Santa Clara*
Wenbao Wang, *New York*
Aaron H Wolfson, *Miami*
Gayle E Woloschak, *Chicago*
Ying Xiao, *Philadelphia*
Juan Xu, *Pittsburgh*
Benjamin M Yeh, *San Francisco*
Terry T Yoshizumi, *Durham*
Jinxing Yu, *Richmond*
Jianhui Zhong, *Rochester*

WJR World Journal of Radiology

Contents

Monthly Volume 3 Number 4 April 28, 2011

World Journal of Radiology
Volume 3 Number 4 April 28, 2011

Contents

NAME OF JOURNAL
World Journal of Radiology

LAUNCH DATE
December 31, 2009

SPONSOR
Beijing Baishideng BioMed Scientific Co., Ltd.,
Room 903, Building D, Ocean International Center,
No. 62 Dongsihuan Zhonglu, Chaoyang District,
Beijing 100025, China
Telephone: +86-10-8538-1892
Fax: +86-10-8538-1893
E-mail: baishideng@wjgnet.com
http://www.wjgnet.com

EDITING
Editorial Board of *World Journal of Radiology*,
Room 903, Building D, Ocean International Center,
No. 62 Dongsihuan Zhonglu, Chaoyang District,
Beijing 100025, China
Telephone: +86-10-8538-1892
Fax: +86-10-8538-1893
E-mail: wjr@wjgnet.com
http://www.wjgnet.com

PUBLISHING
Baishideng Publishing Group Co., Limited,
Room 1701, 17/F, Henan Building,
No.90 Jaffe Road, Wanchai, Hong Kong, China
Fax: +852-3115-8812
Telephone: 00852-5804-2046
E-mail: baishideng@wjgnet.com
http://www.wjgnet.com

SUBSCRIPTION
Beijing Baishideng BioMed Scientific Co., Ltd.,
Room 903, Building D, Ocean International Center,
No. 62 Dongsihuan Zhonglu, Chaoyang District,
Beijing 100025, China
Telephone: +86-10-8538-1892
Fax: +86-10-8538-1893
E-mail: baishideng@wjgnet.com
http://www.wjgnet.com

PUBLICATION DATE
April 28, 2011

ISSN
ISSN 1949-8470 (online)

EDITORIAL OFFICE
Na Ma, Director
World Journal of Radiology
Room 903, Building D, Ocean International Center,
No. 62 Dongsihuan Zhonglu, Chaoyang District,
Beijing 100025, China
Telephone: +86-10-8538-1892
Fax: +86-10-8538-1893
E-mail: wjr@wjgnet.com
http://www.wjgnet.com

INSTRUCTIONS TO AUTHORS
Full instructions are available online at http://www.wjgnet.com/1949-8470/g_info_20100316162358.htm.

ONLINE SUBMISSION
http://www.wjgnet.com/1949-8470office

World Journal of Radiology

Online Submissions: http://www.wjgnet.com/1949-8470office
wjr@wjgnet.com
doi:10.4329/wjr.v3.i4.85

World J Radiol 2011 April 28; 3(4): 85-91
ISSN 1949-8470 (online)

EDITORIAL

Ultrasonography of normal and abnormal appendix in children

Noh Hyuck Park, Hwa Eun Oh, Hee Jin Park, Ji Yeon Park

Noh Hyuck Park, Hee Jin Park, Ji Yeon Park, Department of Radiology, Kwandong University College of Medicine, Myongji Hospital, 697-24 Hwajung-dong, Deokyang-gu, Goyang-si, Gyeonggi-do 412-270, South Korea
Hwa Eun Oh, Department of Pathology, Kwandong University College of Medicine, Myongji Hospital, 697-24 Hwajung-dong, Deokyang-gu, Goyang-si, Gyeonggi-do 412-270, South Korea
Author contributions: Park NH designed the study and wrote the manuscript; Park JY and ParK HJ reviewed the literature related to this study; Oh HE contributed to the pathologic review and illustrations of histologic findings.
Correspondence to: Noh Hyuck Park, MD, PhD, Associate Professor, Department of Radiology, Kwandong University College of Medicine, Myongji Hospital, 697-24 Hwajung-dong, Deokyang-gu, Goyang-si, Gyeonggi-do 412-270, South Korea. nhpark904@kwandong.ac.kr
Telephone: +82-31-8107167 Fax: +82-31-8107173
Received: February 10, 2011 Revised: April 1, 2011
Accepted: April 8, 2011
Published online: April 28, 2011

Abstract

Appendicitis is the most common acute surgical emergency of childhood. Since the original report by Puylaert in 1986, the use of ultrasonography in the diagnosis of appendicitis has been the subject of considerable study. Among the reported diagnostic criteria, the maximal outer diameter (MOD) of the appendix is accepted as the one of the most reliable criteria used to differentiate between a normal appendix and acute appendicitis. However, MOD measurement is subject to inaccuracies because luminal distention by non-compressible, non-inflammatory material such as fecal material, or increased maximal mural thickness due to reactive mucosal lymphoid hyperplasia, or a medical cause due to a generalized gastrointestinal disease, such as Crohn's disease, can cause the measurement to exceed the upper limits of normality. The aim of this article is to introduce the spectrum of ultrasonographic findings in the normal and abnormal appendix and eventually to reduce unnecessary surgery in children.

Key words: Acute appendicitis; Appendix; Children; Ultrasonography

Peer reviewer: Adnan Kabaalioglu, MD, Professor, Akdeniz University Hospital, 07059, Antalya, Turkey

Park NH, Oh HE, Park HJ, Park JY. Ultrasonography of normal and abnormal appendix in children. *World J Radiol* 2011; 3(4): 85-91 Available from: URL: http://www.wjgnet.com/1949-8470/full/v3/i4/85.htm DOI: http://dx.doi.org/10.4329/wjr.v3.i4.85

INTRODUCTION

The appendix is a small organ. However, to clinicians and radiologists, it is a very important organ because acute appendicitis is the most common form of acute abdomen that requires surgery in children. Many clinicians deliberate on the decision to operate following clinical suspicion of acute appendicitis.

The quoted negative appendectomy rate was 15% to 25%, but could be as high as 40% in female patients because many gynecological conditions such as dysmenorrhea and ovarian cyst complications can masquerade as acute appendicitis[1-4].

Since the use of sonography by Puylaert[5] to diagnose acute appendicitis in 1986, ultrasonography became the first line of diagnostic tools to detect or exclude acute appendicitis in many institutes. In addition, with advances in the increased resolution of ultrasonography, the incidence of detection of normal appendix and appendicitis mimicking non-inflamed, distended appendix is increasing. Thus, radiologists should be familiar with the ultrasonographic findings of these conditions. The aim of this

article is to introduce the spectrum of ultrasonographic findings from normal appendix through to overt acute appendicitis.

NORMAL APPENDIX

The appendix is a worm-like extension of the cecum and, for this reason, has been called the vermiform appendix. The average length of the appendix is 8-10 cm (range 2-20 cm). The normal appendix consists of 5 distinct layers; the inner most echogenic layer which represents the interface of mucosa and lumen, the hypoechoic mucosal layer, the echogenic submucosal layer, the hypoechoic muscularis propria layer and the outermost echogenic serosal layer. The typical normal appendix in children has an inner hypoechoic band without folding (Figure 1), and this feature is a distinguishable finding from other bowel structures. Therefore, recognition of this finding reduces the time and effort involved in identifying normal appendix and confidently excluding acute appendicitis[6,7]. This inner hypoechoic band corresponds to the mucosal layer with abundant lymphoid tissue on histologic examination[6] and disappears with aging[8].

Normal appendix is a compressible tubular structure with a blind end. It is generally accepted that normal appendix does not exceed 6 mm in maximal outer diameter (MOD), which is the most important diagnostic criterion to exclude acute appendicitis. However, the MOD may be exaggerated by the presence of intraluminal materials such as gas, feces and non-inflamed fluid. To decrease the false positive rate of this MOD criterion, some radiologists recently tried to determine another size criterion, the maximal mural thickness (MMT) of the appendix[9-12]. Simonovský[9] reported that the differences in the normal appendiceal MMT between groups of young children, adolescents and adults were marginally significant. In addition, a MMT < 3 mm should be regarded as normal in children less than 6 years old.

Wiersma *et al*[10] also reported that the sizes of the MOD and the MMT in a normal appendix in children was 0.21-0.64 cm and 0.11-0.27 cm, respectively.

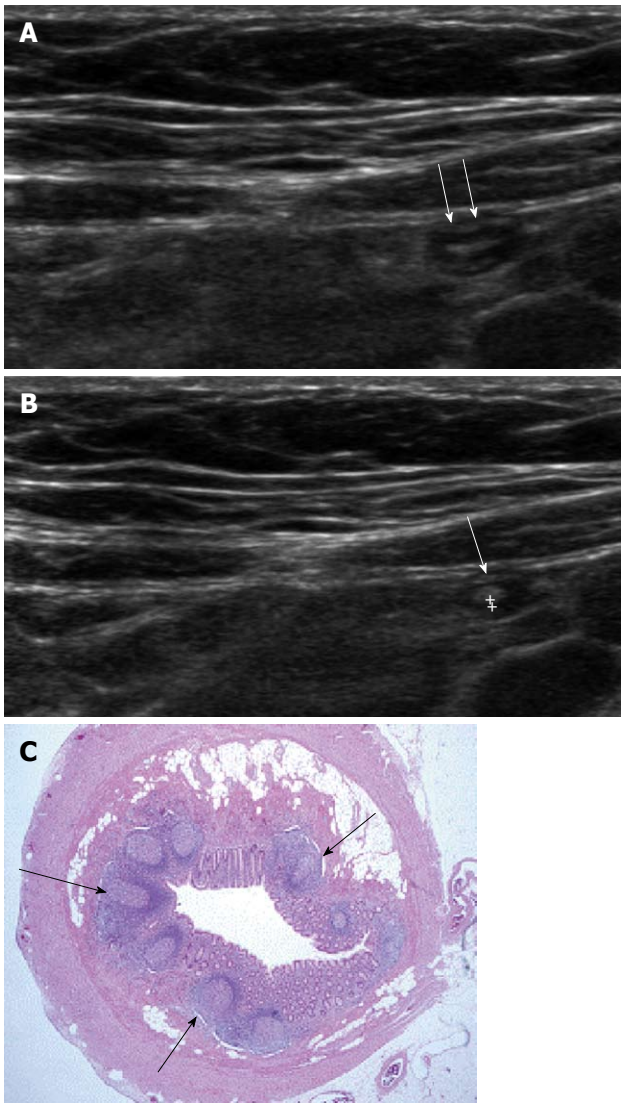

Figure 1 Ultrasonographic and histologic findings of normal appendix. A: Normal appendix (arrows) with thin inner hypoechoic band was seen on high frequency ultrasonography; B: The thickness of the inner hypoechoic band (cursors) of appendix (arrow) was measured as 0.5 mm; C: Low-magnification view of a cross section of the appendix. The inner wall of the appendix is lined by a layer of surface epithelium. The remainder of the mucosa (crypts, surrounding lamina propria, and the inconspicuous muscularis mucosae) surrounds this surface epithelial layer. The characteristic lymphoid nodules (arrows) within the lamina propria were found (× 20, H-E stain).

NORMAL APPENDIX WITH MUCOSAL LYMPHOID HYPERPLASIA

Viral gastroenteritis produces lymphoid hyperplasia in the ileocecal valve region and appendix, altering the intestinal motility and leading to intussusception[13]. Mucosal lymphoid hyperplasia of the appendix is seen as a discernable hypoechoic band without folding in the inner-most layer of the appendix. Although this finding is seen in the normal appendix of children, in conditions of viral gastroenteritis, mesenteric lymphadenitis colitis or other inflammatory conditions, this hypoechoic band becomes thickened and prominent (Figure 2) when compared with that of normal appendix. In one series, the mean thickness of the inner hypoechoic band was measured as 0.80 mm in mesenteric lymphadenitis and 0.74 mm in viral gastroenteritis[6].

Mucosal lymphoid hyperplasia results in an increase in MMT of the appendix, which may lead to the misdiagnosis of acute appendicitis. However, in most cases, we can differentiate it from acute appendicitis by the points of smooth and even hypoechoic band, no demonstrable intraluminal exudates, absence of periappendiceal fat infiltration and absence of blood flow in thickened appendiceal wall[6].

FECAL IMPACTED APPENDIX

Fecal material within the appendiceal lumen was

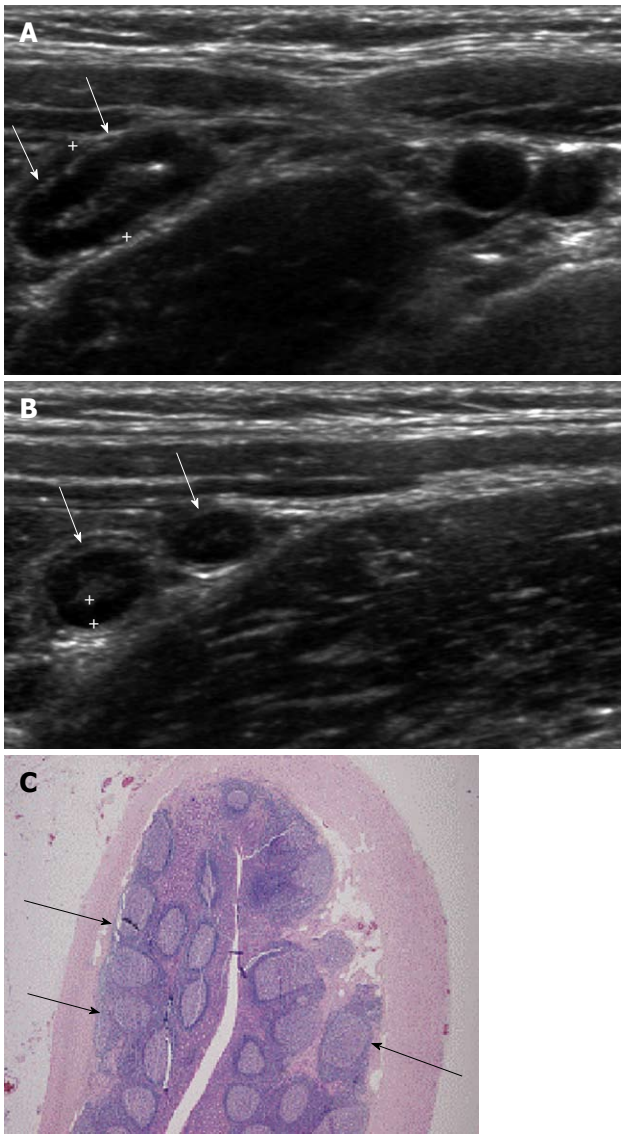

Figure 2 Ultrasonographic and histologic findings of mucosal lymphoid hyperplasia of the appendix. A: Normal appendix with thick inner hypoechoic band was seen (arrows). The maximal outer diameter was measured as 7.3 mm; B: The thickness of the inner hypoechoic band (cursors) of the appendix (arrows) was measured as 1.4 mm; C: Prominent lymphoid follicles (arrows) were found (× 20, H-E stain).

characterized as a heterogeneous mild hyperechoic mass without demonstrable posterior shadowing on ultrasonography[11,14]. The absence of strong hyperechogenicity and posterior shadowing is a distinguishable finding from appendicolith. Fecal material may be present in whole lumen, focal or in a skipped pattern. Fecal impaction of the appendix increases the MOD, frequently leading to a misdiagnosis of acute appendicitis. However, in the fecal impacted appendix, recognition of the sonographic findings of intraluminal fecal material, preservation of the normal wall layering, smaller MOD, thinner MMT, the absence of periappendiceal mesenteric infiltration and no demonstrable increase in blood flow in the appendiceal wall (Figure 3A and B) is helpful in preventing unnecessary surgery[11].

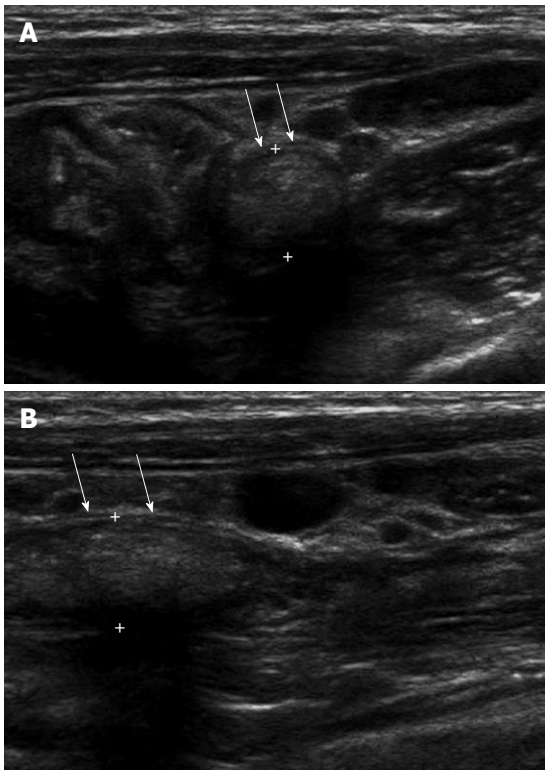

Figure 3 A 5-year-old male with acute abdominal pain. A: Fecal distended appendix (arrows) with thinned maximal mural thickness (0.6 mm) and preservation of wall layers were seen on axial image; B: The maximal outer diameter of fecal distended appendix (arrows) was measured as 8.5 mm.

CROHN'S DISEASE OF APPENDIX

It was shown that 21% of patients with Crohn's disease had appendiceal involvement[15]. This incidence is similar to that reported in pathologic studies (20%-36%)[16]. Appendiceal involvement in Crohn's disease was always associated with segmental thickening of the terminal part of the ileum, cecum, or both.

Newly diagnosed Crohn's disease with involvement of the appendix is difficult to differentiate from acute appendicitis. Distinguishing both entities is important: acute appendicitis usually requires surgery, whereas Crohn's disease does not. On ultrasonography, Crohn's appendicitis shows marked thickening of the appendiceal wall, may be up to 3 cm (Figure 4A and B), which is an unusual finding in primary acute appendicitis. Also periappendiceal fibrofatty proliferation and hyperemia of thickened terminal ileum on color Doppler study are important points in differentiating acute appendicitis[17].

There are two major concerns when isolated Crohn's appendicitis is diagnosed at the time of emergency laparotomy or during subsequent evaluation of the resected specimens, which are: is there concurrent involvement elsewhere in the gastrointestinal tract and what is the potential risk of local recurrence or development of disease elsewhere in the gastrointestinal tract? Both issues are of obvious critical importance for the optimal management of these patients. Yang *et al*[18] and Timmcke[19] reviewed

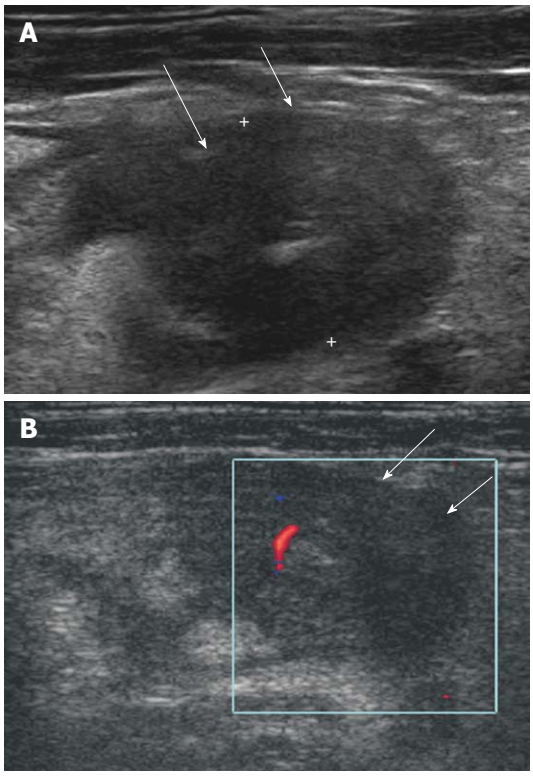

Figure 4 Isolated Crohn's appendicitis. A: Marked thickening with transmural hypoechoic echo-alteration of appendiceal wall (arrows); B: Mild increased blood flow in thickened appendiceal wall (arrows) was seen on color Doppler study.

the literature and noted that concurrent Crohn's disease elsewhere in the gastrointestinal tract was present in approximately 25% of patients with Crohn's appendicitis. The recurrence rate after appendectomy for localized Crohn's disease has been reported to be 14%-50%[18-20].

SECONDARY APPENDICITIS DUE TO A GENERALIZED GASTROINTESTINAL INFECTION

Although rare, there are numerous bacterial, viral, fungal and parasitic infections that can affect the appendix as part of a generalized gastrointestinal disease[13]. It is important to differentiate these disorders from primary acute appendicitis, because the former can be treated with medical therapy for the primary causes and the latter should be treated with surgical therapy. Secondary appendicitis due to a generalized gastrointestinal disease is seen as an increase in MMT with preservation of wall layers, no demonstrable intraluminal exudates and no evidence of periappendiceal change in the setting of the presence of cecal and contiguous colonic wall thickening (Figure 5).

ACUTE APPENDICITIS

Acute appendicitis in children is more difficult to recognize clinically than in adults because most children can-

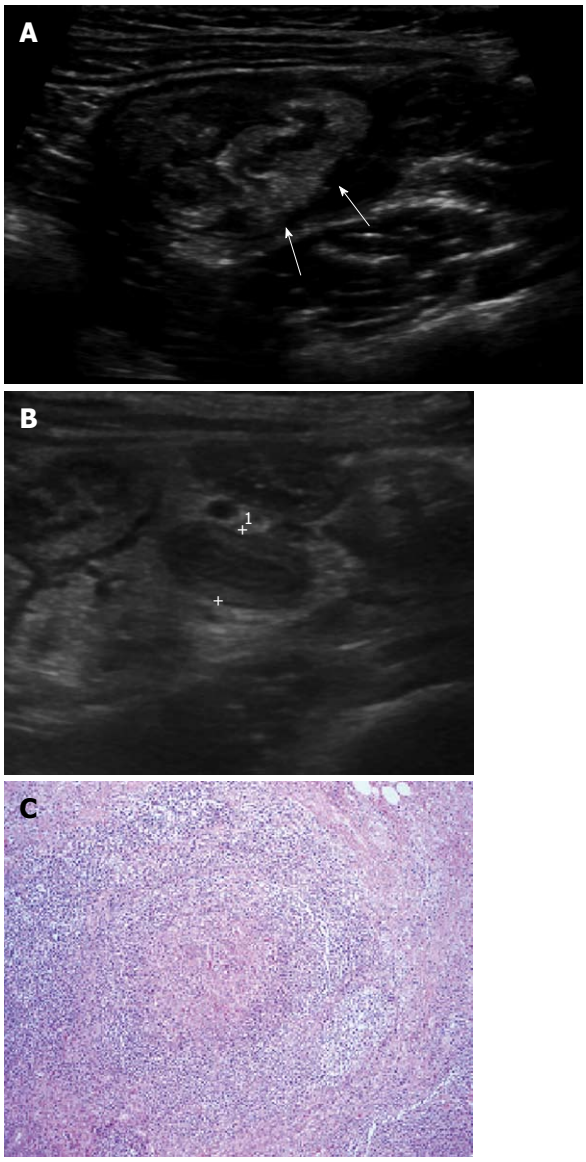

Figure 5 A 4-year-old female with acute colitis. A: Diffuse thickening of the colonic wall including cecum (arrows) was seen; B: Appendix (cursors) was also swollen with a maximal outer diameter of 7.8 mm and mildly increased echogenicity of periappendiceal mesenteric fat, which led to the misdiagnosis of acute appendicitis; C: The lymphoid follicles within the Peyer's patches show granulomas with microabscesses (× 100, H-E stain), suggestive of yersiniosis.

not describe their symptoms clearly and abdominal pain is often poorly localized[21]. The use of high frequency sonography with additional compression in children with acute abdominal pain have improved both diagnostic accuracy and treatment outcome[22].

The exact mechanism of appendicitis is not well characterized. However, the etiology is most likely multifactorial, a combination of ischemic mucosal damage and bacterial overgrowth with some luminal obstruction appears to be the most likely pathogenesis[23,24].

In our experience, non-obstructive appendicitis without luminal distention is frequently present on US examination, although its exact incidence rate is not yet documented. Of course, non-obstructive appendicitis does not have appendicolith or demonstrable intralumi-

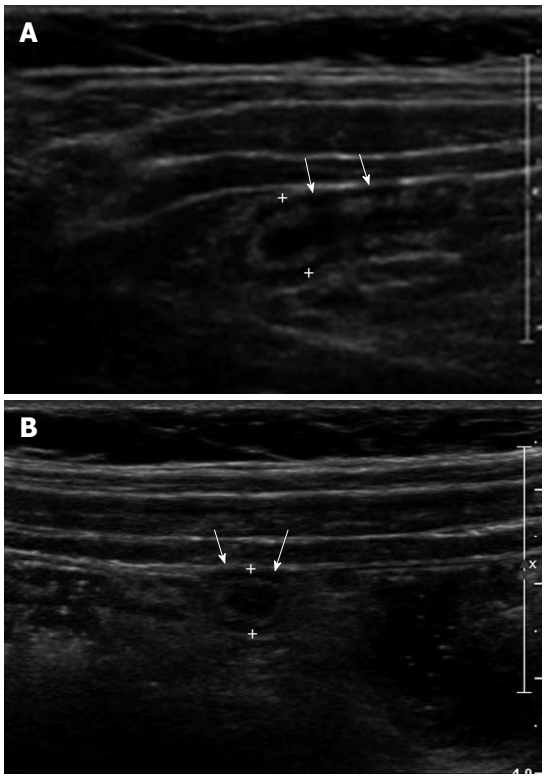

Figure 6 A 10-year-old male with a non-obstructive acute appendicitis. A: Thickening of appendiceal wall (arrows) with a maximal outer diameter (MOD) of 3 mm and some irregularity of the submucosal echogenic layer. However, no evidence of luminal distention and intraluminal appendicolith was found; B: MOD of inflamed appendix (arrows) was measured as 7.1 mm.

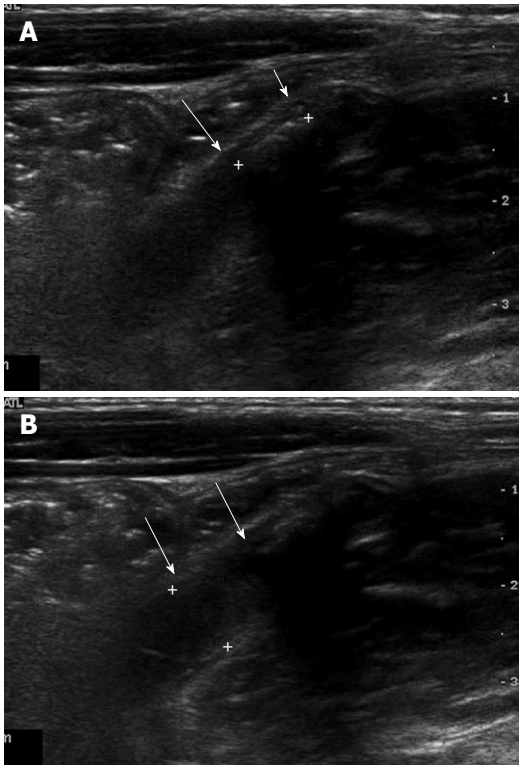

Figure 7 A 7-year-old female with an obstructive acute appendicitis. A: Luminal distention of appendix (arrows) was seen. The maximal outer diameter was measured as approximately 7.9 mm; B: Proximal intraluminal appendicolith (cursors) of appendix (arrows) was identified.

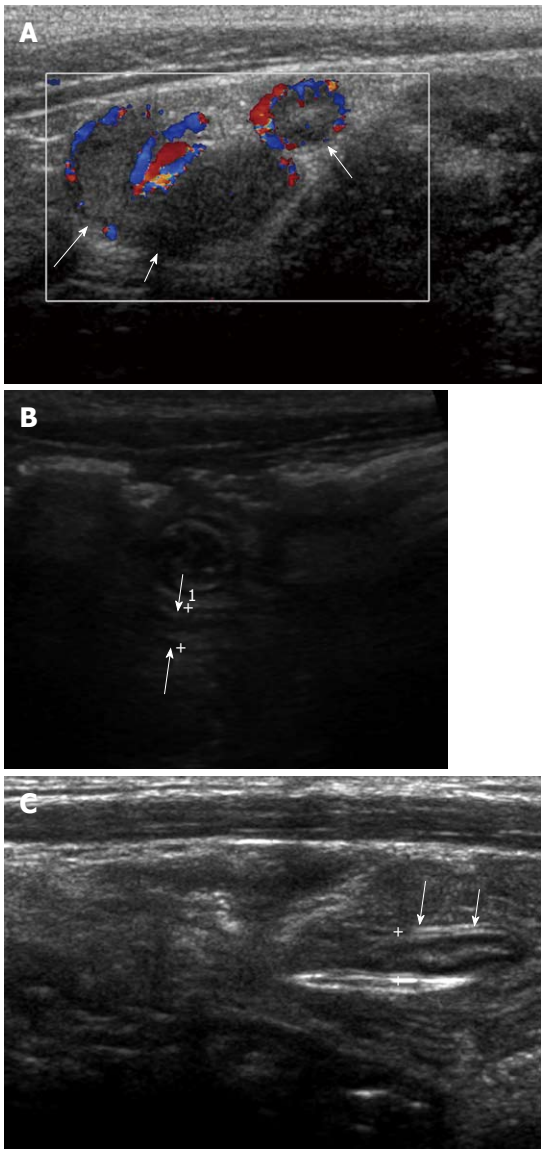

Figure 8 A 6-year-old male with acute appendicitis and fever. A: Distended appendix with dirty intraluminal fluid and hyperemia of appendiceal wall on color Doppler study (arrows). Periappendiceal mesenteric fat infiltration was identified; B: Because of lobar pneumonia, surgery was delayed and antibiotic therapy given. On follow-up ultrasonography 3 d later, the maximal outer diameter of appendix (arrows) was decreased to 4 mm with disappearance of intraluminal content; C: On follow-up after 6 d, the wall layers of the appendix (arrows) had recovered significantly. Periappendiceal mesenteric fat change had almost resolved.

nal obstructive lesion. It has increased MMT with some obliteration of wall layers and periappendiceal fat infiltration (Figure 6A and B). We assume that the incidence of perforation in non-obstructive appendicitis may be lower than obstructive appendicitis (Figure 7A and B). Furthermore, antibiotic therapy with close ultrasonographic observation may be an alternative treatment rather than immediate appendectomy in the case of mild non-obstructive appendicitis when the operation is not allowed due to inadequate systemic condition (Figure 8A-C)[25].

A MOD >6 mm has been regarded as the most reliable feature in diagnosing acute appendicitis. In a recent report, a MOD > 5.7 mm was suggested as the optimal

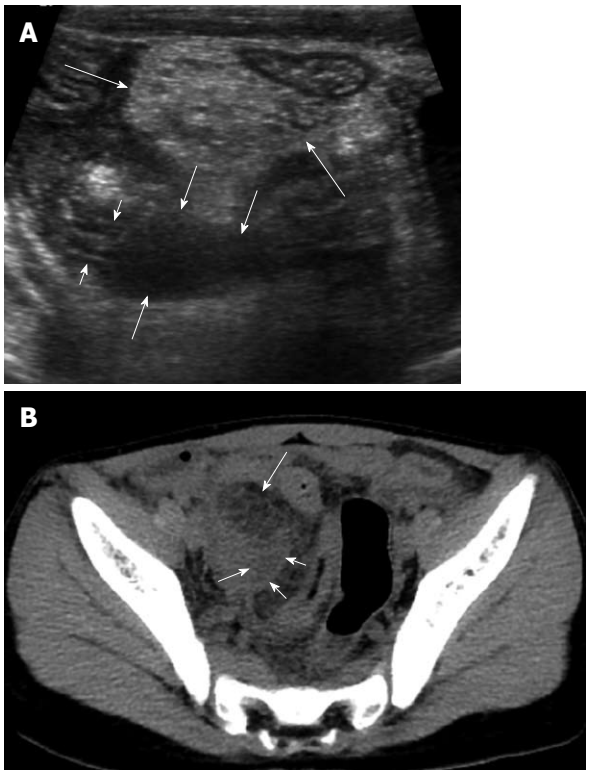

Figure 9 An 8-year-old male with perforated appendicitis. A: Initial US showed a collapsed appendix with distal wall defect (short arrows) and periappendiceal fluid collection (medium sized arrows) in the deep right lower abdomen. In addition, marked mesenteric inflammatory change (long arrows) was seen; B: Subsequent axial CT scan revealed loculated fluid (short arrows) corresponding to the periappendiceal fluid collection on US and marked mesenteric fat change (long arrow) in the right lower abdomen.

criterion to diagnose acute appendicitis in children[11].

However, the MOD may be larger than 6 mm without acute inflammation, due to the presence of intraluminal materials such as gas, feces and fluid[11,14,26,27] or mucosal lymphoid hyperplasia secondary to viral gastroenteritis or mesenteric lymphadenitis. To decrease the false positive rate of the MOD criterion, one should consider the intraluminal content, presence of periappendiceal change, MMT, preservation of wall layers and increase in blood flow in the appendiceal wall in equivocal cases[9-12,14].

PERFORATED APPENDICITIS

The diagnosis of perforated appendicitis can be more difficult because the appendix frequently decompresses with perforation and yet may not "wall off" or form a well-defined abscess. As a result, identifying the appendix can be very difficult[28]. Marked inflammatory change of the mesentery/omentum and abnormal fluid collection or abscess formation in the right lower abdomen or pelvic cavity may be clues to the diagnosis of perforated appendicitis in children (Figure 9).

CONCLUSION

Knowledge of ultrasonographic findings of the normal and abnormal appendix is helpful in reducing the time and effort involved in detecting normal appendix and to diagnose or exclude acute appendicitis confidently.

REFERENCES

1 **Flum DR**, Koepsell T. The clinical and economic correlates of misdiagnosed appendicitis: nationwide analysis. *Arch Surg* 2002; **137**: 799-804; discussion 804
2 **Humes DJ**, Simpson J. Acute appendicitis. *BMJ* 2006; **333**: 530-534
3 **Ma KW**, Chia NH, Yeung HW, Cheung MT. If not appendicitis, then what else can it be? A retrospective review of 1492 appendectomies. *Hong Kong Med J* 2010; **16**: 12-17
4 **Paulson EK**, Kalady MF, Pappas TN. Clinical practice. Suspected appendicitis. *N Engl J Med* 2003; **348**: 236-242
5 **Puylaert JB**. Acute appendicitis: US evaluation using graded compression. *Radiology* 1986; **158**: 355-360
6 **Park NH**, Song SY, Lee EJ, Kim MS, Park CS, Oh HE, Yang GS. Characteristic sonographic appearance of normal appendix in children: inner hypoechoic band without folding. *J Korean Radiol Soc* 2004; **51**: 663-667
7 **Kim BS**, Choi GM, Kim SH, Park JK, Kim K, Kang HW, Kang KS. Usefulness of the inner hypoechoic band of the vermiform appendix as ultrasonographic criteria for the diagnosis of acute appendicitis in children. *J Korean Radiol Soc* 2007; **57**: 483-488
8 Nonneoplastic diseases of the appendix. In: Fenoglio-Preiser CM, Noffsinger AE, Stemmermann GN, Lantz PE, Isaacson PG, editors. Gastrointestinal pathology: an atlas and text. 3rd ed. Philadelphia: Lippincott Williams and Wilkins, 2008: 497-498
9 **Simonovský V**. Normal appendix: is there any significant difference in the maximal mural thickness at US between pediatric and adult populations? *Radiology* 2002; **224**: 333-337
10 **Wiersma F**, Srámek A, Holscher HC. US features of the normal appendix and surrounding area in children. *Radiology* 2005; **235**: 1018-1022
11 **Park NH**, Park CS, Lee EJ, Kim MS, Ryu JA, Bae JM, Song JS. Ultrasonographic findings identifying the faecal-impacted appendix: differential findings with acute appendicitis. *Br J Radiol* 2007; **80**: 872-877
12 **Je BK**, Kim SB, Lee SH, Lee KY, Cha SH. Diagnostic value of maximal-outer-diameter and maximal-mural-thickness in use of ultrasound for acute appendicitis in children. *World J Gastroenterol* 2009; **15**: 2900-2903
13 **Rabah R**. Pathology of the appendix in children: an institutional experience and review of the literature. *Pediatr Radiol* 2007; **37**: 15-20
14 **Rioux M**. Sonographic detection of the normal and abnormal appendix. *AJR Am J Roentgenol* 1992; **158**: 773-778
15 **Ripollés T**, Martínez MJ, Morote V, Errando J. Appendiceal involvement in Crohn's disease: gray-scale sonography and color Doppler flow features. *AJR Am J Roentgenol* 2006; **186**: 1071-1078
16 **Lockhart-Mummery HE**, Morson BC. Crohn's disease (regional enteritis) of the large intestine and its distinction from ulcerative colitis. *Gut* 1960; **1**: 87-105
17 **Agha FP**, Ghahremani GG, Panella JS, Kaufman MW. Appendicitis as the initial manifestation of Crohn's disease: radiologic features and prognosis. *AJR Am J Roentgenol* 1987; **149**: 515-518
18 **Yang SS**, Gibson P, McCaughey RS, Arcari FA, Bernstein J. Primary Crohn's disease of the appendix: report of 14 cases and review of the literature. *Ann Surg* 1979; **189**: 334-339
19 **Timmcke AE**. Granulomatous appendicitis: is it Crohn's disease? Report of a case and review of the literature. *Am J Gastroenterol* 1986; **81**: 283-287
20 **Ewen SW**, Anderson J, Galloway JM, Miller JD, Kyle J. Crohn's disease initially confined to the appendix. *Gastroen-*

terology 1971; **60**: 853-857
21 **Kottmeier PK**. Appendicitis. In: Welch K, Randolph J, Ravitch M, O'Neil J, Rowe M, editors. Pediatric surgery. Chicago: Year Book Medical, 1986: 989-995
22 **Patriquin HB**, Garcier JM, Lafortune M, Yazbeck S, Russo P, Jequier S, Ouimet A, Filiatrault D. Appendicitis in children and young adults: Doppler sonographic-pathologic correlation. *AJR Am J Roentgenol* 1996; **166**: 629-633
23 **Lamps LW**. Appendicitis and infections of the appendix. *Semin Diagn Pathol* 2004; **21**: 86-97
24 **Williams RA**, Myers P. Pathology of the appendix and its surgical treatment. 1st ed. London: Chapman and Hall Medical press, 1994
25 **Styrud J**, Eriksson S, Nilsson I, Ahlberg G, Haapaniemi S, Neovius G, Rex L, Badume I, Granström L. Appendectomy versus antibiotic treatment in acute appendicitis. a prospective multicenter randomized controlled trial. *World J Surg* 2006; **30**: 1033-1037
26 **Hahn HB**, Hoepner FU, Kalle T, Macdonald EB, Prantl F, Spitzer IM, Faerber DR. Sonography of acute appendicitis in children: 7 years experience. *Pediatr Radiol* 1998; **28**: 147-151
27 **Simonovský V**. Sonographic detection of normal and abnormal appendix. *Clin Radiol* 1999; **54**: 533-539
28 **Hayden CK Jr**, Kuchelmeister J, Lipscomb TS. Sonography of acute appendicitis in childhood: perforation versus nonperforation. *J Ultrasound Med* 1992; **11**: 209-216

S- Editor Cheng JX **L- Editor** Webster JR **E- Editor** Zheng XM

World Journal of Radiology

Online Submissions: http://www.wjgnet.com/1949-8470office
wjr@wjgnet.com
doi:10.4329/wjr.v3.i4.92

World J Radiol 2011 April 28; 3(4): 92-104
ISSN 1949-8470 (online)

REVIEW

Clinical significance of magnetic resonance imaging findings in rectal cancer

Charles F Bellows, Bernard Jaffe, Lorenzo Bacigalupo, Salvatore Pucciarelli, Guiseppe Gagliardi

Charles F Bellows, Bernard Jaffe, Guiseppe Gagliardi, Department of Surgery, Tulane University, New Orleans, LA 70112, United States
Lorenzo Bacigalupo, Department of Radiology, Galliera Hospital, Genoa, 16128, Italy
Salvatore Pucciarelli, Department of Surgery, University of Padua, Padua, 35121, Italy
Author contributions: Bellows CF, Jaffe B and Gagliardi G wrote the manuscript; Bacigalupo L and Pucciarelli S contributed materials and wrote sections of the manuscript; Bellows CF and Gagliardi G conceived the idea of the manuscript and performed the literature search.
Correspondence to: Charles F Bellows, MD, Department of Surgery, Tulane University, 1430 Tulane Ave, New Orleans, LA 70112, United States. cbellows@tulane.edu
Telephone: +1-504-9882307 Fax: +1-504-9884762
Received: February 22, 2011 Revised: April 6, 2011
Accepted: April 13, 2011
Published online: April 28, 2011

Abstract

Staging of rectal cancer is essential to help guide clinicians to decide upon the correct type of surgery and determine whether or not neoadjuvant therapy is indicated. Magnetic resonance imaging (MRI) is currently one of the most accurate modalities on which to base treatment decisions for patients with rectal cancer. MRI can accurately detect the mesorectal fascia, assess the invasion of the mesorectum or surrounding organs and predict the circumferential resection margin. Although nodal disease remains a difficult radiological diagnosis, new lymphographic agents and diffusion weighted imaging may allow identification of metastatic nodes by criteria other then size. In light of this, we have reviewed the literature on the accuracy of specific MRI findings for staging the local extent of primary rectal cancer. The aim of this review is to establish a correlation between MRI findings, prognosis, and available treatment options.

Key words: Magnetic resonance imaging; Preoperative staging; Prognostic factors; Rectal cancer

Peer reviewer: Chan Kyo Kim, MD, Assistant Professor, Department of Radiology, Samsung Medical Center, Sungkyunkwan University School of Medicine, 50 Ilwon-dong, Kangnam-gu, Seoul 135-710, South Korea

Bellows CF, Jaffe B, Bacigalupo L, Pucciarelli S, Gagliardi G. Clinical significance of magnetic resonance imaging findings in rectal cancer. *World J Radiol* 2011; 3(4): 92-104 Available from: URL: http://www.wjgnet.com/1949-8470/full/v3/i4/92.htm DOI: http://dx.doi.org/10.4329/wjr.v3.i4.92

INTRODUCTION

In 2010, an estimated 142 570 people were diagnosed with colorectal cancer in the United States, including 39 670 with rectal cancer[1]. In contrast to colon cancer, local recurrences in rectal cancer, which occur in up to 50% of patients with T3 or node positive lesions, have been a significant cause of morbidity[2]. In order to decrease rates of local recurrence, adjuvant treatment, such as radiotherapy with or without chemotherapy, is generally recommended for patients with T3 or higher and/or N+ rectal cancers[3]. Preoperative radiotherapy and chemo-radiotherapy are now preferred to postoperative because they are much better tolerated, thereby increasing treatment compliance. They also result in lower local recurrence rates[4]. However, even if given preoperatively, pelvic radiotherapy can result in deterioration of anal continence and sexual function as well as worsen the quality of life[5]. Importantly, according to data from recent chemoradiotherapy (CRT) trials, 18%-30% of enrolled patients are over-staged and therefore receive unnecessary and potentially harmful therapy[6]. Thus, accurate staging of this disease is essential to spare patients from potentially toxic over-treatment.

The most common pre-operative staging modalities

for rectal cancer include endorectal ultrasonography (EUS), computed tomography (CT) and magnetic resonance imaging (MRI). In two large retrospective studies on rectal cancer patients, over a period of 10 years, the overall accuracy of T and N staging by EUS was shown to be only 69% and 68% respectively[7,8]. Compared to EUS, CT has an even lower accuracy for determining the depth of tumor invasion[9]. In contrast, high definition MRI with phased-array coils has been shown to be more reliable than EUS in staging advanced (stage ≥ Ⅱ) rectal cancer[10]. In fact, MRI has been shown to provide important information about the depth of tumor infiltration within the bowel wall, the relationship between the tumor and mesorectal fascia, and the presence of lymph node and extramural vascular invasion. Information determined from MRI can help guide clinicians to decide upon the correct type of surgery, determine whether or not neoadjuvant therapy, such as chemo-radiation, is indicated, and predict patients' prognosis. This information can be used to maximize the chance of complete oncological resection, improve survival and the quality of life, and minimize morbidity. The aim of this review is to establish a correlation between MRI findings, prognosis, and available treatment options.

MR IMAGING PROTOCOLS

The introduction of phased-array coils has been a major advance in imaging of rectal cancer allowing high spatial resolution, a large field of coverage[10], and visualization of structures 1-2 mm in diameter[11]. Ideally, for rectal MRI, the field of view should be small (i.e. less than 200 mm), the matrix (resolution in 2D) at least 256 × 256 pixels, and the slices 3 mm or less in thickness.

In the most current MRI protocol (Table 1), the tumor is first localized with low-resolution axial and sagittal images of the entire pelvis. The field of view is then restricted to the area of the cancer and high-resolution T2 weighted images are obtained perpendicular to the cranio-caudal axis of the rectum at the level of the tumor (Figure 1A). True axial (i.e. perpendicular) images of the tumor are critical because they reduce the overestimation of the tumor depth of invasion noted upon oblique imaging[12]. Coronal images (parallel to the anus) are important in identifying the relationship of low rectal tumors to the internal sphincter as well as the external sphincter/levators complex[13] (Figure 1B). T2-weighted sagittal images are often necessary to determine the relationship of the tumor to the peritoneal reflection (Figure 1C)[14]. In some cases, axial diffusion weighted imaging (DWI) may be performed to help in the localization of small tumors[15] (Figure 2).

The importance of the imaging protocol for assessment of advanced rectal tumors has recently been reported. Suzuki and associates demonstrated that by including the imaging parameters listed in sequence 2 and 3 (Table 1), the sensitivity and specificity of assessing invasion of anterior organs was 80% and 95% respectively, compared to only 50% and 33% with protocols that employed different imaging parameters[16].

Improving MR image quality can be facilitated with the use of rectal cleaning to limit misinterpretation due to stool residue. Distension of the rectum by air insufflation, gel enema, or intravenous administration of spasmolytic medication also improves evaluation of the rectal wall layers.

MRI FINDINGS IN RECTAL CANCER

In T2 weighted images, rectal cancers typically have a signal-intensity intermediate between that of the perirectal fat, which is bright, and the muscularis propria, which is pitch black. The signal intensity is increased if the tumors contain mucin, but a low signal intensity similar to that of the muscle layer usually indicates a marked desmoplastic reaction of the tumor[17].

The anatomy relevant to rectal cancer imaging is also well visualized in T2 weighted images (Figure 1). The mucosa has a hypointense signal, the submucosa a hyperintense signal, the muscularis propria a hypointense signal, and the mesorectal fat a highly hyperintense signal. The mesorectal fascia can be identified as a thin, low-signal intensity structure that envelopes the mesorectum. However, due to a diminishing thickness of mesorectal fat, the mesorectal fascia is typically better visualized in the upper and middle third as well as the posterior portions of the rectum than the lower third and anterior portions[9]. The presacral fascia is also a thin hypointense layer in T2 weighted images. It covers the pelvic walls and the sacrum and joins with the mesorectum at the level of S4/S5 to form the rectosacral fascia, also known as the Waldayer's fascia (Figure 1B).

Non-enhanced T1 weighted images have limited value in distinguishing the tumor from the layers of the bowel wall[14]. However, after intravenous injection of paramagnetic contrast, the smooth muscle of the internal sphincter brightly enhances, which can sometimes be useful in studying the relationship of the tumor with the sphincter complex[18].

PROGNOSTIC FACTORS ASSESSED BY MRI

The prognostic factors of rectal cancer that significantly influence the management strategy, the type of resection, tumor resectability, and candidacy for neo-adjuvant therapy, depend on the information obtained from preoperative MRI, including depth of tumor infiltration within the bowel wall, involvement of neighboring pelvic organs and/or the peritoneum (T stage), the circumferential resection margin (CRM), the presence of local lymph node metastases (N stage), extramural vascular invasion, and the extent of extramural tumor spread in mm.

T staging

The depth of invasion through the muscle wall is one

Table 1 Optimal rectal MRI protocol

Sequence	Area	Plane	Purpose
1-Low resolution T2 ± T1	Whole pelvis	Axial	Overview of the pelvis and tumor localization
2-High resolution T2	Rectum	Sagittal	Determination of cranio-caudal extension of the tumor, peritoneal reflection and distance from the anal canal
3-High resolution T2	Whole mesorectum	Axial to the tumor	Assessment of the mesorectum and of the CRM
4-High resolution T2	Rectum	Coronal based on the anal canal plane	Assess relation to the sphincter-levator complex

CRM: Circumferential resection margin.

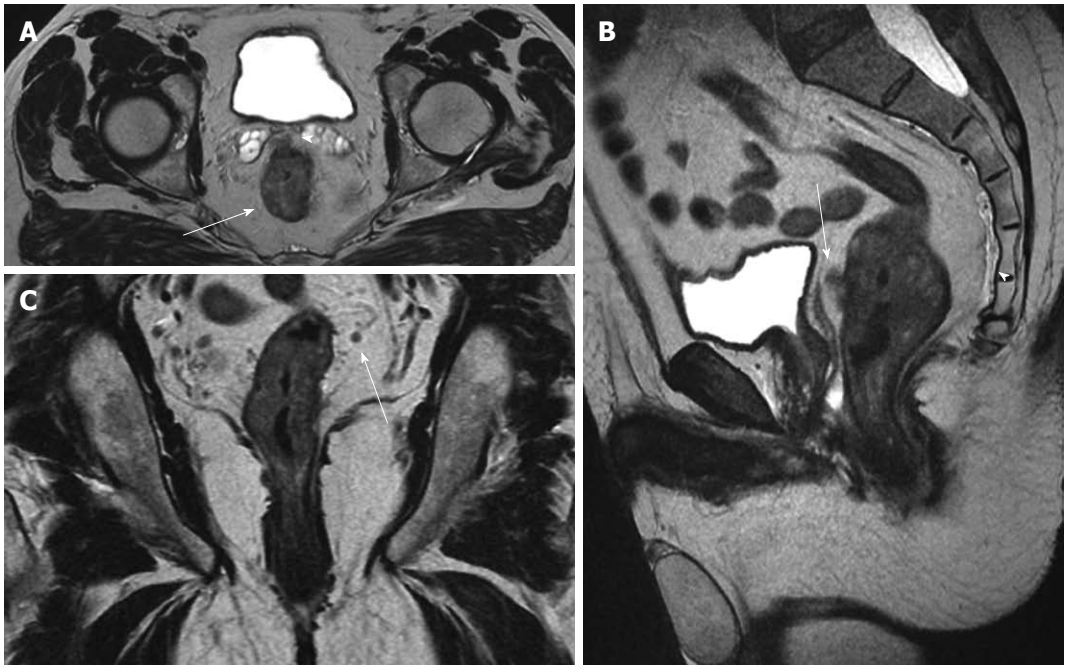

Figure 1 Magnetic resonance imaging staging of rectal cancer before chemoradiation: T3, N+. Pathology result: T3, N1. A: Axial T2w image shows the circumferential tumor (arrow) and the extramural spread anteriorly (arrowhead) close to the seminal vesicles; B: In the sagittal T2w image, the anterior extramural spread (arrow) can be also recognized close to the mesorectal fascia (thin vertical hypointense line posterior to the bladder). The presacral fascia can also be appreciated (arrowhead) continuing inferiorly as the rectosacral fascia; C: In the coronal T2w image, a small mesorectal lymph node (arrow) is seen.

important element seen on MRI that can help guide clinical decision making for patients with rectal cancer. Not only does the incidence of nodal involvement increase with increasing tumor penetration[19,20], but clinical studies have shown that patients with stage I (T1-2 N0) rectal cancer do not benefit from neo-adjuvant radiotherapy[21] and may be amenable to a less than radical surgical treatment[22]. Patients with clinically staged T3-4 tumors typically require preoperative CRT since it reduces the rates of local recurrence more effectively than either postoperative CRT or preoperative radiotherapy alone[23-25]. However, some problems remain with T stage determination on MR imaging. Overall, the agreement between MRI and histology for T staging has ranged from 66%-94%[18,26-28]. One of the main problems of T staging on MRI is the distinction between T2 and T3 tumors. In fact, investigators have shown that the negative predictive value for invasion beyond the muscularis propria varied from 93% (expert reading) to 76% (general radiologist reading)[26]. This difficulty is attributed to the presence of desmoplastic reactions around the tumor. This reaction makes it difficult to distinguish between spiculation in the perirectal fat caused by fibrosis alone from that caused by fibrous tissue that contains tumor cells[26]. In contrast, MRI has been shown to be more accurate in imaging the more advanced tumors (T4)[27,29]. According to a meta-analysis, MRI for T4 lesions has a specificity of 96%[30].

CRM

The CRM (lateral, radial) is defined as the surgical cut surface of the connective tissues (i.e. lymphovascular, fatty and neural tissue) that circumferentially encase the rectum. It equates to the mesorectal fascia that forms the plane of dissection in rectal cancer surgery. It is assessed by marking the outer surface (i.e. the CRM) with ink, taking serial cuts through the specimen and examining the macroscopic and microscopic relations between the tumor and the inked margin (Figure 3A-C). The CRM gives significant information not only about the quality of the performed operation but also prognosis of the disease. Indeed, in a recent study based on the data from a randomized clinical trial, Nagtegaal *et al*[31] demonstrated in a multivariate

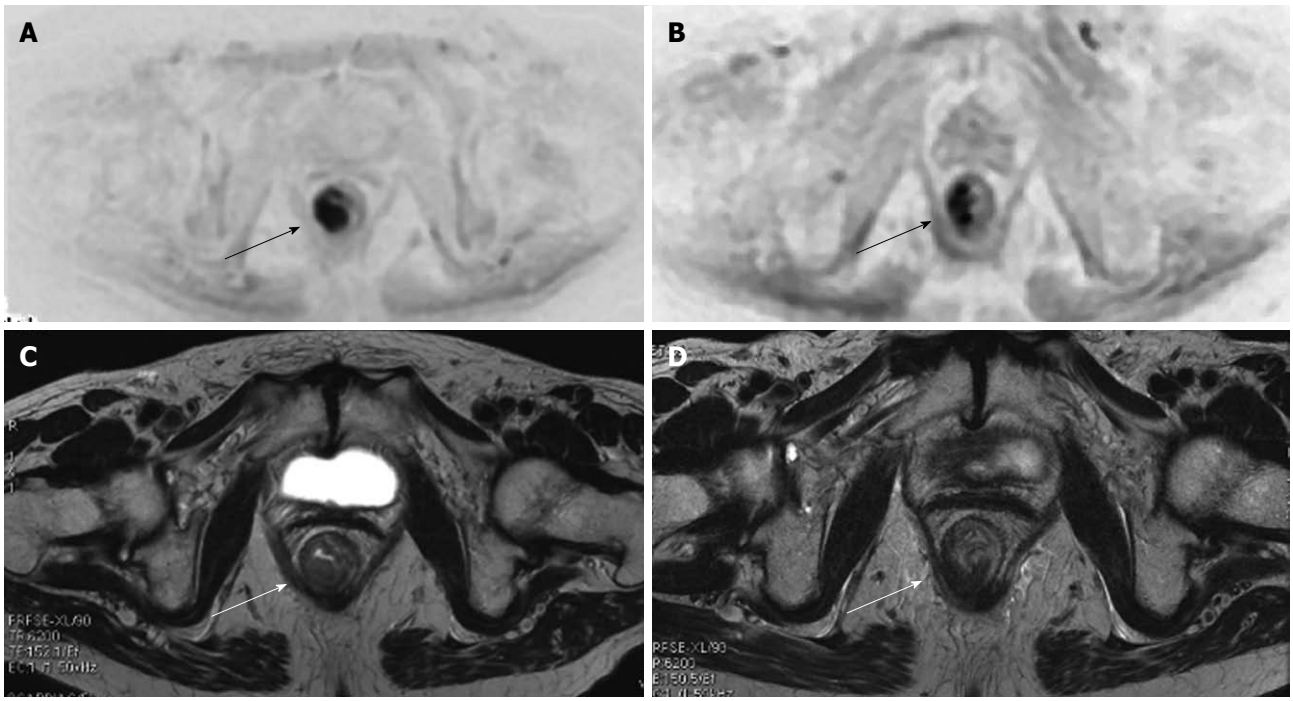

Figure 2 Diffuse weighted imaging and cancer (arrows) of the lower rectum. At initial MR staging T3N1. After neoadjuvant therapy, MR restage was T3N0. At pathology: T3N1 (only one small metastatic mesorectal lymph node). Diffusion weighted imaging (DWI) (A) and axial T2w (B) images show the tumor (arrows) before chemoradiotherapy. The DWI image allows for better recognition of the lesion. DWI (C) and axial T2w (D) images after chemoradiotherapy show a reduction in the dimensions of the lesion (arrows).

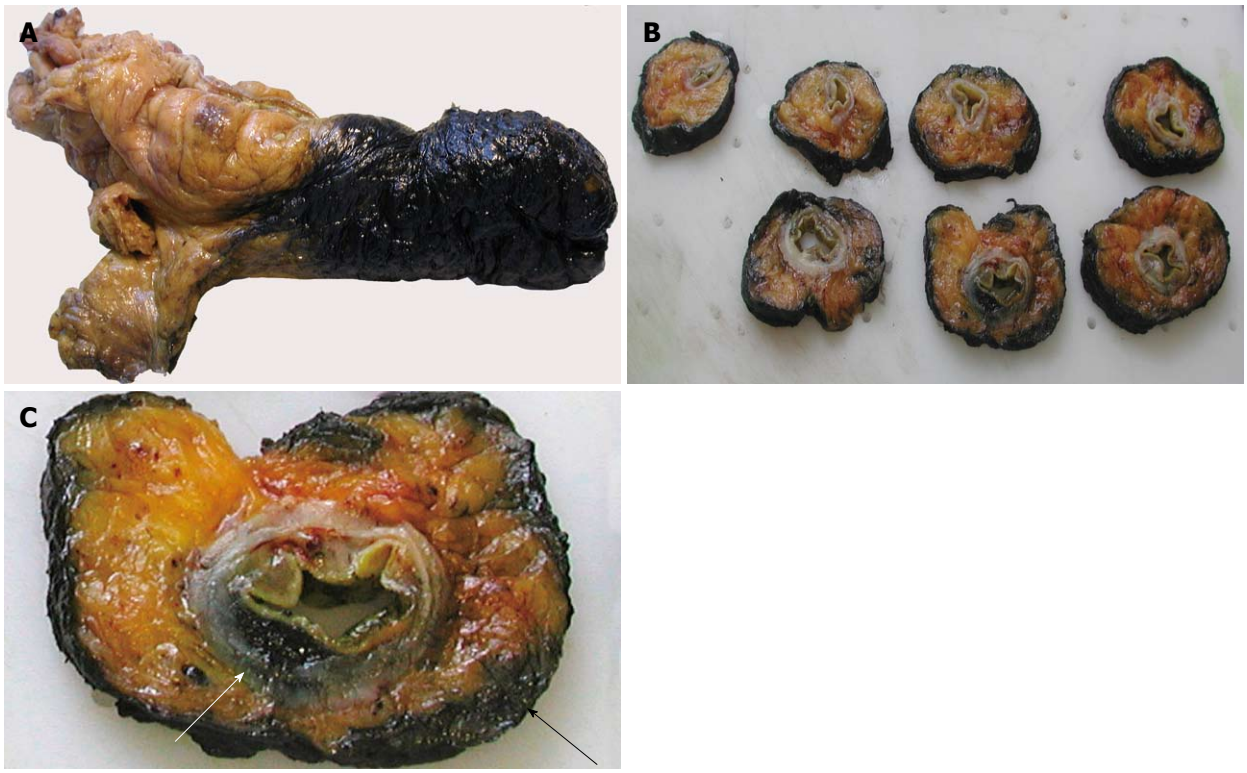

Figure 3 Pathological evaluation of the circumferential resection margin (CRM). A: The excised rectum is dipped in ink; B: Serial sections including the tumor are taken through the entire rectum; C: One of the sections shows the tumor's leading edge (white arrow) and its relation with the CRM (black arrow).

model that the CRM is more important than the T stage for the prognosis of rectal cancer. The definition of a positive CRM remains a matter of debate. A review of the literature in 2006 showed that the majority of studies that dealt with CRM status used the ⩽ 1 mm definition for positive CRM (91.1%; 7373 of 8094 patients)[32].

Six distinct types of CRM involvement have been described; direct tumor spread which occurs in 18% to 29% of cases; discontinuous tumor spread in 14% to 67% of cases; lymph node metastases in 12% to 14% of cases; venous invasion in 14% to 57% of cases; lymphatic invasion in 9% of cases; and perineural tumor spread in 7% to 14% of cases[32]. In approximately 30% of patients, there is more than one type of margin involvement. In contrast to direct tumor spread, the involvement of the CRM by lymph node metastases is not associated with local recurrence[32].

MRI is highly accurate and reliable for prediction of the CRM[33,34]. In their most recent study of 98 rectal cancer patients, Brown *et al*[27] reported a 92% agreement between MRI images and histologic findings for prediction of CRM involvement. In another study assessing the tumor relationship to the mesorectal fascia, two observers independently scored the tumor stage and the distance to the mesorectal fascia on MRI and compared these observations with the final histological findings[26]. For twelve tumors with involved mesorectal fascia, and thus, a CRM of 0 mm, the accuracy in predicting the CRM was 100% for both readers. In 29 patients with a wide CRM (10 mm), the accuracy for predicting the negative margin was 97% (27 of 28) for one reader and 93% (26 of 28) for the other[26].

It is relevant to point out that 5 mm of mesorectal tissue surrounding the lateral tumor edge on MRI was shown to equal a CRM of 2 mm in the surgical specimen[26]. In the report by Nagtegaal *et al*[35], a linear regression curve showed that the crucial distance of at least 2 mm could be predicted with 97% confidence when the distance on MRI is at least 6 mm. Therefore, the safe rule to predict CRM involvement on MRI is considered to be an MRI measurement minus 4 mm due to shrinkage of the specimen with fixation[6]. Of note, the CRM becomes more difficult to identify in low, anterior tumors and in patients with a limited amount of perirectal fat[36].

In a recent study by Frasson *et al*[37], the 5-year local recurrence rates for patients with a preoperative CRM of < 2 mm on MRI or EUS who did not receive preoperative chemoradiation was 19.4% compared to 5.4% for patients with a non threatened margin. It is important to realize that a short course of preoperative radiotherapy has limited ability to control positive CRM. An analysis of more than 17 500 pathologic specimens by Nagtegaal *et al*[32] revealed that the chance of local recurrence was higher for patients with a positive CRM after neoadjuvant treatment (both radiotherapy and radiochemotherapy) than those with a positive CRM following immediate surgery (Hazard ratio 6.3 *vs* 2.0, respectively). Similar results have been reported following postoperative treatment[38]. In the MRC CR-07 trial, patients with positive radial margins who were selected to receive postoperative chemoradiation had a 21% local recurrence rate[39]. Thus, in cases where the tumors are close (< 2 mm) or through the mesorectal margin on preoperative MRI, a more aggressive treatment regimen is required with neoadjuvant CRT or an upfront regimen of chemotherapy before chemoradiation prior to operation. In contrast, patients with a free margin > 2 mm from mesorectal fascia may undergo surgery [total mesorectal excision (TME)] alone, avoiding preoperative chemoradiation.

Interestingly, MRI-based therapy for CRM positive tumors was able to reduce the frequency of neoadjuvant therapy for rectal carcinoma by 35% without the risk of worsening the oncological results[40]. However, omitting preoperative chemoradiation for all CRM-negative tumors on MRI needs to be further investigated in prospective clinical trials before it is adopted as standard therapy.

N staging

The presence of involved lymph nodes is an indicator for the likelihood of systemic disease and local recurrence[41]. Therefore node-positive disease is generally an indication for preoperative chemoradiation. However, radiological evaluation of lymph node metastatic involvement remains a challenge.

Results of anatomic studies show that over half of the metastatic nodes from rectal cancer are within 3 cm of the primary tumor and are smaller than 5 mm in size[42]. With a standard TME, the perirectal nodes are removed with the primary tumor, but the internal iliac and obturator nodes are left in place. Moriya *et al*[43] reported that as many as 28% of lymph node-positive distal rectal cancers have involvement of lateral nodes and in 6% of cases, these were the only nodes involved. This means that in 6% of patients, the disease was incorrectly staged postoperatively as node-negative at TME.

For pre-operative lymph node imaging, MRI at present is only moderately accurate, although this could change with advances in new MR techniques. Currently, the reported accuracy rate of MRI for nodal staging ranges from 71% to 91%[42]. On MRI, lymph nodes typically have lower signal intensity than the perirectal fat but higher signal intensity than arteries and veins (Figure 4). In patients with mucinous carcinoma, metastatic lymph nodes are visualized as hyperintense nodules alone or as hyperintense areas within hypointense nodules. A node is considered enlarged if the major axis length is more than 5 mm (mesorectal), 7 mm (internal iliac), 10 mm (external iliac), or 9 mm (common iliac)[44]. However, the morphological features or signal intensity of the nodes on MRI may more accurately determine metastatic involvement rather than measurement of size. Brown *et al*[45] demonstrated that an irregular border or mixed signal intensity of lymph nodes on MRI improved the specificity of predicting nodal status from 68% (based on size alone) to 97%.

One of the more promising advances of MRI may be the use of new lymphographic agents that help assess tumor spread to lymph nodes. In a recent study, gadofosveset-enhanced MRI improved the specificity of nodal staging from 82% achieved with standard MRI to 97%[46]. Fusion of diffusion-weighted MR with T2-weighted images improves identification of pelvic lymph nodes compared with T2-weighted images alone. Using fusion

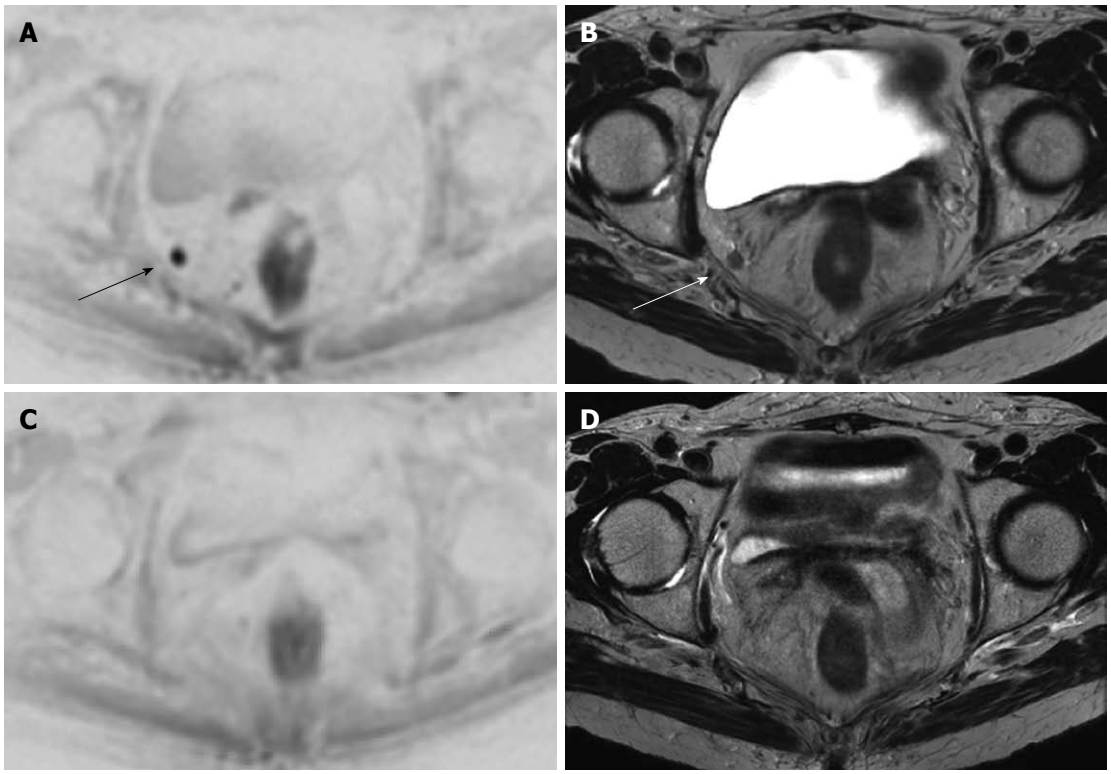

Figure 4 Same case as Figure 2. An enlarged right obturator lymph node is suspected in this patient with a lower third rectal cancer. Diffusion weighted imaging (DWI) (A) and axial T2w (B) images show the enlarged obturator lymph node nicely (arrows). DWI (C) and axial T2w (D) images following chemoradiotherapy show that the lymph node has disappeared

images, 29% additional nodes were detected compared with T2-weighted images alone[47]. The improved nodal identification may aid in treatment planning.

Extramural vascular invasion

Venous invasion is defined as the presence of tumor tissue within an endothelium lined space, either surrounded by a rim of smooth muscle or containing red blood cells. Talbot *et al*[48] showed that extramural venous invasion was present in 52% of rectal cancer specimens examined. Of these, the specimens showing invasion in thick-walled veins were significantly associated with distant metastases and death from tumor recurrence.

On MRI, using contiguous 3-mm slices, the presence of tumor signal intensity within a vascular structure is highly suggestive of extramural vascular invasion[49]. Typically, on T2-weighted images, the tumor signal intensity is intermediate (gray) while the veins are serpiginous or tortuous linear structures beyond the muscle coat[49]. Larger vessels are typically in a consistent anatomic position and appear black owing to signal void. As tumor invades along the vessel lumen, the vessel expands and ultimately the tumor may disrupt the vessel border, making the vessel border appear irregular or nodular[49]. Brown *et al*[50] found that MRI correctly identified 15 of the 26 rectal cancer patients that had extramural venous invasion documented histologically. In the remaining cases, the subtle microscopic extramural venous invasion could not be resolved on MRI.

Using four criteria (tumor margin, tumor location relative to vessels, vessel size, and vessel border), a 5-point grading system for the MRI-based preoperative assessment of extramural vascular invasion has been proposed[51]. Initial data suggests it that has been shown to correlate with clinical outcome. On univariable analysis, relapse-free survival at 3 years was 35% for patients with an extramural vascular invasion score on MRI of 3 to 4, compared with 74% for those with a score of 0 to 2 ($P < 0.001$). Interesting, these scores are similar to relapse-free survival rates noted in patients with histologically positive and negative extramural vascular invasion, respectively (34% *vs* 73.7%, $P < 0.001$). Therefore, the stratification of patients into prognostic groups according to MRI extramural vascular invasion score appears to be clinically accurate for assessing the need for preoperative treatment of patients at high risk.

Extramural spread

Depth of extramural tumor spread is defined as the measured distance of the tumor beyond the outer longitudinal muscle coat. MRI provides valuable information regarding extramural tumor spread[12], except when the tumors are circumferential or have little peri-rectal fat[36].

Pathologists have long recognized that with increasing depth of spread there is an increasing incidence of nodal involvement and extramural vascular invasion[52,53]. Moreover, patients with T3 rectal cancers extending less than 5 mm into the perirectal fat have a significantly better

5-year cancer-related survival rate than do patients with pT3 tumors extending more than 5 mm beyond the rectal wall (85% *vs* 54%, respectively)[52-54]. Based on these observations, neo-adjuvant therapy has not been routinely recommended for patients with pT3 carcinomas invading minimally (< 5 mm) into the perirectal tissue; instead patients should undergo immediate surgery.

However, the use of < 5 mm as the determinant for the therapeutic decision is controversial and should be used with caution when determining treatment options for patients. Merkel *et al*[54] reported that tumors with less than 5 mm extramural spread may still have a 38%-43% rate of nodal metastasis. Moreover, if very advanced tumors and those with positive margins are excluded this prognostic factor no longer correlates with survival[55].

RE-STAGING AFTER CRT

Because of the increasing use of preoperative CRT, MRI is frequently repeated after treatment to re-stage the tumor, assess the response, determine whether it is operable, and establish the extent of surgical resection. However, early studies have questioned the accuracy of MRI in the post-CRT setting with a T-stage correlation of only 47%-54% and an N stage correlation of 64%-68%[46,56-59]. In the study by Kulkarni *et al*[60], MRI performed 6 wk post CRT overestimated the CRM involvement in 56% of cases, while T stages were over-staged in 38% and N stages in 4%. Over-staging was due to lack of discrimination between residual tumor and post-treatment changes, both appearing as a diffuse hypointense signal. Post-treatment changes are due to marked fibrosis of the bowel wall or to peritumoral infiltration of inflammatory cells and proliferating vessels as confirmed by other investigators[46,57].

Recently, improved accuracy of MRI in the post-CRT setting was achieved by lengthening the interval after CRT. In the study by Johnston *et al*[61], the radiological T-stage determined on MRI obtained 10-11 wk after CRT was the same as the pathological T-stage on the resected specimen in 14 out of 17 cases (88%) as compared to only a 59% agreement between the MRI and subsequent post-resection histopathology when the MRI was performed 6 wk after treatment. In this study, the pre-operative MRI showed ongoing response to CRT up to 12 wk after CRT, which has important clinical implications regarding the most appropriate time to operate.

Change in the surgical strategy may occur after CRT, especially for patients who seem to exhibit a complete tumor response. For this subset of patients, transanal excision or non-operative treatment in selected circumstances maybe considered with good prognosis[62]. However, predicting the nodal status for these patients using imaging techniques becomes crucial, since the nodes are not removed at local excision. Importantly, the assessment of tumor spread to lymph nodes may be improved with the use of a novel nanoparticle contrast medium (ultra-small superparamagnetic iron oxide; USPIO)[63,64]. In a recent prospective multicenter study, MRI performed after CRT for rectal cancer using USPIO was able to improve the negative predictive value of the nodal status to 95%[65]. Unfortunately, this product is not currently commercially available.

SPECIAL CONSIDERATION

Adenocarcinoma of the lower rectum

The lower third of the rectum (less than 5 cm from the anal verge) lies below the level of the peritoneal reflection. The majority of published series have shown that tumors arising in this anatomic location have the worst outcome, with local recurrence rates as high as 30%. This is due, in part, to the fact that compared to the tumors of the upper rectum, the surgical dissection for these low rectal tumors is less straightforward and is associated with a higher rate of perforation through the correct oncologic plane compared to the tumors of the upper rectum. Anatomically, the mesorectum thins out towards the lower third of the rectum and disappears at the level of the internal sphincter. There is less space for the tumor to traverse before it reaches the surgical plane of resection. Consequently, the CRM is more often positive in the surgical specimen for tumors located in the lower rectum, than for those located in the middle and upper rectum[32].

To overcome this shortcoming, a new operation, the "cylindrical" abdominoperineal resection (APR), has been pioneered in Europe[66,67]. In this operation, instead of following the mesorectum all the way to the levator muscles, the surgeon stops when the coccyx is visualized. The remaining dissection is performed from the perineum and is facilitated by the prone position. In the standard APR the perineal operator enters the levators anteriorly to the coccyx and the amount of levator muscle and ischiorectal fat removed around the tumor is not standardized. Instead in the cylindrical APR once the levators and the coccyx are encountered the coccyx is excised and the levators are followed laterally to their origin from the lateral pelvic sidewalls where they are transected. In the case of anterior tumors, the posterior vaginal wall and part of the prostate are also removed *en bloc*[66]. One disadvantage of the technique is that it leaves a very large pelvic gap that can not be primarily closed and therefore a muscle flap reconstruction with the gracilis, the rectus abdominis or the gluteus maximus is often required[66]. Comparing 27 cylindrical to 99 conventional APRs, West *et al*[68] found a 70% increase in the amount of tissue removed around the tumor and no violation of the oncologic plane of dissection in the former group as well as a much lower rate of positive CRM 15% *vs* 40%, respectively. While many series advocate a wide perineal resection, and report low rates of local recurrence, these enhanced perineal resections have not become standard of care and prospective data are lacking[69]. Perineal wound infection, wound breakdown, and neurological dysfunctions are major problems for patients who receive radiation followed by abdominoperineal excision[69]. Primary closure with a flap overcomes some of these difficulties by bringing non-irradiated tissue into the perineal wound.

In a prospective study of 40 rectal tumors ≤ 5 cm from the dentate line from a single institution, MRI with intravenous contrast medium was universally successful in detecting invasion of the internal and external sphincters[70]. For low-lying rectal tumors that are restricted to the rectal wall or internal sphincter, spare the external sphincter and levator ani, and are not amenable to local excision as determined by preoperative MRI, there are several advantages to performing inter-sphincteric APR. While the standard APR removes the whole sphincter complex in this procedure the dissection is carried out in the inter-sphincteric plane, the external sphincter is left in place and the perineal defect is easily closed by approximating the external sphincter margins. This not only minimizes the problems with wound healing and postoperative pain but also reduces risk of damage to the erigentes nerves, hypogastric plexus, and the neurovascular bundles of Walsh (containing the cavernous nerves). Damage to these nerves causes both sexual and bladder dysfunction in men and women. Overall, this represents an anatomic and well-standardized dissection, which decreases the risk of rectal perforation and positive margins.

Among the sphincter-saving options, the inter-sphincteric TME, which removes only the upper half of the internal sphincter, has been recently found to be a valid option for selected tumors of the lower rectum[71]. The procedure is similar to a TME with a manual colo-anal anastomosis. In a TME with a manual colo-anal anstomosis the surgeon performs a mucosectomy above the dentate line leaving the internal sphincter intact. In the inter-sphincteric TME the surgeon cuts through the internal sphincter at the level of the dentate line, enters and dissects along the inter-sphinteric plane until establishing a connection with the abdominal operator. The proximal bowel is then manually anastomosed to the dentate line leaving the distal part of the internal sphincter intact. This allows one to achieve negative distal margins for tumors down to the ano-rectal junction while still providing good functional and oncologic results[71]. This procedure is indicated for T1-2 tumors that are well or moderately differentiated and for selected T3 tumors that have responded well to CRT.

For some tumors of the lower rectum, a trans-perineal approach overcomes the lack of exposure due to the angled pelvic anatomy and the rectum being surrounded by the levators[72]. In this approach the external sphincter and the perineal body is exposed through a transverse incision between the anus and the vagina or scrotum. This dissection allows the last 2-3 cm of rectum to be directly visualized.

These new procedures are not part of the standard surgical armamentarium and have to be planned in advance. MRI can offer the surgeon a road map to select the safest plane of dissection and plan the most appropriate procedure (Figure 5)[13].

Currently, the majority of tumors of the lower third of the rectum are irradiated preoperatively and MRI is not accurate for detecting residual microscopic sites of disease[57]. Thus, it is not advisable to make decisions about sphincter preservation based purely on MRI assessments of post-radiation tumor response. In this specific circumstance, EUS repeated after irradiation provided a 100% sensitivity but only a 53% positive predictive value for invasion of the sphincters[73].

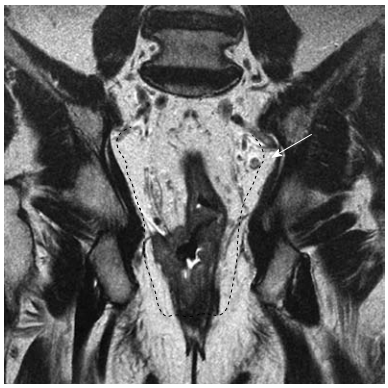

Figure 5 This case highlights the importance of the coronal plane in the assessment of the extension of the T4 lesion across the right levator complex into the right ischiorectal fossa, also shown (arrow) an enlarged and suspect lymph node. In this case, the surgeon may choose a modified APR resection (black dotted line).

Mucinous carcinomas

MRI in rectal carcinoma provides information on the mucinous status in addition to local tumor stage. The definition of mucinous carcinoma originates from histopathological examinations designating carcinomas with a mucin proportion of > 50% within the tumor volume[74]. Because of the high signal intensity in T2-weighted imaging, MRI can identify mucin pools in rectal carcinomas with a 97% accuracy and high inter-observer agreement[75]. Mucinous rectal tumors diagnosed at pre-therapeutic MRI have been associated with a noticeably worse response to chemoradiation as compared to that observed in non-mucinous carcinomas which allows an estimation of response before initiating neoadjuvant treatment[76,77].

NEW DEVELOPMENTS

There have been many advances in MRI techniques. The spatial resolution has improved, the speed of the examinations has been increased, DWI sequences have been used for body applications, and new contrast media have been developed. The newest 3 Tesla scanners provide excellent spatial resolution. High-resolution T2 sequences can be acquired in a shorter time[78] and isotropic (cubic) voxels can be acquired. In the near future, 3D T2 sequences with isotropic voxels will probably be available and the accurate positioning of imaging planes will no longer be an issue.

DWI is one of the most interesting developments of MR, allowing it to become an alternative to FDG-positron emission tomography (PET) in oncological imaging. DWI provides MR images with a signal intensity sensitized to the random motion of free water molecules[79,80]. In the

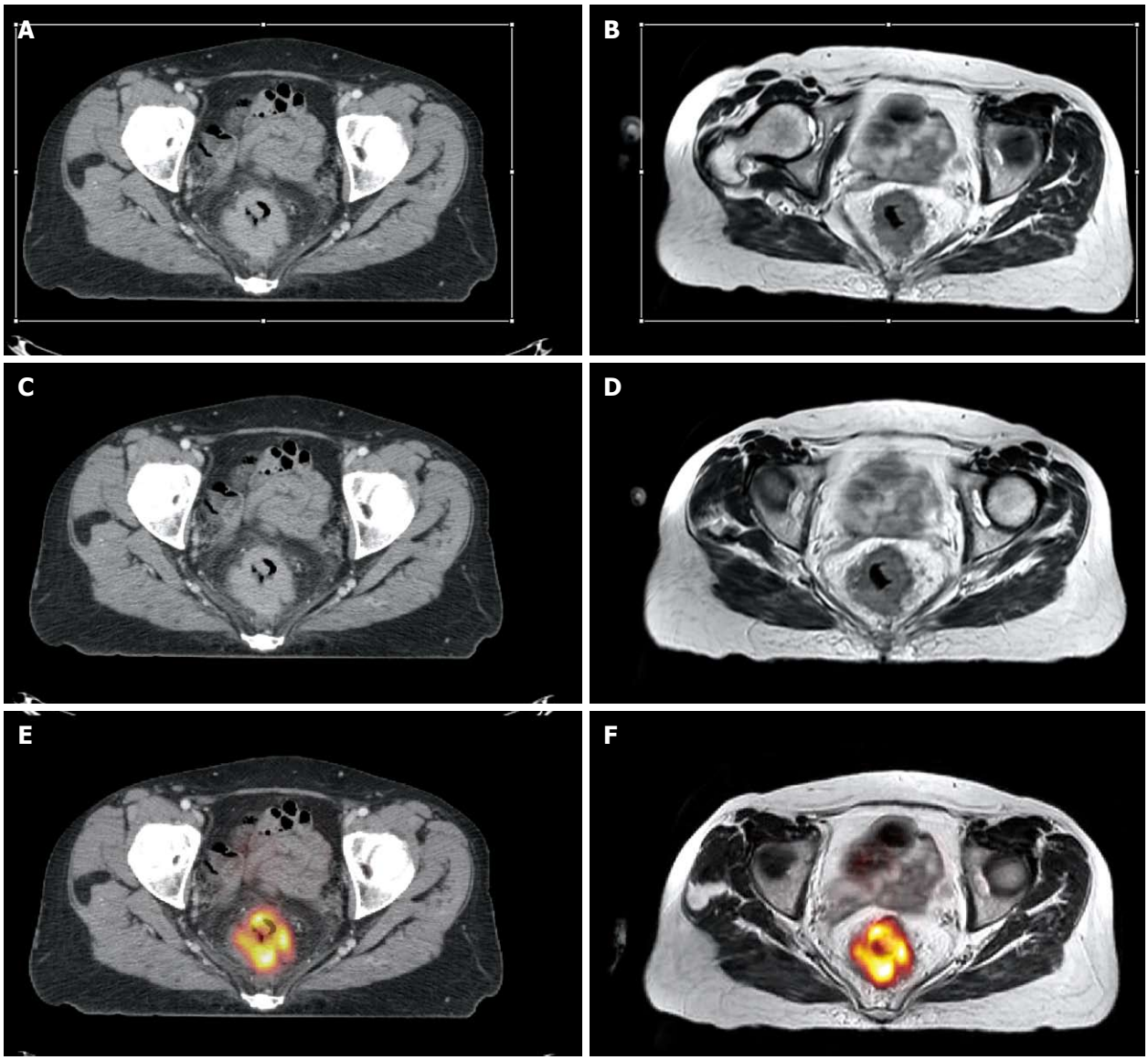

Figure 6 Multimodal image registration can be performed to improve staging and radiotherapy planning of rectal cancer. Axial contrast enhanced computed tomography (CT) at the portal phase (A) and rigid registration of the axial T2w magnetic resonance (MR) image (B). Rigid registration reduces the misalignment between the anatomical structures in the two modalities. A, B: Volume selection (rectangular white thin line) for non-rigid registration is performed; C, D: Non-rigid registration compensates for the more complex deformations due to the different acquisition setting; E, F: Following non rigid registration, MR can be fused with the positron emission tomography (PET) image (F) and the result is super-imposable on the PET-CT image (E).

rectum it is able to distinguish neoplastic from surrounding normal tissue (Figure 2). As such it may help in the detection of small tumors. However, the major challenge of MRI for rectal cancer is to reliably define the response to neoadjuvant therapy. Predicting a tumor's response to treatment can be of considerable clinical benefit. Interestingly, preliminary results indicate that DWI might be effective in predicting treatment outcomes and for detecting the early tumor response[81-83]. In quantitative DWI, the magnetic resonance signal arises from both intracellular and extracellular compartments, and the result is given in terms of the apparent diffusion coefficient (ADC). Changes in the tumor ADC have been shown to correlate with the development of intra-tumoral fibrosis after chemoradiation[83], histologically proven apoptotic cell death[84] and regression in tumor size after chemotherapy and chemoradiation[81]. Other authors have supported the use of ADC values in combination with other MR imaging criteria in improving the discrimination between malignant and benign lymph nodes even after chemoradiation[46,63,85] (Figure 4). The main limitation to DWI imaging today is the variability in ADC values that are obtained with different magnets and imaging protocols. Further studies will be necessary to prove the possible value of DWI on predicting therapy outcome.

There are also alternative imaging techniques. CT has so far had a limited role in the local staging of rectal cancer. Today, perfusion imaging represents one of the most interesting fields of CT development. Perfusion imaging of large volumes is possible with multi-detector CT scanners. This technique has shown promise in predicting the response to neoadjuvant treatment[86]. CT perfusion data

cannot currently be obtained with dynamic contrast-enhanced MR[87] and this represents a strong point in favor of CT.

PET and CT-PET scans are used mainly in the assessment of metastatic rectal cancer and local recurrence. Sequential determination of fluorodeoxyglucose uptake on PET/CT has proved useful in differentiating responsive from nonresponsive tumors during and at the end of neoadjuvant therapy[88]. However, radionuclide techniques have limitations, such as low spatial resolution and high cost. Large studies are needed to establish the most effective morphologic and functional imaging modalities for post-neoadjuvant therapy restaging of rectal cancer[86].

Over the last several years many strategies have been developed to overcome the limitations of radiotherapy planning using noncontrast-enhanced CT. Radiotherapy guided by MRI is possible using strategies that allow fusion and/or co-registration of MR images with those from other imaging techniques[88]. PET-CT, contrast enhanced CT, and non contrast enhanced CT and MR images can all be fused together to improve the assessment of rectal lesions and radiotherapy planning[89-91] (Figure 6). However, PET-guided radiotherapy has not yet provided a clear advantage. Better delineation of pelvic anatomy and pathology will become progressively more important as radiotherapy protocols are developed that include a boost on the gross tumor volume with documented improvement in patient outcome[92].

CONCLUSION

Rectal cancer is a global disease associated with poor outcomes if not properly staged and treated. The increased use of preoperative chemoradiation and refinement of surgical techniques have led to a greater proportion of patients being considered for curative resection. New surgical options exist for these patients in the form of sphincter saving resection or transanal excision in selected circumstances. For the vast majority of rectal carcinomas, MRI is currently the most accurate modality on which to base treatment decisions for patients with rectal cancer. Traditionally, the decision to apply preoperative treatment for rectal cancer patients has been based on the T- and N-stage. Lately, other MRI findings such as the radial distance of the tumor to the CRM and extramural vascular invasion score have been identified as important risk factors for local failure and survival. We strongly believe that every center that treats patients with rectal cancer should develop a multidisciplinary team featuring a description of the MRI findings and their implementation in the treatment strategy with the aim of increasing resectability, reducing the local recurrence and treatment morbidity, and improving the quality of life.

REFERENCES

1 **Jemal A**, Siegel R, Xu J, Ward E. Cancer statistics, 2010. *CA Cancer J Clin* 2010; **60**: 277-300

2 **Rich T**, Gunderson LL, Lew R, Galdibini JJ, Cohen AM, Donaldson G. Patterns of recurrence of rectal cancer after potentially curative surgery. *Cancer* 1983; **52**: 1317-1329

3 NCCN clinical practice guidelines in Oncology. accessed on October 13, 2010. Available from: URL: http://www.nccn.org/professionals/physician_gls/f_guidelines.asp

4 **Valentini V**, Aristei C, Glimelius B, Minsky BD, Beets-Tan R, Borras JM, Haustermans K, Maingon P, Overgaard J, Pahlman L, Quirke P, Schmoll HJ, Sebag-Montefiore D, Taylor I, Van Cutsem E, Van de Velde C, Cellini N, Latini P. Multidisciplinary Rectal Cancer Management: 2nd European Rectal Cancer Consensus Conference (EURECA-CC2). *Radiother Oncol* 2009; **92**: 148-163

5 **Kosaras B**, Kirschner DA. Radial component of CNS myelin: junctional subunit structure and supramolecular assembly. *J Neurocytol* 1990; **19**: 187-199

6 **Bosset JF**. Adjuvant treatment of rectal cancer: improving patient selection. *Gastrointest Cancer Res* 2008; **2**: 37-38

7 **Garcia-Aguilar J**, Pollack J, Lee SH, Hernandez de Anda E, Mellgren A, Wong WD, Finne CO, Rothenberger DA, Madoff RD. Accuracy of endorectal ultrasonography in preoperative staging of rectal tumors. *Dis Colon Rectum* 2002; **45**: 10-15

8 **Kauer WK**, Prantl L, Dittler HJ, Siewert JR. The value of endosonographic rectal carcinoma staging in routine diagnostics: a 10-year analysis. *Surg Endosc* 2004; **18**: 1075-1078

9 **Ju H**, Xu D, Li D, Chen G, Shao G. Comparison between endoluminal ultrasonography and spiral computerized tomography for the preoperative local staging of rectal carcinoma. *Biosci Trends* 2009; **3**: 73-76

10 **Gagliardi G**, Bayar S, Smith R, Salem RR. Preoperative staging of rectal cancer using magnetic resonance imaging with external phase-arrayed coils. *Arch Surg* 2002; **137**: 447-451

11 **Ginsberg GG**, Lewis JH, Gallagher JE, Fleischer DE, al-Kawas FH, Nguyen CC, Mundt DJ, Benjamin SB. Diazepam versus midazolam for colonoscopy: a prospective evaluation of predicted versus actual dosing requirements. *Gastrointest Endosc* 1992; **38**: 651-656

12 **Brown G**, Richards CJ, Newcombe RG, Dallimore NS, Radcliffe AG, Carey DP, Bourne MW, Williams GT. Rectal carcinoma: thin-section MR imaging for staging in 28 patients. *Radiology* 1999; **211**: 215-222

13 **Shihab OC**, Heald RJ, Rullier E, Brown G, Holm T, Quirke P, Moran BJ. Defining the surgical planes on MRI improves surgery for cancer of the low rectum. *Lancet Oncol* 2009; **10**: 1207-1211

14 **Brown G**, Daniels IR, Richardson C, Revell P, Peppercorn D, Bourne M. Techniques and trouble-shooting in high spatial resolution thin slice MRI for rectal cancer. *Br J Radiol* 2005; **78**: 245-251

15 **Soyer P**, Lagadec M, Sirol M, Dray X, Duchat F, Vignaud A, Fargeaudou Y, Placé V, Gault V, Hamzi L, Pocard M, Boudiaf M. Free-breathing diffusion-weighted single-shot echo-planar MR imaging using parallel imaging (GRAPPA 2) and high b value for the detection of primary rectal adenocarcinoma. *Cancer Imaging* 2010; **10**: 32-39

16 **Suzuki C**, Torkzad MR, Tanaka S, Palmer G, Lindholm J, Holm T, Blomqvist L. The importance of rectal cancer MRI protocols on interpretation accuracy. *World J Surg Oncol* 2008; **6**: 89

17 **Akasu T**, Iinuma G, Takawa M, Yamamoto S, Muramatsu Y, Moriyama N. Accuracy of high-resolution magnetic resonance imaging in preoperative staging of rectal cancer. *Ann Surg Oncol* 2009; **16**: 2787-2794

18 **Hoeffel C**, Marra MD, Azizi L, Tran Van K, Crema MD, Lewin M, Arrivé L, Tubiana JM. [External phased-array MR imaging preoperative assessment of rectal cancer]. *J Radiol* 2006; **87**: 1821-1830

19 **Mellgren A**, Sirivongs P, Rothenberger DA, Madoff RD, García-Aguilar J. Is local excision adequate therapy for early rectal cancer? *Dis Colon Rectum* 2000; **43**: 1064-1071; discus-

sion 1071-1074
20 **Bueno CG**, de Barros JJ, Terres JS, Pereira DS Júnior. [Mandibular osteoradionecrosis. Clinical study and presentation of two cases]. *Quintessencia* 1978; **5**: 55-73
21 Improved survival with preoperative radiotherapy in resectable rectal cancer. Swedish Rectal Cancer Trial. *N Engl J Med* 1997; **336**: 980-987
22 **Bailey HR**, Huval WV, Max E, Smith KW, Butts DR, Zamora LF. Local excision of carcinoma of the rectum for cure. *Surgery* 1992; **111**: 555-561
23 **Sauer R**, Becker H, Hohenberger W, Rödel C, Wittekind C, Fietkau R, Martus P, Tschmelitsch J, Hager E, Hess CF, Karstens JH, Liersch T, Schmidberger H, Raab R. Preoperative versus postoperative chemoradiotherapy for rectal cancer. *N Engl J Med* 2004; **351**: 1731-1740
24 **Bosset JF**, Collette L, Calais G, Mineur L, Maingon P, Radosevic-Jelic L, Daban A, Bardet E, Beny A, Ollier JC. Chemotherapy with preoperative radiotherapy in rectal cancer. *N Engl J Med* 2006; **355**: 1114-1123
25 **Gérard JP**, Conroy T, Bonnetain F, Bouché O, Chapet O, Closon-Dejardin MT, Untereiner M, Leduc B, Francois E, Maurel J, Seitz JF, Buecher B, Mackiewicz R, Ducreux M, Bedenne L. Preoperative radiotherapy with or without concurrent fluorouracil and leucovorin in T3-4 rectal cancers: results of FFCD 9203. *J Clin Oncol* 2006; **24**: 4620-4625
26 **Beets-Tan RG**, Beets GL, Vliegen RF, Kessels AG, Van Boven H, De Bruine A, von Meyenfeldt MF, Baeten CG, van Engelshoven JM. Accuracy of magnetic resonance imaging in prediction of tumour-free resection margin in rectal cancer surgery. *Lancet* 2001; **357**: 497-504
27 **Brown G**, Radcliffe AG, Newcombe RG, Dallimore NS, Bourne MW, Williams GT. Preoperative assessment of prognostic factors in rectal cancer using high-resolution magnetic resonance imaging. *Br J Surg* 2003; **90**: 355-364
28 **Videhult P**, Smedh K, Lundin P, Kraaz W. Magnetic resonance imaging for preoperative staging of rectal cancer in clinical practice: high accuracy in predicting circumferential margin with clinical benefit. *Colorectal Dis* 2007; **9**: 412-419
29 **Sebag-Montefiore D**. Treatment of T4 tumours: the role of radiotherapy. *Colorectal Dis* 2003; **5**: 432-435
30 **Bipat S**, Glas AS, Slors FJ, Zwinderman AH, Bossuyt PM, Stoker J. Rectal cancer: local staging and assessment of lymph node involvement with endoluminal US, CT, and MR imaging--a meta-analysis. *Radiology* 2004; **232**: 773-783
31 **Nagtegaal ID**, Gosens MJ, Marijnen CA, Rutten HJ, van de Velde CJ, van Krieken JH. Combinations of tumor and treatment parameters are more discriminative for prognosis than the present TNM system in rectal cancer. *J Clin Oncol* 2007; **25**: 1647-1650
32 **Nagtegaal ID**, Quirke P. What is the role for the circumferential margin in the modern treatment of rectal cancer? *J Clin Oncol* 2008; **26**: 303-312
33 **Mulla M**, Deb R, Singh R. MRI in T staging of rectal cancer: How effective is it? *Indian J Radiol Imaging* 2010; **20**: 118-121
34 **Wieder HA**, Rosenberg R, Lordick F, Geinitz H, Beer A, Becker K, Woertler K, Dobritz M, Siewert JR, Rummeny EJ, Stollfuss JC. Rectal cancer: MR imaging before neoadjuvant chemotherapy and radiation therapy for prediction of tumor-free circumferential resection margins and long-term survival. *Radiology* 2007; **243**: 744-751
35 **Nagtegaal ID**, Marijnen CA, Kranenbarg EK, van de Velde CJ, van Krieken JH. Circumferential margin involvement is still an important predictor of local recurrence in rectal carcinoma: not one millimeter but two millimeters is the limit. *Am J Surg Pathol* 2002; **26**: 350-357
36 **Kim YW**, Cha SW, Pyo J, Kim NK, Min BS, Kim MJ, Kim H. Factors related to preoperative assessment of the circumferential resection margin and the extent of mesorectal invasion by magnetic resonance imaging in rectal cancer: a prospective comparison study. *World J Surg* 2009; **33**: 1952-1960
37 **Frasson M**, Garcia-Granero E, Roda D, Flor-Lorente B, Roselló S, Esclapez P, Faus C, Navarro S, Campos S, Cervantes A. Preoperative chemoradiation may not always be needed for patients with T3 and T2N+ rectal cancer. *Cancer* 2011; Epub ahead of print
38 **Baik SH**, Kim NK, Lee YC, Kim H, Lee KY, Sohn SK, Cho CH. Prognostic significance of circumferential resection margin following total mesorectal excision and adjuvant chemoradiotherapy in patients with rectal cancer. *Ann Surg Oncol* 2007; **14**: 462-469
39 **Sebag-Montefiore D**, Stephens RJ, Steele R, Monson J, Grieve R, Khanna S, Quirke P, Couture J, de Metz C, Myint AS, Bessell E, Griffiths G, Thompson LC, Parmar M. Preoperative radiotherapy versus selective postoperative chemoradiotherapy in patients with rectal cancer (MRC CR07 and NCIC-CTG C016): a multicentre, randomised trial. *Lancet* 2009; **373**: 811-820
40 **Strassburg J**, Junginger T, Trinh T, Püttcher O, Oberholzer K, Heald RJ, Hermanek P. Magnetic resonance imaging (MRI)-based indication for neoadjuvant treatment of rectal carcinoma and the surrogate endpoint CRM status. *Int J Colorectal Dis* 2008; **23**: 1099-1107
41 **Kapiteijn E**, Marijnen CA, Nagtegaal ID, Putter H, Steup WH, Wiggers T, Rutten HJ, Pahlman L, Glimelius B, van Krieken JH, Leer JW, van de Velde CJ. Preoperative radiotherapy combined with total mesorectal excision for resectable rectal cancer. *N Engl J Med* 2001; **345**: 638-646
42 **Beets-Tan RG**, Beets GL. Rectal cancer: review with emphasis on MR imaging. *Radiology* 2004; **232**: 335-346
43 **Moriya Y**, Sugihara K, Akasu T, Fujita S. Importance of extended lymphadenectomy with lateral node dissection for advanced lower rectal cancer. *World J Surg* 1997; **21**: 728-732
44 **Grubnic S**, Vinnicombe SJ, Norman AR, Husband JE. MR evaluation of normal retroperitoneal and pelvic lymph nodes. *Clin Radiol* 2002; **57**: 193-200; discussion 201-204
45 **Brown G**, Richards CJ, Bourne MW, Newcombe RG, Radcliffe AG, Dallimore NS, Williams GT. Morphologic predictors of lymph node status in rectal cancer with use of high-spatial-resolution MR imaging with histopathologic comparison. *Radiology* 2003; **227**: 371-377
46 **Lambregts DM**, Beets GL, Maas M, Kessels AG, Bakers FC, Cappendijk VC, Engelen SM, Lahaye MJ, de Bruïne AP, Lammering G, Leiner T, Verwoerd JL, Wildberger JE, Beets-Tan RG. Accuracy of gadofosveset-enhanced MRI for nodal staging and restaging in rectal cancer. *Ann Surg* 2011; **253**: 539-545
47 **Mir N**, Sohaib SA, Collins D, Koh DM. Fusion of high b-value diffusion-weighted and T2-weighted MR images improves identification of lymph nodes in the pelvis. *J Med Imaging Radiat Oncol* 2010; **54**: 358-364
48 **Talbot IC**, Ritchie S, Leighton MH, Hughes AO, Bussey HJ, Morson BC. The clinical significance of invasion of veins by rectal cancer. *Br J Surg* 1980; **67**: 439-442
49 **Smith NJ**, Shihab O, Arnaout A, Swift RI, Brown G. MRI for detection of extramural vascular invasion in rectal cancer. *AJR Am J Roentgenol* 2008; **191**: 1517-1522
50 **Brown G**, Daniels IR. Preoperative staging of rectal cancer: the MERCURY research project. *Recent Results Cancer Res* 2005; **165**: 58-74
51 **Smith NJ**, Barbachano Y, Norman AR, Swift RI, Abulafi AM, Brown G. Prognostic significance of magnetic resonance imaging-detected extramural vascular invasion in rectal cancer. *Br J Surg* 2008; **95**: 229-236
52 **Dukes CE**, Bussey HJ. The spread of rectal cancer and its effect on prognosis. *Br J Cancer* 1958; **12**: 309-320
53 **Cawthorn SJ**, Parums DV, Gibbs NM, A'Hern RP, Caffarey SM, Broughton CI, Marks CG. Extent of mesorectal spread and involvement of lateral resection margin as prognostic factors after surgery for rectal cancer. *Lancet* 1990; **335**: 1055-1059
54 **Merkel S**, Mansmann U, Papadopoulos T, Wittekind C, Hohenberger W, Hermanek P. The prognostic inhomogeneity

of colorectal carcinomas Stage III: a proposal for subdivision of Stage III. *Cancer* 2001; **92**: 2754-2759
55 **Picon AI**, Moore HG, Sternberg SS, Minsky BD, Paty PB, Blumberg D, Quan SH, Wong WD, Cohen AM, Guillem JG. Prognostic significance of depth of gross or microscopic perirectal fat invasion in T3 N0 M0 rectal cancers following sharp mesorectal excision and no adjuvant therapy. *Int J Colorectal Dis* 2003; **18**: 487-492
56 **Kim DJ**, Kim JH, Lim JS, Yu JS, Chung JJ, Kim MJ, Kim KW. Restaging of Rectal Cancer with MR Imaging after Concurrent Chemotherapy and Radiation Therapy. *Radiographics* 2010; **30**: 503-516
57 **Kuo LJ**, Chern MC, Tsou MH, Liu MC, Jian JJ, Chen CM, Chung YL, Fang WT. Interpretation of magnetic resonance imaging for locally advanced rectal carcinoma after preoperative chemoradiation therapy. *Dis Colon Rectum* 2005; **48**: 23-28
58 **Allen SD**, Padhani AR, Dzik-Jurasz AS, Glynne-Jones R. Rectal carcinoma: MRI with histologic correlation before and after chemoradiation therapy. *AJR Am J Roentgenol* 2007; **188**: 442-451
59 **Vliegen RF**, Beets GL, Lammering G, Dresen RC, Rutten HJ, Kessels AG, Oei TK, de Bruïne AP, van Engelshoven JM, Beets-Tan RG. Mesorectal fascia invasion after neoadjuvant chemotherapy and radiation therapy for locally advanced rectal cancer: accuracy of MR imaging for prediction. *Radiology* 2008; **246**: 454-462
60 **Kulkarni T**, Gollins S, Maw A, Hobson P, Byrne R, Widdowson D. Magnetic resonance imaging in rectal cancer downstaged using neoadjuvant chemoradiation: accuracy of prediction of tumour stage and circumferential resection margin status. *Colorectal Dis* 2008; **10**: 479-489
61 **Johnston DF**, Lawrence KM, Sizer BF, Arulampalam TH, Motson RW, Dove E, Lacey N. Locally advanced rectal cancer: histopathological correlation and predictive accuracy of serial MRI after neoadjuvant chemotherapy. *Br J Radiol* 2009; **82**: 332-336
62 **Borschitz T**, Wachtlin D, Möhler M, Schmidberger H, Junginger T. Neoadjuvant chemoradiation and local excision for T2-3 rectal cancer. *Ann Surg Oncol* 2008; **15**: 712-720
63 **Lahaye MJ**, Beets GL, Engelen SM, Kessels AG, de Bruïne AP, Kwee HW, van Engelshoven JM, van de Velde CJ, Beets-Tan RG. Locally advanced rectal cancer: MR imaging for restaging after neoadjuvant radiation therapy with concomitant chemotherapy. Part II. What are the criteria to predict involved lymph nodes? *Radiology* 2009; **252**: 81-91
64 **Engelen SM**, Beets-Tan RG, Lahaye MJ, Kessels AG, Beets GL. Location of involved mesorectal and extramesorectal lymph nodes in patients with primary rectal cancer: preoperative assessment with MR imaging. *Eur J Surg Oncol* 2008; **34**: 776-781
65 **Engelen SM**, Beets-Tan RG, Lahaye MJ, Lammering G, Jansen RL, van Dam RM, Konsten J, Leijtens JW, van de Velde CJ, Beets GL. MRI after chemoradiotherapy of rectal cancer: a useful tool to select patients for local excision. *Dis Colon Rectum* 2010; **53**: 979-986
66 **Marr R**, Birbeck K, Garvican J, Macklin CP, Tiffin NJ, Parsons WJ, Dixon MF, Mapstone NP, Sebag-Montefiore D, Scott N, Johnston D, Sagar P, Finan P, Quirke P. The modern abdominoperineal excision: the next challenge after total mesorectal excision. *Ann Surg* 2005; **242**: 74-82
67 **Holm T**, Ljung A, Häggmark T, Jurell G, Lagergren J. Extended abdominoperineal resection with gluteus maximus flap reconstruction of the pelvic floor for rectal cancer. *Br J Surg* 2007; **94**: 232-238
68 **West NP**, Finan PJ, Anderin C, Lindholm J, Holm T, Quirke P. Evidence of the oncologic superiority of cylindrical abdominoperineal excision for low rectal cancer. *J Clin Oncol* 2008; **26**: 3517-3522
69 **Guillem JG**, Minsky BD. Extended perineal resection of distal rectal cancers: surgical advance, increased utilization of neoadjuvant therapies, proper patient selection or all of the above? *J Clin Oncol* 2008; **26**: 3481-3482
70 **Holzer B**, Urban M, Hölbling N, Feil W, Novi G, Hruby W, Rosen HR, Schiessel R. Magnetic resonance imaging predicts sphincter invasion of low rectal cancer and influences selection of operation. *Surgery* 2003; **133**: 656-661
71 **Rullier E**, Laurent C, Bretagnol F, Rullier A, Vendrely V, Zerbib F. Sphincter-saving resection for all rectal carcinomas: the end of the 2-cm distal rule. *Ann Surg* 2005; **241**: 465-469
72 **Williams NS**, Murphy J, Knowles CH. Anterior Perineal PlanE for Ultra-low Anterior Resection of the Rectum (the APPEAR technique): a prospective clinical trial of a new procedure. *Ann Surg* 2008; **247**: 750-758
73 **Assenat E**, Thézenas S, Samalin E, Bibeau F, Portales F, Azria D, Quenet F, Rouanet P, Saint Aubert B, Senesse P. The value of endoscopic rectal ultrasound in predicting the lateral clearance and outcome in patients with lower-third rectal adenocarcinoma. *Endoscopy* 2007; **39**: 309-313
74 **Hamilton SR**, Aaltonen LA. World Health Organization Classification of Tumours. Pathology and Genetics of Tumours of the Digestive System. Lyon: IARC Press, 2000: 105-120
75 **Kim MJ**, Park JS, Park SI, Kim NK, Kim JH, Moon HJ, Park YN, Kim WH. Accuracy in differentiation of mucinous and nonmucinous rectal carcinoma on MR imaging. *J Comput Assist Tomogr* 2003; **27**: 48-55
76 **Grillo-Ruggieri F**, Mantello G, Berardi R, Cardinali M, Fenu F, Iovini G, Montisci M, Fabbietti L, Marmorale C, Guerrieri M, Saba V, Bearzi I, Mattioli R, Bonsignori M, Cascinu S. Mucinous rectal adenocarcinoma can be associated to tumor downstaging after preoperative chemoradiotherapy. *Dis Colon Rectum* 2007; **50**: 1594-1603
77 **Oberholzer K**, Menig M, Kreft A, Schneider A, Junginger T, Heintz A, Kreitner KF, Hötker AM, Hansen T, Düber C, Schmidberger H. Rectal Cancer: Mucinous Carcinoma on Magnetic Resonance Imaging Indicates Poor Response to Neoadjuvant Chemoradiation. *Int J Radiat Oncol Biol Phys* 2011; Epub ahead of print
78 **Kim H**, Lim JS, Choi JY, Park J, Chung YE, Kim MJ, Choi E, Kim NK, Kim KW. Rectal cancer: comparison of accuracy of local-regional staging with two- and three-dimensional preoperative 3-T MR imaging. *Radiology* 2010; **254**: 485-492
79 **Torricelli P**, Pecchi A, Luppi G, Romagnoli R. Gadolinium-enhanced MRI with dynamic evaluation in diagnosing the local recurrence of rectal cancer. *Abdom Imaging* 2003; **28**: 19-27
80 **Kremser C**, Judmaier W, Hein P, Griebel J, Lukas P, de Vries A. Preliminary results on the influence of chemoradiation on apparent diffusion coefficients of primary rectal carcinoma measured by magnetic resonance imaging. *Strahlenther Onkol* 2003; **179**: 641-649
81 **Dzik-Jurasz A**, Domenig C, George M, Wolber J, Padhani A, Brown G, Doran S. Diffusion MRI for prediction of response of rectal cancer to chemoradiation. *Lancet* 2002; **360**: 307-308
82 **Barbaro B**, Vitale R, Leccisotti L, Vecchio FM, Santoro L, Valentini V, Coco C, Pacelli F, Crucitti A, Persiani R, Bonomo L. Restaging locally advanced rectal cancer with MR imaging after chemoradiation therapy. *Radiographics* 2010; **30**: 699-716
83 **Hein PA**, Kremser C, Judmaier W, Griebel J, Pfeiffer KP, Kreczy A, Hug EB, Lukas P, DeVries AF. Diffusion-weighted magnetic resonance imaging for monitoring diffusion changes in rectal carcinoma during combined, preoperative chemoradiation: preliminary results of a prospective study. *Eur J Radiol* 2003; **45**: 214-222
84 **Chinnaiyan AM**, Prasad U, Shankar S, Hamstra DA, Shanaiah M, Chenevert TL, Ross BD, Rehemtulla A. Combined effect of tumor necrosis factor-related apoptosis-inducing ligand and ionizing radiation in breast cancer therapy. *Proc Natl Acad Sci USA* 2000; **97**: 1754-1759
85 **Ono K**, Ochiai R, Yoshida T, Kitagawa M, Omagari J, Kobayashi H, Yamashita Y. Comparison of diffusion-weighted MRI and 2-[fluorine-18]-fluoro-2-deoxy-D-glucose positron

emission tomography (FDG-PET) for detecting primary colorectal cancer and regional lymph node metastases. *J Magn Reson Imaging* 2009; **29**: 336-340
86 **Bellomi M**, Travaini LL. Imaging as a surveillance tool in rectal cancer. *Expert Rev Med Devices* 2010; **7**: 99-112
87 **Kierkels RG**, Backes WH, Janssen MH, Buijsen J, Beets-Tan RG, Lambin P, Lammering G, Oellers MC, Aerts HJ. Comparison between perfusion computed tomography and dynamic contrast-enhanced magnetic resonance imaging in rectal cancer. *Int J Radiat Oncol Biol Phys* 2010; **77**: 400-408
88 **Schiepers C**, Haustermans K, Geboes K, Filez L, Bormans G, Penninckx F. The effect of preoperative radiation therapy on glucose utilization and cell kinetics in patients with primary rectal carcinoma. *Cancer* 1999; **85**: 803-811
89 **Anderson H**, Singh N, Miles K. Tumour response evaluation with fluorodeoxyglucose positron emission tomography: research technique or clinical tool? *Cancer Imaging* 2010; **10** Spec no A: S68-S72
90 **Bassi MC**, Turri L, Sacchetti G, Loi G, Cannillo B, La Mattina P, Brambilla M, Inglese E, Krengli M. FDG-PET/CT imaging for staging and target volume delineation in preoperative conformal radiotherapy of rectal cancer. *Int J Radiat Oncol Biol Phys* 2008; **70**: 1423-1426
91 **Garlaschi A**, Bacigalupo LE, Biscaldi E, Chiusano G, Basso C, Rollandi GA. Multi-modal non-rigid image registration of MR and PET-CT for staging and therapy of rectal adenocarcinoma. Presented as a Scientific Poster at the Radiological Society of North America November 29 - December 4, 2009; Chicago, IL. Abstract Book, 921
92 **Roels S**, Slagmolen P, Nuyts J, Lee JA, Loeckx D, Maes F, Vandecaveye V, Stroobants S, Ectors N, Penninckx F, Haustermans K. Biological image-guided radiotherapy in rectal cancer: challenges and pitfalls. *Int J Radiat Oncol Biol Phys* 2009; **75**: 782-790

S- Editor Cheng JX **L- Editor** O'Neill M **E- Editor** Zheng XM

World Journal of Radiology

Online Submissions: http://www.wjgnet.com/1949-8470office
wjr@wjgnet.com
doi:10.4329/wjr.v3.i4.105

World J Radiol 2011 April 28; 3(4): 105-113
ISSN 1949-8470 (online)

BRIEF ARTICLE

Applications of multi-nuclear magnetic resonance spectroscopy at 7T

Mary C Stephenson, Frances Gunner, Antonio Napolitano, Paul L Greenhaff, Ian A MacDonald, Nadeem Saeed, William Vennart, Susan T Francis, Peter G Morris

Mary C Stephenson, Susan T Francis, Peter G Morris, The Sir Peter Mansfield Magnetic Resonance Centre, School of Physics and Astronomy, University of Nottingham, Nottingham NG7 2RD, United Kingdom
Frances Gunner, Paul L Greenhaff, Ian A MacDonald, School of Biomedical Sciences, University of Nottingham Medical School, Nottingham NG7 2UH, United Kingdom
Antonio Napolitano, Academic Radiology, University of Nottingham, Nottingham NG7 2UH, United Kingdom
Nadeem Saeed, William Vennart, Molecular Medicine, Pfizer, Sandwich, Kent CT13 9NJ, United Kingdom
Author contributions: Stephenson MC, Gunner F, Morris PG, Francis ST, Saeed N, MacDonald IA, Greenhaff PL and Vennart W designed the research; Stephenson MC and Gunner F performed the research; Stephenson MC analyzed the data; Napolitano A contributed new analytic tools; Stephenson MC and Morris PG wrote the paper.
Supported by The Haldane-Spearman Consortium for PhD funding for Dr. Gunner F, Swecarb AB for provision of the carbohydrate drink, and Pfizer for funding the 1H Repeatability work. Dr.Stephenson M was supported by the University of Nottingham's Mansfield Fellowship scheme. 7T work was supported by grant G9900259 from the Medical Research Council; Pfizer and grant G0901321 from the Medical Research Council; The 7 T MR Scanner in Nottingham, was funded by a Joint Infrastructure Fund Grant from the Wellcome Trust UK
Correspondence to: Mary C Stephenson, PhD, The Sir Peter Mansfield Magnetic Resonance Centre, School of Physics and Astronomy, University of Nottingham, Nottingham NG7 2RD, United Kingdom. mary.stephenson@nottingham.ac.uk
Telephone: +44-115-9566881 Fax: +44-115-9515166
Received: October 22, 2010 Revised: April 2, 2011
Accepted: April 9, 2011
Published online: April 28, 2011

Abstract

AIM: To discuss the advantages of ultra-high field (7T) for ^{1}H and ^{13}C magnetic resonance spectroscopy (MRS) studies of metabolism.

METHODS: Measurements of brain metabolites were made at both 3 and 7T using ^{1}H MRS. Measurements of glycogen and lipids in muscle were measured using ^{13}C and ^{1}H MRS respectively.

RESULTS: In the brain, increased signal-to-noise ratio (SNR) and dispersion allows spectral separation of the amino-acids glutamate, glutamine and γ-aminobutyric acid (GABA), without the need for sophisticated editing sequences. Improved quantification of these metabolites is demonstrated at 7T relative to 3T. SNR was 36% higher, and measurement repeatability (% coefficients of variation) was 4%, 10% and 10% at 7T, *vs* 8%, 29% and 21% at 3T for glutamate, glutamine and GABA respectively. Measurements at 7T were used to compare metabolite levels in the anterior cingulate cortex (ACC) and insula. Creatine and glutamate levels were found to be significantly higher in the insula compared to the ACC ($P < 0.05$). In muscle, the increased SNR and spectral resolution at 7T enables interleaved studies of glycogen (^{13}C) and intra-myocellular lipid (IMCL) and extra-myocellular lipid (EMCL) (^{1}H) following exercise and re-feeding. Glycogen levels were significantly decreased following exercise (-28% at 50% VO_2 max; -58% at 75% VO_2 max). Interestingly, levels of glycogen in the hamstrings followed those in the quadriceps, despite reduce exercise loading. No changes in IMCL and EMCL were found in the study.

CONCLUSION: The demonstrated improvements in brain and muscle MRS measurements at 7T will increase the potential for use in investigating human metabolism and changes due to pathologies.

Key words: Magnetic resonance spectroscopy; ^{13}C; ^{1}H; 7 Tesla; Glutamate; Glutamine; γ-aminobutyric acid

Peer reviewer: Kubilay Aydin, MD, Professor, Istanbul University, Istanbul Faculty of Medicine, Department of Radiology, Neuroradiology Division Capa, Istanbul, Turkey

Stephenson MC, Gunner F, Napolitano A, Greenhaff PL, MacDonald IA, Saeed N, Vennart W, Francis ST, Morris PG. Applications of multi-nuclear magnetic resonance spectroscopy at 7T. *World J Radiol* 2011; 3(4): 105-113 Available from: URL: http://www.wjgnet.com/1949-8470/full/v3/i4/105.htm DOI: http://dx.doi.org/10.4329/wjr.v3.i4.105

INTRODUCTION

Magnetic resonance spectroscopy (MRS) is a versatile technique which can be used for measurement of metabolite levels, studies of bioenergetics, and measurement of chemical reaction rates without the need for invasive procedures such as biopsy. Whilst magnetic resonance imaging has quickly become one of the most widely used clinical tools, progress in MRS has been much slower. MRS has the potential to become a vital tool for aiding the understanding of changes due to pathology in specific regions of the body, as well as for clinical diagnosis and treatment monitoring. Improvements in hardware, which have allowed higher field spectrometers to be developed, provide increased sensitivity and spectral resolution. Many studies have demonstrated these improvements with increasing field[1-10], however the extent has been variable, with increases in signal-to-noise ratio (SNR) of 20% to 46% reported between 1.5 and 3T[1,4-6] and 80% from 1.5T to 4T[2]. This paper compares SNR and measurement reproducibility for ^{1}H and ^{13}C MRS measurements in the human brain and skeletal muscle, and discusses applications of ^{1}H and ^{13}C MRS for studying human metabolism, utilizing the increased sensitivity and spectral resolution at 7T.

Improved ^{1}H MRS reproducibility of glutamate, glutamine and γ-aminobutyric acid measurements in the human brain at 7T

Levels of metabolites, measurable in the human brain with ^{1}H MRS, are important in understanding changes involved in neurological[11,12] and psychiatric diseases[13-17], and potential therapies[18-19]. Studies at low field strength (≤ 1.5T) tend to concentrate on measurement of N-acetyl aspartate (NAA), Creatine (Cr) and Choline (Cho). Measurement of glutamate (Glu), glutamine (Gln) and γ-aminobutyric acid (GABA) is difficult at low field strength due to their overlapping resonances with each other, and with those of other molecules such as myo-Inositol (mI) and NAA. Thus, at low field, the concentrations of Glu and Gln are often combined as Glx = Glu + Gln. This could mask relative changes in Glu and Gln, such as might be expected if the rate of the glutamate/glutamine cycle is altered. Many different methods have been suggested for individual measurement of Glu, Gln and GABA, including constant time point resolved spectroscopy[20], chemical shift selective filters[21], 2D J-resolved spectroscopy[22] and MEGA-editing sequences[23,24]. However, these techniques are often time consuming, or may result in the loss of other metabolite signals which may be of interest. At higher fields, increasing spectral resolution enables metabolites to be accurately quantified without the need for sophisticated editing, and various sequences, optimized to give maximum separation, have been proposed[25-29]. Little work has been done to compare optimized sequences, or to establish levels of reproducibility based on different sequences. The aim of this study was to compare the ^{1}H MRS reproducibility of measurements of Glu, Gln and GABA at 3 and 7T using both a short TE STEAM sequence (TE/TM = 16/17 ms for optimum SNR) and a long TE STEAM sequence (TE/TM = 74/68 ms, shown to give pseudo-singlets for these metabolites[29]). Levels of variation in neurotransmitter concentrations over a week were then assessed in the anterior cingulate cortex (ACC) and insula (Ins) using the sequence which provided the most reproducible results.

Ultra-high field studies of skeletal muscle energy stores

Glycogen, intra-myocellular lipid (IMCL) and extra-myocellular lipid (EMCL) are the major sources of energy in human skeletal muscle[30] and can be measured *in vivo* using ^{13}C[31-33] and ^{1}H MRS respectively[34-40]. Studies of energy stores in skeletal muscle (or hepatic tissue) can provide much information on utilization during exercise or during postprandial replenishment[41-45], and are important for understanding diseases where glucose or lipid metabolism is thought to be perturbed. Due to the low natural abundance and low relative sensitivity of the ^{13}C nucleus, natural abundance ^{13}C MRS acquisition times tend to be long. Increased signal, available at 7T, allows for shorter acquisition times, which can be used to achieve better temporal resolution for dynamic studies. Shorter acquisition times for dynamic studies allow ^{13}C MRS measurements of glycogen to be made sequentially with ^{1}H MRS measurements of lipid stores thus allowing both of the major sources of energy to be observed on a reasonable timescale. The separation of IMCL and EMCL peaks in ^{1}H MR spectra is determined by the orientation of the muscle fibres in the magnetic field[40]. For well aligned fibres, orientated with the static magnetic field, the resonances from EMCL shift approximately 0.2 ppm from their respective IMCL resonances. Thus, at higher field, increased spectral resolution should provide more accurate quantitation as well as enabling separation of peaks in muscles with reduced alignment, for example the quadriceps and hamstrings in the human thigh.

Previous studies of energy stores have shown that muscle glycogen depletion during exercise is dependent on muscle fibre type[46] as well as exercise intensity[47] and duration[48]. Much less is known about the role of IMCL in muscle substrate selection and maintaining performance during exercise, although it is suggested that at higher exercise intensities IMCL contributes little to meeting energy demand, whereas at lower intensities IMCL may be oxidised to provide energy[49]. Here, a study was performed to assess the feasibility of sequential monitoring muscle glycogen and IMCL levels, in thigh muscles, prior to and following exercise, by utilizing the higher SNR and spectral resolution available at 7T.

MATERIALS AND METHODS

Ethical permission was obtained from the University of

Nottingham Medical School Ethics Committee and all subjects provided informed written consent before participation in the study. All measurements were performed on the Philips Achieva 3T and 7T systems at the Sir Peter Mansfield Magnetic Resonance Centre, Nottingham.

^{1}H reproducibility study

3T scans were acquired using an 8-channel SENSE head coil with transmission on the Q-Body coil. 7T scans were acquired on a 16-channel SENSE head, with transmission on a head volume coil.

Sequence reproducibility: Twelve healthy male subjects (age = 28 ± 11 years) attended two scan visits, 8 ± 2 d apart. On each visit subjects were scanned for 1h in each scanner, the protocol consisted of 3 survey images (to allow voxel positioning within the ACC) and 3 ^{1}H MRS acquisitions. Subjects were asked to reposition their head between repeats. For each spectral acquisition a 1 mm isotropic anatomical T_1 weighted Turbo-field Echo (TFE) image was acquired with TE/TR = 3.8/8.3 ms. This image was used to estimate the tissue percentage within the voxel to allow correction of metabolite concentrations since metabolites (with the exception of Gln and lactate) are present in much lower concentrations in the cerebrospinal fluid (CSF) compartment (levels of Gln are given without correction).

3T spectra were acquired with a bandwidth (BW) = 3000 Hz, and the number of points (No. samples) = 2048. 7T spectra were acquired with BW = 4000 Hz, No. samples = 2048. At both 3T and 7T the "short TE" STimulated Echo Acquisition Mode (STEAM) sequence was acquired with TE/TM/TR = 16/17/2000 ms, and the "long TE" sequence with TE/TM/TR = 74/68/2000 ms. The volume of interest (VOI) = 20 mm × 18 mm × 25 mm was placed in the ACC. Spectra for metabolite analysis consisted of 288 water-suppressed averages. Reference spectra consisted of 18 averages without water suppression.

Regional and longitudinal variation: 12 healthy male subjects (age = 30 ± 5 years) were scanned twice 7 ± 0 d apart. On visit 1, three repeat spectra (7T short TE) were acquired from the insula (VOI = 40 mm × 12 mm × 18 mm), to assess single session repeatability, and one spectrum acquired from the ACC. On visit 2, one spectrum was acquired from the ACC and one from the insula.

Post-processing: All spectra were processed in jMRUI. The water suppressed spectra were summed in jMRUI before analysis using LCModel and sequence specific basis-datasets based on 10 metabolites: N-acetyl aspartate (NAA), Creatine (Cr), Choline (Cho), Glu, Gln, GABA, Myo-Inositol (mI), Aspartate (Asp), Taurine (Tau) and Guanidinoacetate (Gua). Cramer-Rao lower bounds (CRLB) > 100% were eliminated from averages. Metabolite concentrations from LCModel were then corrected for tissue concentrations (by dividing by the tissue fraction). Metabolite concentrations are given in arbitrary units and no correction has been made for relaxation effects. Estimated standard deviations (%SDs) were taken directly from LCModel and average values were calculated across all subjects. Coefficients of variation [%CV = (SD/mean) × 100] were calculated across the three repeat measures in a single visit in ACC and insula cortex. Longitudinal variation [%LV = (SD/mean) × 100] was calculated from repeat measures over a week. SNR measurements were calculated from post-processed spectra using an in-house Matlab script [SNR = peak height/(1.96 × RMS_{noise})]. Significance was calculated using a Wilcoxon signed ranks test in SPSS 17 (SPSS for Windows, Chicago Ill, USA).

3T vs 7T comparisons of muscle glycogen and IMCL measurements

Subjects: Four healthy subjects (age 18-30 years) were scanned for ^{1}H MRS measurement of lipid levels in muscle on both the 3 and 7T scanners. 3T ^{1}H IMCL scans were acquired using the Q-Body coil for signal transmission and reception. 7T ^{1}H IMCL scans were acquired using a transmit/receive quadrature ^{1}H coil (with inbuilt ^{13}C quadrature coil), supplied by Philips (Cleveland, Ohio, USA). Spectra were acquired from the soleus muscle using a PRESS sequence with TE/TR = 40/7000 ms and the following parameters: VOI = 30 mm × 30 mm × 50 mm, with 16 water-suppressed averages. Reference spectra consisted of 16 acquisitions without water suppression. At 3T BW = 2000 Hz, No. samples = 1024, and at 7T BW = 4000 Hz, No. samples = 2048. To assess the repeatability of measurements, three measurements were made in a single subject.

For measurement of glycogen SNRs, spectra were acquired from a phantom containing 250 mol/L oyster glycogen. 3T ^{13}C glycogen measurements were acquired using a transmit/receive 13cm diameter ^{13}C coil with quadrature ^{1}H decouple coils (PulseTeq Ltd, Gloucestershire, UK). 7T glycogen measurements were acquired using a transmit/receive ^{13}C quadrature coil with quadrature ^{1}H decouple coils. Spectra were acquired using a pulse-acquire sequence with optimized adiabatic pulses and narrowband decoupling (3T BW = 8000 Hz, No. samples = 256; 7T BW = 16 000 Hz, No. samples = 256). Eight spectra, each with 80 averages, were collected at each time point (total scan time 11 min) before signal averaging in jMRUI.

^{1}H and ^{13}C MRS of muscle energy stores

Subjects: Six healthy, recreationally active, male volunteers (age = 26 ± 1.5 years, body mass index = 23.7 ± 0.9 kg/m^2, VO_2 max = 53.4 ± 2.7 mL/kg per minute) underwent preliminary testing to establish VO_2 max, before attending two study visits, separated by at least 1 wk. Subjects were overnight fasted and had refrained from alcohol, caffeine and strenuous exercise for 24 h and were requested to consume the same quantity and type of food prior to each study visit.

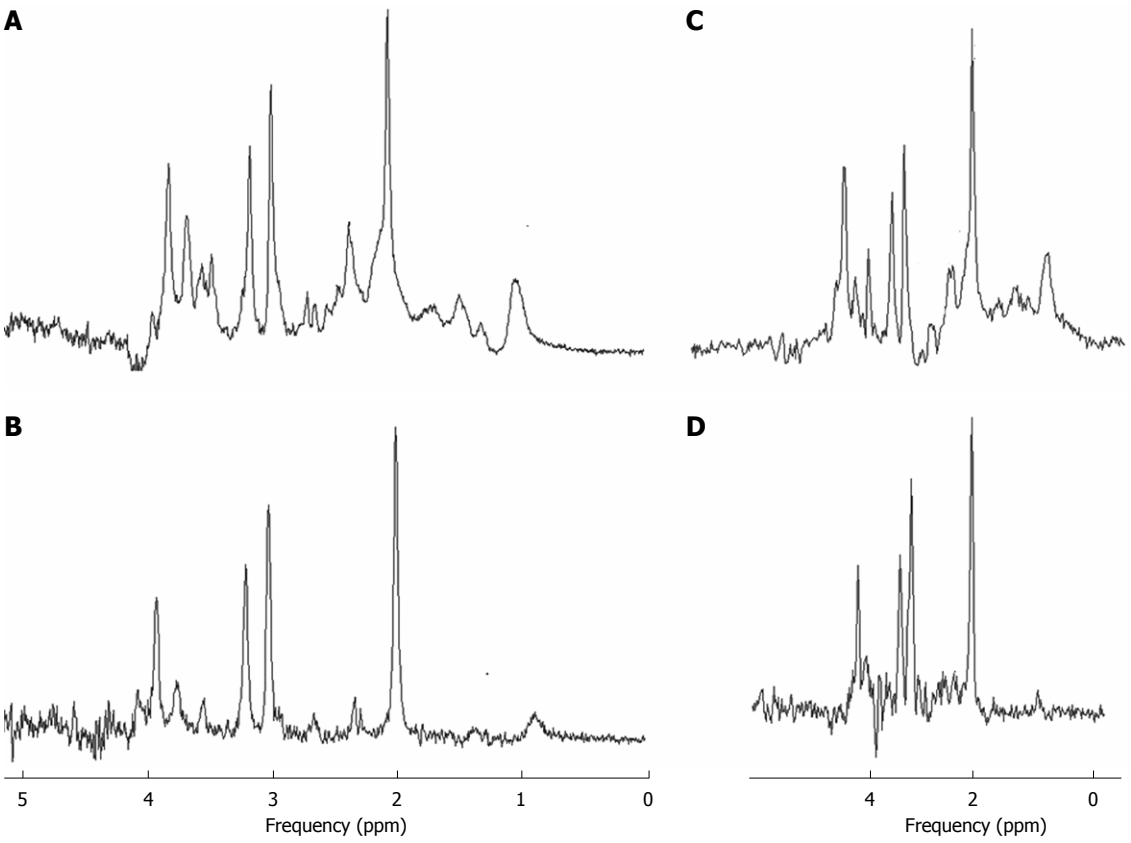

Figure 1 Example spectra acquired from subject 1 using 7T short TE (A), 7T long TE (B), 3T short TE (C) and 3T long TE (D) sequence.

Experimental protocol: On each visit, subjects underwent two baseline scan sessions with the RF coil positioned on the front and the back of the thigh respectively. Measurements were made of IMCL and glycogen. Following the baseline scans, subjects cycled for 1h at either 50% VO_2 max (50.8% ± 0.7%) or 75% VO_2 max (74.9% ± 1.9%) with exercise intensity randomized across the subject's two visits. A post exercise (PE) scan was carried out on the front of the thigh to measure glycogen levels before subjects were given a carbohydrate drink (t = 20 min PE) consisting of a 1 litre solution containing 100 g of a commercially available glucose polymer. Following ingestion of the drink, ^{13}C scans for measurement of glycogen were acquired at t = 20, 80, and 120 min in the quadriceps, and t = 50 and 100 min in the hamstring muscle group. Measurements of ^{1}H IMCL were carried out at t = 20 and 80 min in the vastus intermedius (VI) muscle and at t = 50 and 110 min in the semitendinosus (ST) muscle.

^{13}C MRS: ^{13}C spectra were acquired using a proton-decoupled pulse acquire sequence with adiabatic pulses and narrowband decoupling (BW = 16 000 Hz, No. samples = 256, TR = 1000 ms) for measurement of glycogen concentrations. Eight spectra, each with 80 averages, were collected at each time point (total scan time 11 min). ^{13}C spectra were post-processed by signal averaging and 50 Hz Lorentzian line broadening added before a phase correction was applied using jMRUI. Glycogen/external reference peak areas were determined using in-house software built in Matlab.

^{1}H MRS: ^{1}H MR spectra, for measurement of IMCL and EMCL, were acquired from the VI and the ST muscles using a STEAM sequence with the following parameters: TE/TM/TR = 11/13/8000 ms, VOI = 18 mm × 18 mm × 30 mm, No. samples = 4096, BW = 4000 Hz. Sixteen water-suppressed averages, and 4 reference spectra were acquired. Spectra were post-processed by realigning and phase correcting using jMRUI. Peak areas were calculated using the AMARES algorithm[50], fitting to Gaussian lineshapes. Values were converted to absolute levels as described by Szczepaniak *et al*[51], using T_2 values measured at 7T[52].

RESULTS

^{1}H reproducibility study

Sequence optimization: Example spectra, acquired in the ACC for a single subject, are shown in Figure 1. Average ACC SNR values, calculated for each sequence from the unfiltered NAA peak at 2.008 ppm, were highest for the 7T short TE sequence (SNR = 69 ± 7), which was significantly better than the 3T short TE sequence (SNR = 51 ± 6, $P < 0.002$). Similarly the 7T long TE sequence produced significantly higher SNR values than the 3T long TE sequence (SNR = 37 ± 9 *vs* 27 ± 6, $P = 0.006$).

The mean estimated error in metabolite quantifica-

Table 1 Mean Cramer-Rao lower bounds (SD) from LCModel averaged across all subjects

	NAA	Glu	Gln	mI	GABA	Cr	Cho
7T short	2 (0)	2 (0)	6 (1)	5 (1)	9 (2)	3 (2)	2 (0)
3T short	3 (1)	8 (2)	24 (8)	6 (1)	24 (10)	12 (3)	7 (7)
7T long	2 (1)	8 (1)	28 (13)	10 (3)	26 (9)	2 (0)	2 (0)
3T long	3 (1)	16 (5)	40 (15)	13 (6)	50 (20)	12 (5)	5 (1)

NAA: N-acetyl aspartate; Glu: Glutamate; Gln: Glutamine; mI: Myo-Inositol; GABA: γ-aminobutyric acid; Cr: Creatine; Cho: Choline.

Table 2 Mean % coefficients of variation (SD) averaged across all subjects

	NAA	Glu	Gln	mI	GABA	Cr	Cho
Uncorrected							
7T short	3 (2)	4 (2)	10 (6)	9 (3)	10 (6)	3 (2)	5 (4)
3T short	5 (3)	8 (6)	29 (11)	8 (4)	21 (14)	10 (4)	16 (16)
7T long	6 (6)	10 (6)	29 (19)	19 (10)	16 (8)	7 (6)	8 (6)
3T long	6 (6)	16 (9)	32 (30)	22 (10)	36 (25)	22 (13)	8 (7)
Tissue corrected							
7T short	4 (3)	5 (2)	10 (5)	9 (4)	10 (6)	4 (2)	6 (3)
3T short	6 (4)	8 (6)	29 (12)	8 (5)	22 (15)	10 (5)	17 (16)
7T long	6 (6)	10 (7)	29 (19)	20 (10)	15 (6)	6 (6)	8 (6)
3T long	7 (6)	16 (10)	32 (30)	23 (10)	38 (25)	22 (14)	9 (7)

NAA: N-acetyl aspartate; Glu: Glutamate; Gln: Glutamine; mI: Myo-Inositol; GABA: γ-aminobutyric acid; Cr: Creatine; Cho: Choline.

Table 3 Mean Cramer-Rao lower bounds (SD) from LCModel averaged across all subjects

	NAA	Glu	Gln	mI	GABA	Cr	Cho
CRLB ACC	2 (0)	2 (0)	6 (1)	5 (1)	9 (2)	3 (2)	2 (0)
CRLB Ins	3 (1)	3 (1)	9 (3)	7 (1)	11 (3)	2 (0)	2 (1)

CRLB: Cramer-Rao lower bounds; ACC: Anterior cingulate cortex; NAA: N-acetyl aspartate; Glu: Glutamate; Gln: Glutamine; mI: Myo-Inositol; GABA: γ-aminobutyric acid; Cr: Creatine; Cho: Choline.

tion, the Cramer-Rao lower bounds (CRLB), from LCModel analysis are shown in Table 1. CRLBs for Glu, Gln and GABA were lowest for the 7T short TE sequence, as expected from the SNR values. CRLB values for the 3T short TE and 7T long TE sequence were similar, despite much increased SNR for the 3T short spectra. CRLBs were highest for the 3T long TE sequence. The signals from Gln and GABA were not measurable (CRLB > 100%) in one spectrum using the 7T long TE sequence, and GABA was not found in 9 spectra using the 3T long TE sequence.

The intra-subject coefficients of variation for repeat measures of ACC metabolite levels are shown in Table 2. Values are given both uncorrected (direct from LCModel) and following correction for the voxel tissue fraction.

Regional and longitudinal variation

Spectral SNRs, averaged across all subjects, were significantly higher in the ACC than in the insula cortex (ACC SNR = 63 ± 10, insula SNR = 36 ± 11, $P = 0.002$) despite similar VOIs (9.00 mL *vs* 8.64 mL respectively) and similar average tissue fractions (0.94 ± 0.2 and 0.94 ± 0.1, calculated from 1 mm isotropic images)(Tables 3-5).

Table 4 Mean % coefficients of variation (SD) and % longitudinal variation (SD) averaged across all subjects

	NAA	Glu	Gln	mI	GABA	Cr	Cho
%CV							
ACC	4 (3)	5 (2)	10 (5)	9 (4)	10 (6)	4 (2)	6 (3)
Ins	6 (6)	8 (6)	12 (9)	10 (6)	21 (11)	7 (7)	6 (4)
%LV							
ACC	6 (3)	8 (7)	11 (9)	13 (13)	16 (13)	8 (9)	9 (10)
Ins	6 (5)	8 (10)	18 (18)	18 (11)	20 (24)	6 (6)	6 (6)

CV: Coefficients of variation; LV: Longitudinal variation; ACC: Anterior cingulate cortex; NAA: N-acetyl aspartate; Glu: Glutamate; Gln: Glutamine; mI: Myo-Inositol; GABA: γ-aminobutyric acid; Cr: Creatine; Cho: Choline.

Table 5 Mean (SD) metabolite levels (AU)

	NAA	Glu	Gln	mI	GABA	Cr	Cho
ACC	6.3 (0.7)	11.0 (1.4)	2.3 (0.4)	3.8 (0.3)	1.7 (0.4)	6.1 (0.6)	1.6 (0.2)
Ins	7.1 (0.6)	12.1 (1.3)	2.5 (0.5)	3.8 (0.5)	1.9 (0.4)	6.5 (0.4)	1.7 (0.2)

ACC: Anterior cingulate cortex; NAA: N-acetyl aspartate; Glu: Glutamate; Gln: Glutamine; mI: Myo-Inositol; GABA: γ-aminobutyric acid; Cr: Creatine; Cho: Choline.

3T vs 7T comparisons of muscle glycogen and IMCL measurements: measurements of glycogen and lipid

The SNR for the C1 peak of glycogen at 100.4 ppm (measured using ^{13}C MRS) was increased by 60% at 7T compared with the 3T values (11 *vs* 7) for the same number of acquisitions. Using ^{1}H MRS, SNRs (measured for the water peak) at 7T were 90% higher than values measured at 3T. %CVs for measurement of EMCL levels at 7T were much lower compared with the 3T measurements (6% *vs* 20% respectively). Similarly, repeat measurement of IMCL levels showed improved repeatability at 7T compared with 3T (2% *vs* 6%).

^{1}H and ^{13}C MRS of muscle energy stores

Basal glycogen levels were not significantly altered between each subject's visits. Similarly there were no basal differences in glycogen levels between the 50% VO_2 max visit and the 75% VO_2 max visit. Basal glycogen concentrations in the quadriceps tended to be higher than in the hamstrings, although this did not reach significance (front = 204 ± 56 mmol/L, back = 171 ± 49 mmol/L, $P = 0.2$).

Levels of glycogen (Figure 2) decreased significantly in the quadriceps following exercise ($t = 10$ min) at both 50% and 75% VO_2 max (-28% ± 20% and -52% ± 10%, $P < 0.05$) and were significantly lower when the subjects cycled at 75% VO_2 max compared with 50% VO_2 max ($P < 0.05$). Levels remained significantly below baseline levels at 20 and

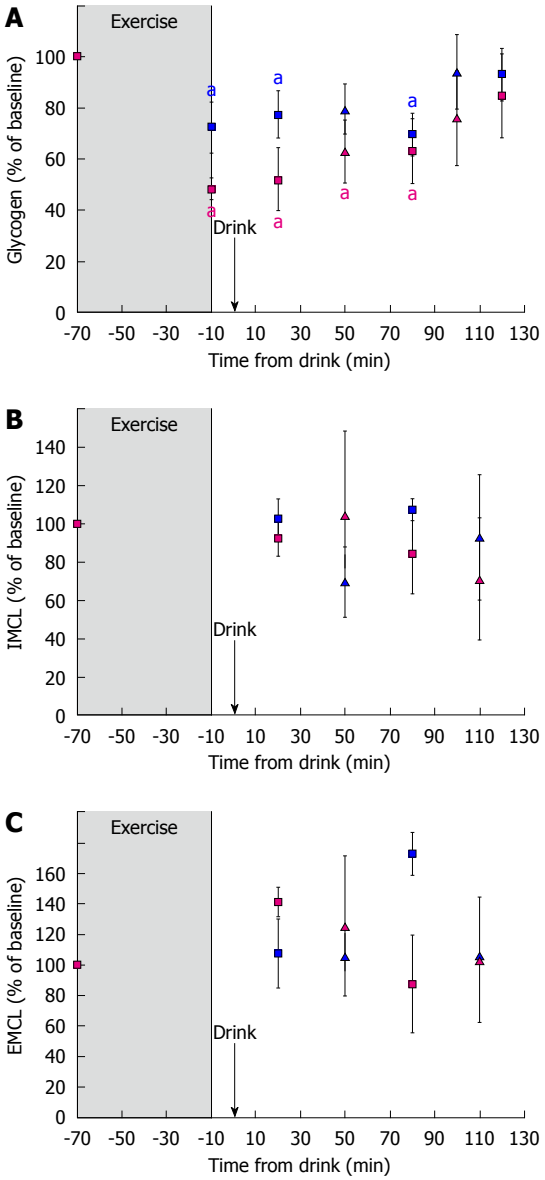

Figure 2 Percentage changes in glycogen (A), intra-myocellular lipid (B) and extra-myocellular lipid (C) levels due to exercise and following recovery. Values are mean ± SE. Squares represent measurements in the front of thigh, triangles represent measurements in the back of thigh. Points shown in blue and pink indicate exercise at 50% and 75% VO_2 max respectively ($^aP < 0.05$). IMCL: Intra-myocellular lipid; EMCL: Extra-myocellular lipid.

80 min following the drink (-23% ± 21% and -30% ± 19% respectively following cycling at 50% VO_2 max and -48% ± 28% and -37% ± 29% respectively at 75% VO_2 max). By 2 h after ingestion of the carbohydrate rich drink, glycogen levels in the front of the thigh were recovering towards baseline level (-7% ± 23% and -15% ± 37% following cycling at 50% VO_2 max and 75% VO_2 max respectively).

Post-exercise concentrations of glycogen in the hamstrings were not measured until 50 min after ingestion of the drink. Despite this, glycogen levels were still significantly below baseline level following exercise at 75% VO_2 max (-37% ± 28%) but had recovered towards baseline by 100 min (-24% ± 19%). Measurements of glycogen were not significantly different from baseline levels in the back of the thigh following exercise at 50% VO_2 max. As expected, mean glycogen concentrations were consistently lower in both the quadriceps and hamstrings following exercise at 75% compared with exercise at 50%.

IMCL and EMCL content

Basal IMCL content in the VI was not significantly different from levels in the ST muscle (0.4% ± 0.2% *vs* 0.3% ± 0.1%). No significant differences in IMCL were measured at any time point following exercise and re-feeding. Levels of EMCL were significantly larger in the ST compared with the VI (2.2% ± 0.3% *vs* 0.8% ± 0.3%, $P < 0.05$). No changes in EMCL levels were observed following exercise and re-feeding.

DISCUSSION

^1H reproducibility study

Increases in SNR from 3 to 7T are approximately 35% and 37% for the short TE and long TE sequence, respectively. Previous studies have reported various levels of increase in SNR with increasing field; however it is likely the 7T sequence would suffer from increased T_2 relaxation effects at the same TE, as well as increased saturation of signal due to longer T_1 relaxation values. Due to these relaxation effects, the 3T short TE sequence produced significantly higher SNR values than the 7T long TE sequence ($P = 0.002$).

As shown in Table 2, CVs for Glu, Gln and GABA from repeat measures are much lower for the 7T short TE sequence than for the 3T short TE sequence. It is possible this is in part due to reduced SNR; however, %CVs for GABA, using the 7T long TE sequence, are lower than those measured using the 3T short TE sequence despite the reduced SNR. This improvement in quantification is likely due to increased spectral resolution, as previously shown by Tkác *et al*[10].

Regional and longitudinal variation

Differences in SNR values, measured in the ACC and insula are likely due to increased field inhomogeneities for the long, thin VOI used in the insula (linewidths were measured to be approximately 15% wider in the insula compared with the ACC, $P = 0.05$), and poorer water suppression.

In spite of the much reduced SNR levels in the insula, CRLBs (Table 3) are only slightly increased. This is in agreement with single session CVs which, with the exception of GABA, are only slightly larger in the insula compared with the ACC. The reduced ability to accurately measure GABA is likely due to decreased spectral resolution as a consequence of the increased linewidths in the insula since the measured concentrations of GABA in the insula are similar to those measured in the ACC (Table 5).

%LVs tend to be larger than %CVs for all metabolites in the ACC (Table 4). This implies biological variation over a week, greater than the reproducibility of the measurements. %LVs for Gln and GABA were also larger

than %CVs in the insula. In contrast, %LVs for NAA, Cr, Cho, and Glu in the insula were not larger than %CVs. It is possible that there is some biological variation occurring in these levels which is masked by decreased single session repeatability in the insula.

Metabolite concentrations from the ACC and insula showed levels of Glu and Cr were significantly higher in the insula compared with the ACC ($P = 0.05$ and $P = 0.02$ respectively). No other differences in metabolites levels were found.

3T vs 7T comparisons of muscle glycogen and IMCL measurements: measurements of glycogen and lipid

Assuming that signal increases linearly with the number of averages (N_{ave}) while noise increases with $\sqrt{N_{ave}}$, obtaining the same SNR as measured for the C1 glycogen peak at 7T would take approximately 2.5 times longer at 3T. Utilizing this increase in signal strength at 7T allows either increased temporal resolution or improved measurement accuracy.

Improved measurement repeatability at 7T is likely due to the increase in spectral separation of IMCL and EMCL at 7T compared to 3T. However, repeatability of lipid measurements (particularly EMCL) in muscle is extremely susceptible to voxel repositioning errors. The voxels used for these measurements are quite large and so there are limited positions in which the voxel can be placed whilst avoiding adipose lipids and bone (particularly at 7T where chemical shifts between fat and water are increased). This may make repositioning between repeat measurements less variable and therefore improve measurement repeatability.

^{1}H and ^{13}C MRS of muscle energy stores

As expected, levels of glycogen in exercising muscles decreased significantly during exercise, with larger decreases following higher intensity exercise. At 2 h, levels of glycogen were returned to baseline levels indicating replenishment of glycogen stores due to carbohydrate refeeding. Interestingly, levels of glycogen in the hamstrings followed those in the quadriceps, despite the expected reduced exercise load.

No changes were measured in levels of IMCL due to exercise. If there are changes, they are likely to be small, and poor measurement repeatability (due to large spatial variation in levels of IMCL[40]) may mask these changes. It is thought that EMCL turnover is slow in contrast to IMCL, so EMCL levels would not be expected to change significantly over the timescale observed.

Increased spectral resolution at 7T allows improved ^{1}H MRS measurement of Glu, Gln and GABA concentrations which are thought to be perturbed in many neurodegenerative disorders and psychiatric diseases. Quantification is further improved by increases in sensitivity with increasing field strength. Using a short TE STEAM sequence, Glu, Gln and GABA were measured repeatedly in the ACC with coefficients of variation of 5%, 10% and 10% respectively within 15 min. Measurements made 1 wk apart showed increased variability indicating biological change in excess of single session reproducibility levels.

Increased sensitivity and spectral resolution available at 7T allows dynamic changes in glycogen and lipid levels in skeletal muscles to be observed with increasing temporal resolution. Measurements following exercise and re-feeding show the expected[45-50,53,54] decrease in glycogen levels in muscle, with a larger decrease in levels for increased exercise intensity. Levels of lipid were not significantly altered despite cycling for 1 h at 50% and 75% VO_2 max.

COMMENTS

Background

Magnetic resonance spectroscopy (MRS) has the potential to become a vital tool to aid the understanding of changes due to pathology in specific regions of the body, as well as for clinical diagnosis and treatment monitoring. Since signal increases with magnetic field strength, the use of ultra-high field (7T) scanners allows increased potential for measuring metabolite concentrations more accurately as well as allowing measurement of low concentration metabolites not seen at lower field.

Research frontiers

Levels of metabolites, particularly neurotransmitters glutamate and γ-aminobutyric acid (GABA), as well as glutamine, are thought to be important in understanding changes involved in neurological and psychiatric diseases. This study shows increased reproducibility for ^{1}H MRS measurement of glutamate, glutamine and GABA at 7T compared with 3T. In addition, measurement of energy stores [glycogen and intra-myocellular lipid (IMCL)] in skeletal muscle using ^{13}C and ^{1}H MRS respectively, are shown to be improved at 7T compared to 3T. This study utilizes the increased signal to noise to improve temporal resolution for subsequent measurements of IMCL and glycogen, and shows that higher intensity exercise (70% VO_2 max *vs* 50% VO_2 max) increases utilization of glycogen. No change in IMCL levels were measured due to exercise.

Innovations and breakthroughs

Little work has been done to compare optimized sequences and to establish levels of reproducibility based on different sequences for measurement of glutamate, glutamine and GABA. This paper contains single session repeatability for various proposed sequences at 3 and 7T, as well as measuring levels of biological variation over time. This paper also shows improved measurement of glycogen and IMCL at 7T, and is one of the first papers to sequentially measure dynamic changes in IMCL and glycogen levels at 7T.

Applications

Measurement of metabolite levels are important in understanding changes involved in neurological and psychiatric diseases, as well as for monitoring potential therapies. More accurate measurements will allow smaller changes to be measured which may provide new information for treatments.

Peer review

The current paper discusses the advantages of ultra-high field MR spectroscopy. It is a very well designed exceptional study.

REFERENCES

1 **Barker PB**, Hearshen DO, Boska MD. Single-voxel proton MRS of the human brain at 1.5T and 3.0T. *Magn Reson Med* 2001; **45**: 765-769

2 **Bartha R**, Drost DJ, Menon RS, Williamson PC. Comparison of the quantification precision of human short echo time (1)H spectroscopy at 1.5 and 4.0 Tesla. *Magn Reson Med* 2000; **44**: 185-192

3 **Dydak U**, Schär M. MR spectroscopy and spectroscopic imaging: comparing 3.0 T versus 1.5 T. *Neuroimaging Clin N Am* 2006; **16**: 269-283, x

4 **Gonen O**, Gruber S, Li BS, Mlynárik V, Moser E. Multivoxel 3D proton spectroscopy in the brain at 1.5 versus 3.0 T:

signal-to-noise ratio and resolution comparison. *AJNR Am J Neuroradiol* 2001; **22**: 1727-1731
5 **Inglese M**, Spindler M, Babb JS, Sunenshine P, Law M, Gonen O. Field, coil, and echo-time influence on sensitivity and reproducibility of brain proton MR spectroscopy. *AJNR Am J Neuroradiol* 2006; **27**: 684-688
6 **Kantarci K**, Reynolds G, Petersen RC, Boeve BF, Knopman DS, Edland SD, Smith GE, Ivnik RJ, Tangalos EG, Jack CR Jr. Proton MR spectroscopy in mild cognitive impairment and Alzheimer disease: comparison of 1.5 and 3 T. *AJNR Am J Neuroradiol* 2003; **24**: 843-849
7 **Otazo R**, Mueller B, Ugurbil K, Wald L, Posse S. Signal-to-noise ratio and spectral linewidth improvements between 1.5 and 7 Tesla in proton echo-planar spectroscopic imaging. *Magn Reson Med* 2006; **56**: 1200-1210
8 **Posse S**, Otazo R, Caprihan A, Bustillo J, Chen H, Henry PG, Marjanska M, Gasparovic C, Zuo C, Magnotta V, Mueller B, Mullins P, Renshaw P, Ugurbil K, Lim KO, Alger JR. Proton echo-planar spectroscopic imaging of J-coupled resonances in human brain at 3 and 4 Tesla. *Magn Reson Med* 2007; **58**: 236-244
9 **Srinivasan R**, Vigneron D, Sailasuta N, Hurd R, Nelson S. A comparative study of myo-inositol quantification using LCmodel at 1.5 T and 3.0 T with 3 D 1H proton spectroscopic imaging of the human brain. *Magn Reson Imaging* 2004; **22**: 523-528
10 **Tkác I**, Oz G, Adriany G, Uğurbil K, Gruetter R. In vivo 1H NMR spectroscopy of the human brain at high magnetic fields: metabolite quantification at 4T vs. 7T. *Magn Reson Med* 2009; **62**: 868-879
11 **Antuono PG**, Jones JL, Wang Y, Li SJ. Decreased glutamate + glutamine in Alzheimer's disease detected in vivo with (1)H-MRS at 0.5 T. *Neurology* 2001; **56**: 737-742
12 **Kantarci K**, Jack CR Jr, Xu YC, Campeau NG, O'Brien PC, Smith GE, Ivnik RJ, Boeve BF, Kokmen E, Tangalos EG, Petersen RC. Regional metabolic patterns in mild cognitive impairment and Alzheimer's disease: A 1H MRS study. *Neurology* 2000; **55**: 210-217
13 **Moore CM**, Breeze JL, Gruber SA, Babb SM, Frederick BB, Villafuerte RA, Stoll AL, Hennen J, Yurgelun-Todd DA, Cohen BM, Renshaw PF. Choline, myo-inositol and mood in bipolar disorder: a proton magnetic resonance spectroscopic imaging study of the anterior cingulate cortex. *Bipolar Disord* 2000; **2**: 207-216
14 **Rosenberg DR**, Macmaster FP, Mirza Y, Smith JM, Easter PC, Banerjee SP, Bhandari R, Boyd C, Lynch M, Rose M, Ivey J, Villafuerte RA, Moore GJ, Renshaw P. Reduced anterior cingulate glutamate in pediatric major depression: a magnetic resonance spectroscopy study. *Biol Psychiatry* 2005; **58**: 700-704
15 **Auer DP**, Pütz B, Kraft E, Lipinski B, Schill J, Holsboer F. Reduced glutamate in the anterior cingulate cortex in depression: an in vivo proton magnetic resonance spectroscopy study. *Biol Psychiatry* 2000; **47**: 305-313
16 **Auer DP**, Wilke M, Grabner A, Heidenreich JO, Bronisch T, Wetter TC. Reduced NAA in the thalamus and altered membrane and glial metabolism in schizophrenic patients detected by 1H-MRS and tissue segmentation. *Schizophr Res* 2001; **52**: 87-99
17 **Hoerst M**, Weber-Fahr W, Tunc-Skarka N, Ruf M, Bohus M, Schmahl C, Ende G. Correlation of glutamate levels in the anterior cingulate cortex with self-reported impulsivity in patients with borderline personality disorder and healthy controls. *Arch Gen Psychiatry* 2010; **67**: 946-954
18 **Carrey N**, MacMaster FP, Fogel J, Sparkes S, Waschbusch D, Sullivan S, Schmidt M. Metabolite changes resulting from treatment in children with ADHD: a 1H-MRS study. *Clin Neuropharmacol* 2003; **26**: 218-221
19 **Pollack MH**, Jensen JE, Simon NM, Kaufman RE, Renshaw PF. High-field MRS study of GABA, glutamate and glutamine in social anxiety disorder: response to treatment with levetiracetam. *Prog Neuropsychopharmacol Biol Psychiatry* 2008; **32**: 739-743
20 **Mayer D**, Spielman DM. Detection of glutamate in the human brain at 3 T using optimized constant time point resolved spectroscopy. *Magn Reson Med* 2005; **54**: 439-442
21 **Schulte RF**, Trabesinger AH, Boesiger P. Chemical-shift-selective filter for the in vivo detection of J-coupled metabolites at 3T. *Magn Reson Med* 2005; **53**: 275-281
22 **Ryner LN**, Sorenson JA, Thomas MA. Localized 2D J-resolved 1H MR spectroscopy: strong coupling effects in vitro and in vivo. *Magn Reson Imaging* 1995; **13**: 853-869
23 **Mescher M**, Merkle H, Kirsch J, Garwood M, Gruetter R. Simultaneous in vivo spectral editing and water suppression. *NMR Biomed* 1998; **11**: 266-272
24 **Terpstra M**, Ugurbil K, Gruetter R. Direct in vivo measurement of human cerebral GABA concentration using MEGA-editing at 7 Tesla. *Magn Reson Med* 2002; **47**: 1009-1012
25 **Hu J**, Yang S, Xuan Y, Jiang Q, Yang Y, Haacke EM. Simultaneous detection of resolved glutamate, glutamine, and gamma-aminobutyric acid at 4 T. *J Magn Reson* 2007; **185**: 204-213
26 **Tkác I**, Starcuk Z, Choi IY, Gruetter R. In vivo 1H NMR spectroscopy of rat brain at 1 ms echo time. *Magn Reson Med* 1999; **41**: 649-656
27 **Thompson RB**, Allen PS. Sources of variability in the response of coupled spins to the PRESS sequence and their potential impact on metabolite quantification. *Magn Reson Med* 1999; **41**: 1162-1169
28 **Thompson RB**, Allen PS. Response of metabolites with coupled spins to the STEAM sequence. *Magn Reson Med* 2001; **45**: 955-965
29 **Yang S**, Hu J, Kou Z, Yang Y. Spectral simplification for resolved glutamate and glutamine measurement using a standard STEAM sequence with optimized timing parameters at 3, 4, 4.7, 7, and 9.4T. *Magn Reson Med* 2008; **59**: 236-244
30 **Campbell I**. Intermediary metabolism. *Anaesth Intens Care Med* 2004; **5**: 141-143
31 **Taylor R**, Price TB, Rothman DL, Shulman RG, Shulman GI. Validation of 13C NMR measurement of human skeletal muscle glycogen by direct biochemical assay of needle biopsy samples. *Magn Reson Med* 1992; **27**: 13-20
32 **Stevens AN**, Iles RA, Morris PG, Griffiths JR. Detection of glycogen in a glycogen storage disease by 13C nuclear magnetic resonance. *FEBS Lett* 1982; **150**: 489-493
33 **Gruetter R**, Magnusson I, Rothman DL, Avison MJ, Shulman RG, Shulman GI. Validation of 13C NMR measurements of liver glycogen in vivo. *Magn Reson Med* 1994; **31**: 583-588
34 **Thomsen C**, Becker U, Winkler K, Christoffersen P, Jensen M, Henriksen O. Quantification of liver fat using magnetic resonance spectroscopy. *Magn Reson Imaging* 1994; **12**: 487-495
35 **Longo R**, Pollesello P, Ricci C, Masutti F, Kvam BJ, Bercich L, Crocè LS, Grigolato P, Paoletti S, de Bernard B. Proton MR spectroscopy in quantitative in vivo determination of fat content in human liver steatosis. *J Magn Reson Imaging* 1995; **5**: 281-285
36 **Garbow JR**, Lin X, Sakata N, Chen Z, Koh D, Schonfeld G. In vivo MRS measurement of liver lipid levels in mice. *J Lipid Res* 2004; **45**: 1364-1371
37 **Tarasów E**, Siergiejczyk L, Panasiuk A, Kubas B, Dzienis W, Prokopowicz D, Walecki J. MR proton spectroscopy in liver examinations of healthy individuals in vivo. *Med Sci Monit* 2002; **8**: MT36-MT40
38 **Szczepaniak LS**, Nurenberg P, Leonard D, Browning JD, Reingold JS, Grundy S, Hobbs HH, Dobbins RL. Magnetic resonance spectroscopy to measure hepatic triglyceride content: prevalence of hepatic steatosis in the general population. *Am J Physiol Endocrinol Metab* 2005; **288**: E462-E468
39 **Schick F**, Eismann B, Jung WI, Bongers H, Bunse M, Lutz O. Comparison of localized proton NMR signals of skeletal

muscle and fat tissue in vivo: two lipid compartments in muscle tissue. *Magn Reson Med* 1993; **29**: 158-167

40 **Boesch C**, Slotboom J, Hoppeler H, Kreis R. In vivo determination of intra-myocellular lipids in human muscle by means of localized 1H-MR-spectroscopy. *Magn Reson Med* 1997; **37**: 484-493

41 **Taylor R**, Magnusson I, Rothman DL, Cline GW, Caumo A, Cobelli C, Shulman GI. Direct assessment of liver glycogen storage by 13C nuclear magnetic resonance spectroscopy and regulation of glucose homeostasis after a mixed meal in normal subjects. *J Clin Invest* 1996; **97**: 126-132

42 **Moriarty KT**, Mclntyre DGO, Bingham K, Coxon R, Glover PM, Greenhaff PL, Macdonald IA, Bachelard HS, Morris PG. Glycogen resynthesis in liver and muscle after exercise: measurement of the rate of resynthesis by 13C magnetic resonance spectroscopy. *Magma Magn Reson Mater Phys Biol Med* 1994; **2**: 429-432

43 **Casey A**, Mann R, Banister K, Fox J, Morris PG, Macdonald IA, Greenhaff PL. Effect of carbohydrate ingestion on glycogen resynthesis in human liver and skeletal muscle, measured by (13)C MRS. *Am J Physiol Endocrinol Metab* 2000; **278**: E65-E75

44 **Franklin RM**, Ploutz-Snyder LL, Szeverenyi NM, Kanaley JA. The effects of an acute resistance exercise bout on IMCL content in obese younger and older women. *Med Sci Sport Exer* 2010; **42**: 1

45 **Awad S**, Stephenson MC, Placidi E, Marciani L, Constantin-Teodosiu D, Gowland PA, Spiller RC, Fearon KC, Morris PG, Macdonald IA, Lobo DN. The effects of fasting and refeeding with a 'metabolic preconditioning' drink on substrate reserves and mononuclear cell mitochondrial function. *Clin Nutr* 2010; **29**: 538-544

46 **Vøllestad NK**, Blom PC. Effect of varying exercise intensity on glycogen depletion in human muscle fibres. *Acta Physiol Scand* 1985; **125**: 395-405

47 **Gollnick PD**, Piehl K, Saubert CW 4th, Armstrong RB, Saltin B. Diet, exercise, and glycogen changes in human muscle fibers. *J Appl Physiol* 1972; **33**: 421-425

48 **Price TB**, Rothman DL, Avison MJ, Buonamico P, Shulman RG. 13C-NMR measurements of muscle glycogen during low-intensity exercise. *J Appl Physiol* 1991; **70**: 1836-1844

49 **van Loon LJ**, Greenhaff PL, Constantin-Teodosiu D, Saris WH, Wagenmakers AJ. The effects of increasing exercise intensity on muscle fuel utilisation in humans. *J Physiol* 2001; **536**: 295-304

50 **Vanhamme L**, van den Boogaart A, Van Huffel S. Improved method for accurate and efficient quantification of MRS data with use of prior knowledge. *J Magn Reson* 1997; **129**: 35-43

51 **Szczepaniak LS**, Babcock EE, Schick F, Dobbins RL, Garg A, Burns DK, McGarry JD, Stein DT. Measurement of intracellular triglyceride stores by H spectroscopy: validation in vivo. *Am J Physiol* 1999; **276**: E977-E989

52 **Ren J**, Sherry AD, Malloy CR. 1H MRS of intramyocellular lipids in soleus muscle at 7 T: spectral simplification by using long echo times without water suppression. *Magn Reson Med* 2010; **64**: 662-671

53 **Krssak M**, Petersen KF, Bergeron R, Price T, Laurent D, Rothman DL, Roden M, Shulman GI. Intramuscular glycogen and intramyocellular lipid utilization during prolonged exercise and recovery in man: a 13C and 1H nuclear magnetic resonance spectroscopy study. *J Clin Endocrinol Metab* 2000; **85**: 748-754

54 **Price TB**, Rothman DL, Taylor R, Avison MJ, Shulman GI, Shulman RG. Human muscle glycogen resynthesis after exercise: insulin-dependent and -independent phases. *J Appl Physiol* 1994; **76**: 104-111

S- Editor Cheng JX **L- Editor** O'Neill M **E- Editor** Zheng XM

World Journal of Radiology

Online Submissions: http://www.wjgnet.com/1949-8470office
wjr@wjgnet.com
doi:10.4329/wjr.v3.i4.114

World J Radiol 2011 April 28; 3(4): 114-119
ISSN 1949-8470 (online)

CASE REPORT

Imaging features of a huge spermatic cord leiomyosarcoma: Review of the literature

Irene Kyratzi, Evangelos Lolis, Eleni Antypa, Maria Alexandra Lianou, Demetrios Exarhos

Irene Kyratzi, Eleni Antypa, Demetrios Exarhos, Department of Radiology, Evaggelismos General Hospital, Ipsilantou 45-47, 10676, Athens, Greece
Evangelos Lolis, Second Department of Surgery, Evaggelismos General Hospital, Ipsilantou 45-47, 10676, Athens, Greece
Maria Alexandra Lianou, Department of Pathology, Evaggelismos General Hospital, Ipsilantou 45-47, 10676, Athens, Greece
Author contributions: All authors contributed in the therapeutic approach of the patient (U/S: Antypa E and Kyratzi I, CT: Exarhos D and Kyratzi I, Surgery: Lolis E, Pathologic exams: Lianou MA) and they wrote the part of the paper corresponding to their exam; Kyratzi I made literature searching and wrote the paper; Exarhos D made the supervision of the paper.
Correspondence to: Irene Kyratzi, MD, Department of Radiology, Evaggelismos General Hospital, Ipsilantou 45-47, 10676, Athens, Greece. ekyratzi@yahoo.com
Telephone: +30-21-21021560 Fax: +30-21-6015227
Received: November 13, 2010 Revised: January 25, 2011
Accepted: February 1, 2011
Published online: April 28, 2011

Abstract

Spermatic cord leiomyosarcomas (LMSs) are rare tumors which may cause significant morbidity and mortality if inadequately diagnosed or treated. We report a case of a paratesticular LMS in a 60-year-old man who presented with a right scrotal mass. The patient was evaluated by scrotal ultrasound and computed tomography of the abdomen and pelvis (including scans of the scrotum), which revealed a large extratesticular mass. The lesion proved to be malignant and the patient underwent radical orchiectomy with high cord ligation. To improve the assignment of this lesion, we further analyze the imaging features of LMS and correlate them with pathologic findings.

Key words: Spermatic cord leiomyosarcoma; Extratesticular sarcoma; Scrotum

Peer reviewer: Ahmed A Shokeir, MD, PhD, FEBU, Professor, Urology Department, Urology and Nephrology Center, Mansoura University, Mansoura 35516, Egypt

Kyratzi I, Lolis E, Antypa E, Lianou MA, Exarhos D. Imaging features of a huge spermatic cord leiomyosarcoma: Review of the literature. *World J Radiol* 2011; 3(4): 114-119 Available from: URL: http://www.wjgnet.com/1949-8470/full/v3/i4/114.htm DOI: http://dx.doi.org/10.4329/wjr.v3.i4.114

INTRODUCTION

Leiomyosarcoma (LMS) accounts for 5%-10% of soft tissue sarcomas. However, LMS of the spermatic cord is rare and only approximately 110 cases have been reported in the literature so far[1]. The spermatic cord is the most common site of extratesticular neoplasia but only 30% of them are malignant, 90% of which are sarcomas. Approximately 10% of paratesticular sarcomas are LMSs[2]. This type of lesion is reported in all age groups but is mostly diagnosed in the 6th decade[3]. A case of LMS is presented with description of its imaging features [ultrasound (U/S), computed tomography (CT)].

CASE REPORT

A 60 year-old male presented at the outpatient clinic with a right hydrocele and a small right scrotal lump, 4 mo after having had a mesh repair of bilateral inguinal hernias and mesh repair of an incisional midline hernia. Further work up was recommended during the consultation but the patient did not comply. Eighteen months later he presented once more at the outpatient clinic with a slightly painful, firm and obviously larger than previously right scrotal mass. The patient denied any lower urinary tract symptoms. On physical examination a firm, lobulated mass was palpated in the right hemiscrotum extending proximal up to a few centimeters from the right external

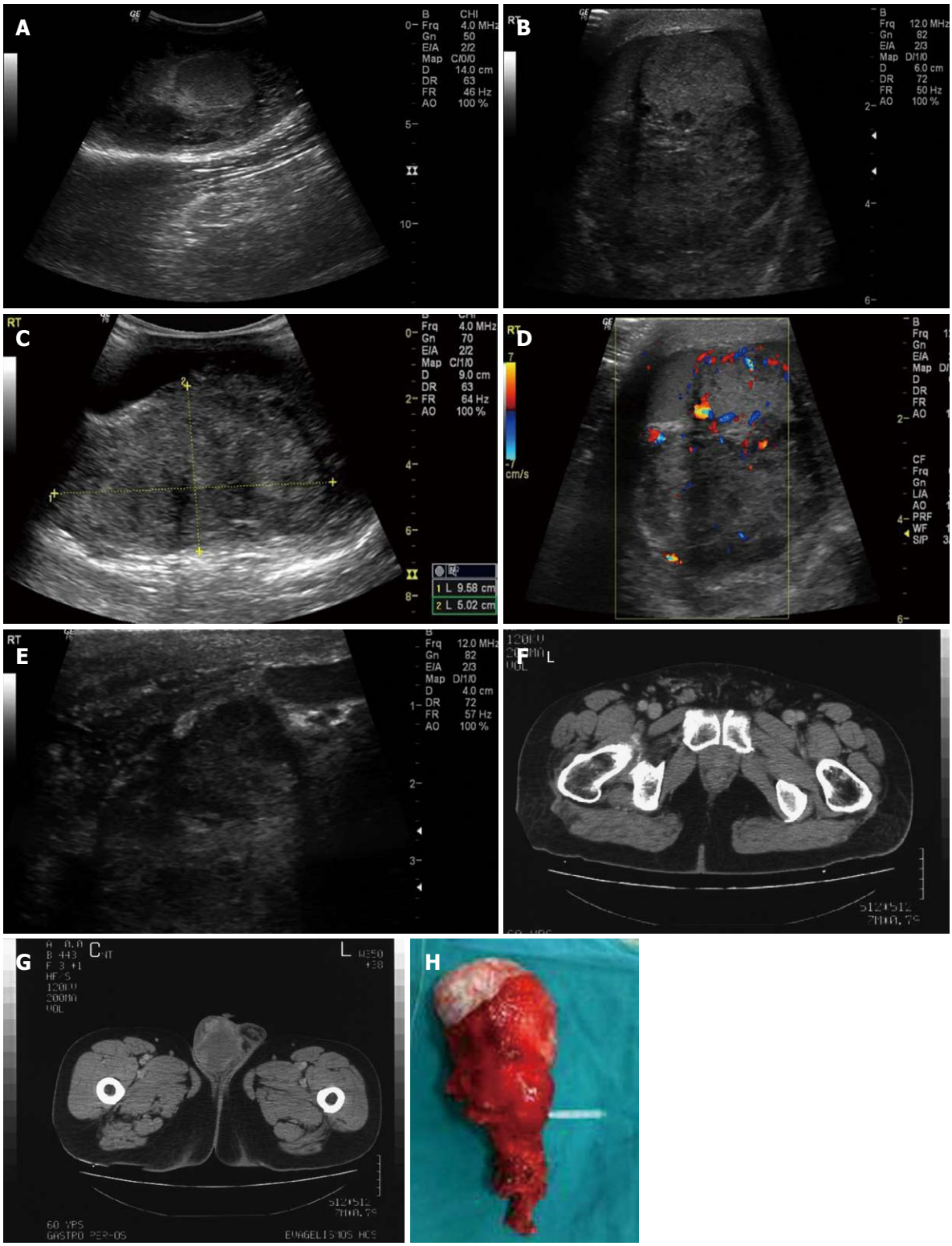

Figure 1 Leiomyosarcoma. A: Extratesticular mass located posterior-superiorly to the right testis; B: Large mass of heterogenous echotexture located posterior-superiorly to the testis without obvious signs of infiltration; C: Presence of calcifications and hypoechoic areas - hydrocele (use of convex probe due to the size of the mass); D: Colour Doppler image revealing vascularity within the tumour; E: Thickening of the spermatic cord in the inguinal canal; F: Thickening of the spermatic cord and dilated vessels present; G: Mass within the right hemiscrotum with irregular, mostly peripheral vascularity; H: Surgical specimen.

inguinal ring. The right spermatic cord was thick and hard on palpation. Recurrence of the right inguinal hernia with mass migration into the scrotum was excluded clinically. Right inguinal lymph nodes were palpated, but they were soft, painless and mobile.

Scrotal ultrasound was performed using a 10 MHz linear transducer and a 4 MHz convex transducer, revealing a large mass of mixed echogenicity with calcifications, measuring approximately 10 cm × 5 cm × 8 cm, located posterior-superiorly to the right testis (Figure 1A). The

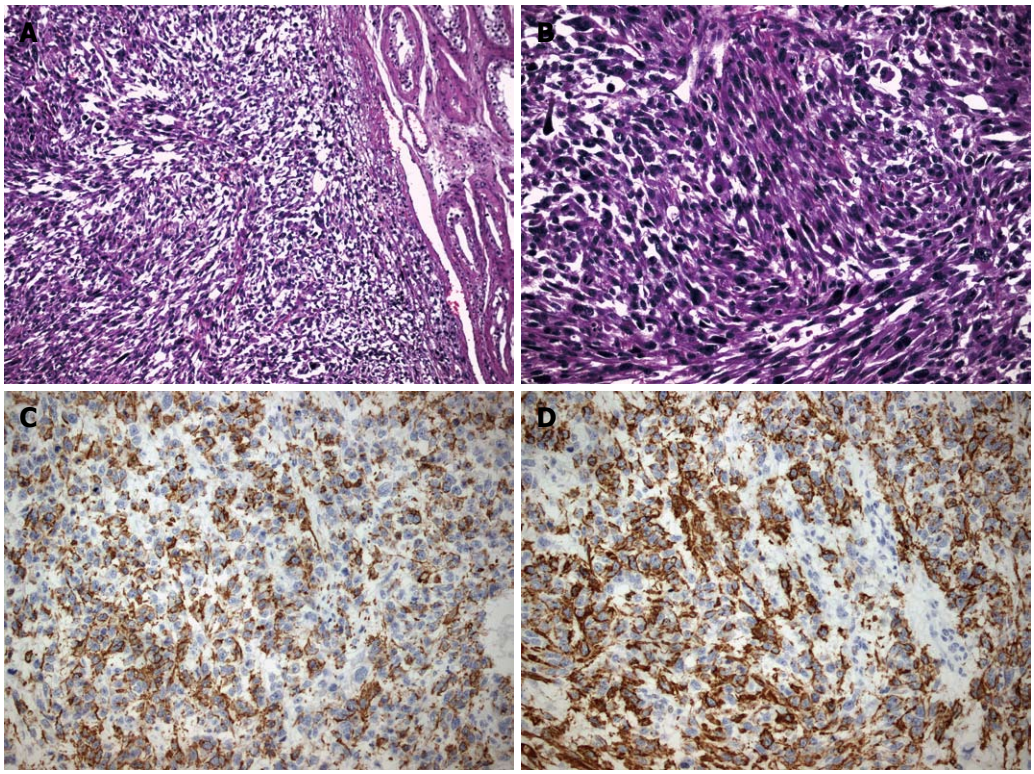

Figure 2 Pathological evidence of spermatic cord leiomyosarcoma. A: A fascicular growth pattern of spindle neoplastic cells is evident, which is highly indicative of leiomyosarcoma; B: A high degree of atypia and cellular pleomorphism is noticed on the above picture; C: Positivity for desmin is shown; D: Positivity for specific muscle actin is shown.

mass was depicted in close proximity to the testis, without obvious signs of infiltration (Figure 1B and C). Colour Doppler revealed increased, mostly peripheral, irregular vascularity (Figure 1D), as well as dilatation and congestion of the vessels within the spermatic cord. The right testis had normal dimensions, echotexture and vascularity. It was impossible to visualize the right epididymis. A significant complex hydrocele was also present. The examination was further expanded into the inguinal canal, to exclude a possible groin hernia. There were no signs of hernia; the walls of the ductus deferens, however, were thick in comparison to the left side (Figure 1E). The wall of the right hemiscrotum was also thick. A few inguinal lymph nodes were detected, without signs of inflammation or infiltration. The findings of the left hemiscrotum were unremarkable. Even though the extratesticular location of the mass was indicative of a benign etiology, the irregularity of the vascularity along with the inability to depict the epididymis led us to the admission of the patient for further investigation.

All laboratory examinations were within normal limits, including α-fetoprotein and β-human chorionic gonadotropin (β-HCG). Plain chest X-ray was normal. A CT scan of the abdomen and the pelvis with intravenous contrast material was performed and the scrotum was also included. The right spermatic cord was edematous with dilated vessels along its course (Figure 1F). A mass with a greater diameter of approximately 10 cm was located in the right hemiscrotum, with peripheral enhancement after intravenous injection of contrast material (Figure 1G). Soft tissue densities (HU 20-65), which did not imply the presence of fat, were detected throughout the mass. A few inguinal lymph nodes were depicted but without suspicious characteristics of infiltration. No para-aortic or pelvic lymph nodes were detected. There was no evidence of other pathologic conditions. Malignancy was confirmed by a core biopsy.

A transinguinal right radical orchiectomy was carried out with high cord ligation. Two right inguinal lymph nodes were sampled. The patient's post-operative course was uneventful.

Macroscopically, a firm, solid, grey-white tumor measuring 12 cm × 9.5 cm × 6 cm involved the right spermatic cord, displacing the testicle inferiorly, without invading it (Figure 1H). The right epididymis was not recognized. Seven neoplastic lesions along the spermatic cord with undefined borders were noted with diameters up to 2.5 cm.

Microscopically, an adequate degree of cellular and nuclear atypia as well as pleomorphism were revealed. In addition to that, multiple mitoses and widespread, coagulant necrotic areas were seen. Immunohistochemical stain results were: desmin (+), specific muscle actin (a-SMA) (+), CD68 (+), myogenic differentiation 1 (MyoD1) (+), Caldesmon (-) (Figure 2A-D). The findings were compatible with the diagnosis of a highly malignant, grade Ⅲ leiomyosarcoma of low differentiation. Other pathological findings concerning extension of the mass included multiple neoplastic emboli in the tumor periphery, infiltration

of the vessel walls and absence of testicular or tunica infiltration. The sampled lymph nodes were not infiltrated.

Chest CT was performed after the pathological diagnosis was established and revealed multiple nodules throughout the parenchyma of the lungs, compatible with secondary deposits. It was not carried out immediately after malignancy was diagnosed by core biopsy, because it would not have changed the surgical plan. The operation could not have been avoided because the patient was symptomatic and the mass was locally advanced. Moreover, the operation aimed at controlling local disease, regardless secondary lung depositions. Nevertheless, due to the rarity of the disease, there were not sufficient data and clear guidelines regarding the surgical management of these tumors in relation to the stage.

Two courses of adjuvant chemotherapy were administered (doxorubicin hydrochloride, trabectedin), after which progressive disease was still detected on chest CT. A second line of chemotherapy (dacarbazine, cyclophosphamide, vincristine sulfate) was administered and the metastatic disease showed evidence of remission in follow up CT after the third course (approximately 6 mo after the operation). By the end of the sixth course of the second line of chemotherapy, however, progressive disease was detected (increase of the size and number of secondary lung depositions, as well as a block of external iliac lymph nodes). Chemotherapy was switched to paclitaxel and gemcitabine, which is currently administered to the patient (9 mo after the operation).

DISCUSSION

Malignant neoplasms of non testicular origin located in the scrotum are uncommon and are usually sarcomas. In a series of 1583 adult soft tissue sarcomas at the Memorial Sloan-Kettering Cancer Center, 43 were urological and 14 (0.8%) were paratesticular (5 rhabdomyosarcoma, 4 leiomyosarcoma, 3 liposarcoma, 1 malignant fibrous histiocytoma and 1 undifferentiated sarcoma)[4]. One of the largest series of solid extratesticular masses in literature with 91 patients included, all of whom underwent surgical resection, reports an overall malignancy rate of 3%[5]. However, another series of 19 patients with extratesticular masses evaluated with scrotal U/S, reports a malignancy rate of 16%, with a limitation of selection bias[6]. Even though a few reviews of a small number of series are available, LMS seems to be the second most common histological variety following liposarcoma, with a peak incidence in the sixth decade[7]. Most patients present with a painless or slightly painful mass in the scrotum as our patient did. Only one case was reported where the mass was extremely painful and this was related to overproduction of β-HCG[8].

LMS is the result of neoplastic transformation of smooth muscle cells or multi-potential mesenchymal cells in various sites of the body. Its behavior is related to the site, histological grade of the lesion and the presence of nodal or distant metastases. It is subdivided topographically into 3 groups: LMS of the deep soft tissue, LMS of the cutaneous and subcutaneous tissue and LMS of vascular origin. According to the American Joint Committee on Cancer Staging System, paratesticular sarcomas should belong to the deep subtype[9].

Paratesticular LMS originates from the spermatic cord, the scrotum (testicular tunica, dartos muscle and scrotal subcutis) or the epididymis. The most common type arises from undifferentiated mesenchymal cells of the cremasteric muscle and vas deferens. The epididymal form is less frequent and arises from the smooth muscle surrounding the basement membrane of the epididymis canal. The dartous layer is the origin of the scrotal types. The first two aforementioned types drain into the retroperitoneal lymph nodes in contrast with the last type, which drains into the inguinal, external and internal iliac nodes[10,11].

Grading of paratesticular LMS is based on the evaluation of the number of mitoses (the mean number of mitoses in 5 HPF [high power field] in a part of tumor with the highest mitosis rate and cellularity), the percentage of necrosis and the severity of nuclear pleomorphism[3]. This LMS was classified grade Ⅲ due to its multiple necrosis, widespread necrotic areas nuclear atypia and nuclear pleomorphism.

Radical orchiectomy is the cornerstone of treatment in the management of this neoplasm, but the reported survival rates indicate the need for additional treatment[3,9]. It is important to note that negative histological margins are particularly hard to achieve during primary surgery[10]. Comprehension of the pattern of spread is essential, but this task is difficult by the rare occurrence of this disease. The most common means of dissemination are by regional lymph nodes spread (external, common iliac, hypogastric and retroperitoneal lymph nodes), haematogenous metastases (most commonly to the lungs) and by local extension (local infiltration of the scrotum, inguinal canal or pelvis, along the pathway of vas deferens)[11]. Involvement of the anterior abdominal wall is also possible[12]. In 1966, Kyle stated that the ratio of haematogenous to lymphatic spread is 3:1[13]. Further series suggested that lymph node dissection (especially retroperitoneal) should not be performed unless enlarged lymph nodes are encountered on CT scans or palpated during surgery[13,14].

Even though the study of a rare disease treated over several decades contains inherent biases that makes firm conclusions difficult to draw, the results of several studies suggest that adjuvant radiation, following radical orchiectomy, may control local microscopic disease and reduce the risk of locoregional relapse[10]. At present the role of chemotherapy remains controversial and restricted to the presence of metastatic disease[7].

In this case report, ultrasound examination of the patient revealed a heterogeneous mass, with calcifications and hypoechoic to anechoic areas, with irregular, mostly peripheral vascularity overtaking the right hemiscrotum, pressing the testicle inferiorly, without obviously obscuring its borders. It was impossible to depict the right epididy-

Table 1 Correlation of imaging and pathologic findings

U/S findings	CT findings	Pathologic findings
Hypoechoic to anechoic areas	Heterogeneous lesion with cystic areas	Necrotic areas
Disability to visualize the epididymis		Epididymal infiltration
Location in the root of the hemiscrotum, superiorly to the testis	Location in the root of the hemiscrotum, superiorly to the testis	Spermatic cord origin
Definite testicular borders		No testicular infiltration
Thick and edematous appearance of spermatic cord	Thick and edematous appearance of spermatic cord	Neoplastic lesions within the cord
Distended vessels within the cord	Distended vessels within the cord	Spermatic cord vessels' infiltration
	HU 20-65	Cystic, solid and calcified areas - absence of fat

U/S: Ultrasound; CT: Computed tomography.

mis. The majority of the LMSs described in the literature are heterogeneous lesions like the aforementioned[6,11,15,16] although some LMSs appear to be hypoechoic[8,14]. Calcifications are not mentioned in the majority of the cases described[1,2,6,8,11,14-16]. Colour Doppler ultrasonography shows either minimal[8], or increased vascularity[11,16]. The appearance is mostly related to the size of the lesion and the differentiation of the mesenchymal components[16]. This mass appears to be the largest LMS ever to have been reported in literature until now, with a maximum diameter of 12 cm. LMSs described until now ranged in size from 2-9 cm with a mean of 5 cm[8,17]. CT scan was not performed for the evaluation of the lesion itself, but in order to estimate the extent of disease, since the mass was suspected to be malignant. The only relevant bibliographic references besides staging concern the exclusion of the extension of retroperitoneal sarcoma into the scrotum[12]. A non-homogeneous mass with irregular, peripheral contrast enhancement and HU between 20 and 65, indicative of cystic, solid and calcified areas were found. A thickened and edematous spermatic cord with distended vessels was also depicted. The above CT findings parallel the sonographic ones. In addition to that, absence of areas with negative HU excluded the presence of fat within the lesion.

The afore-mentioned are pathologically correlated to necrotic areas within the tumor (cystic areas), infiltration of the epididymis (epididymis not visualized), origin from the spermatic cord (high position of the lesion within the scrotum), absence of testicular infiltration (definite testicular borders), neoplastic lesions within the spermatic cord (thick and edematous appearance) and infiltration of the vessels (vessel distention within the cord) (Table 1).

Even though there are circumstances where MR imaging is very helpful in the assessment of the scrotum, since it is far more specific than U/S (depiction of lipomas, fibrous pseudotumors, polyorchidism), it was considered that it would not limit the aforementioned differential diagnosis[18] or change the surgical procedure.

Although the ultrasound findings alone should have raised the probability of malignancy, the differential diagnosis of the extratesticular lesions in general is not so limited. Apart from purely cystic extratesticular lesions (epididymal cyst, scrotal tunica cyst) most of the solid lesions, either benign (adenoid tumor, papillary epididymal cystadenoma, fibrous pseudotumor, inguinoscrotal hernia, lipoma, leiomyoma) or malignant (rhabdomyosarcoma, liposarcoma, leiomyosarcoma, mesothelioma), frequently have overlapping characteristics, making it extremely difficult to exclude malignancy[18,19]. Considering the above imaging features the mass was more compatible with a leiomyosarcoma (exclusion of rhabdomyosarcoma due to the age of the patient), even though the diagnosis of a benign leiomyoma or a fibrous pseudotumor could not be completely excluded[18-20].

In conclusion, dealing with an extratesticular lesion can be confusing and troublesome, especially when a young patient is involved. Malignant extratesticular tumors are rare, but even if the malignancy rate of these lesions is much lower than that of the intratesticular masses, it is high enough to be of concern. Sonography should be the initial imaging modality since it can determine the origin of the lesion and even though the imaging characteristics are not adequate to reach a single diagnosis, the heterogeneous appearance along with the irregular, often increased vascularity of the tumor may allow the diagnosis of a sarcoma. Correlation with case history of the patients and CT/MR findings can further limit the differential diagnosis and lead to a better management of the patient.

REFERENCES

1 **Vogelaar FJ**, Schuttevaer HM, Willems JM. A patient with an inguinal mass: a groin hernia? *Neth J Med* 2009; **67**: 399-400
2 **Lopes RI**, Leite KR, Lopes RN. Paratesticular leiomyosarcoma treated by enucleation. *Int Braz J Urol* 2006; **32**: 66-67
3 **Mohammadi Torbati P**, Zham H. Epithelioid type of paratesticular leiomyosarcoma: a case report and literature review. *Urol J* 2004; **1**: 215-217
4 **Russo P**. Urologic sarcoma in adults. Memorial Sloan-Kettering Cancer Center experience based on a prospective database between 1982 and 1989. *Urol Clin North Am* 1991; **18**: 581-588
5 **Beccia DJ**, Krane RJ, Olsson CA. Clinical management of non-testicular intrascrotal tumors. *J Urol* 1976; **116**: 476-479
6 **Frates MC**, Benson CB, DiSalvo DN, Brown DL, Laing FC, Doubilet PM. Solid extratesticular masses evaluated with sonography: pathologic correlation. *Radiology* 1997; **204**: 43-46

7 **Coleman J**, Brennan MF, Alektiar K, Russo P. Adult spermatic cord sarcomas: management and results. *Ann Surg Oncol* 2003; **10**: 669-675
8 **Ou SM**, Lee SS, Peng YJ, Sheu LF, Yao NS, Chang SY. Production of beta-HCG by spermatic cord leiomyosarcoma: a paraneoplastic syndrome? *J Androl* 2006; **27**: 643-644
9 **Alberghini M**, Zanella L, Bacchini P, Maltarello MC, Maraldi NM, Bertoni F. Leiomyosarcoma of the spermatic cord: a light and ultrastructural description of one case. *Pathol Res Pract* 2004; **200**: 487-491
10 **Fagundes MA**, Zietman AL, Althausen AF, Coen JJ, Shipley WU. The management of spermatic cord sarcoma. *Cancer* 1996; **77**: 1873-1876
11 **Dangle P**, Basavaraj DR, Bhattarai S, Paul AB, Biyani CS. Leiomyosarcoma of the spermatic cord: case report and literature review. *Can Urol Assoc J* 2007; **1**: 55-58
12 **Cardenosa G**, Papanicolaou N, Fung CY, Tung GA, Yoder IC, Althausen AF, Shipley WU. Spermatic cord sarcomas: sonographic and CT features. *Urol Radiol* 1990; **12**: 163-167
13 **Kyle VN**. Leiomyosarcoma of the spermatic cord: a review of the literature and report of an additonal case. *J Urol* 1966; **96**: 795-800
14 **Stein A**, Kaplun A, Sova Y, Zivan I, Laver B, Lurie M, Lurie A. Leiomyosarcoma of the spermatic cord: report of two cases and review of the literature. *World J Urol* 1996; **14**: 59-61
15 **Watanabe J**, Soma T, Kawa G, Hida S, Koisi M. Leiomyosarcoma of the spermatic cord. *Int J Urol* 1999; **6**: 536-538
16 **Secil M**, Kefi A, Gulbahar F, Aslan G, Tuna B, Yorukoglu K. Sonographic features of spermatic cord leiomyosarcoma. *J Ultrasound Med* 2004; **23**: 973-976; quiz 977-978
17 **Fisher C**, Goldblum JR, Epstein JI, Montgomery E. Leiomyosarcoma of the paratesticular region: a clinicopathologic study. *Am J Surg Pathol* 2001; **25**: 1143-1149
18 **Woodward PJ**, Schwab CM, Sesterhenn IA. From the archives of the AFIP: extratesticular scrotal masses: radiologic-pathologic correlation. *Radiographics* 2003; **23**: 215-240
19 **Kim W**, Rosen MA, Langer JE, Banner MP, Siegelman ES, Ramchandani P. US MR imaging correlation in pathologic conditions of the scrotum. *Radiographics* 2007; **27**: 1239-1253
20 **Garriga V**, Serrano A, Marin A, Medrano S, Roson N, Pruna X. US of the tunica vaginalis testis: anatomic relationships and pathologic conditions. *Radiographics* 2009; **29**: 2017-2032

S- Editor Cheng JX **L- Editor** O'Neill M **E- Editor** Zheng XM

World Journal of Radiology

Online Submissions: http://www.wjgnet.com/1949-8470office
wjr@wjgnet.com
doi:10.4329/wjr.v3.i4.120

World J Radiol 2011 April 28; 3(4): 120-124
ISSN 1949-8470 (online)

Feng Chen's work on translational and clinical imaging

Feng Chen

Feng Chen, Section of Radiology, Department of Medical Diagnostic Sciences, Faculty of Medicine, University of Leuven, 3000 Leuven, Belgium
Feng Chen, Molecular Small Animal Imaging Center, University of Leuven, 3000 Leuven, Belgium
Feng Chen, Department of Radiology, Zhong Da Hospital, Southeast University, Nanjing 210009, Jiangsu Province, China
Author contributions: Chen F solely contributed to this manuscript.
Supported by Health Bureau of Jiangsu Province, China; Chinese Scholarship Council; National Natural Science Foundation of China; European Congress of Radiology 2000, EAR-ECR Research and Education Fund Fellowship Grant; European Union Asia-Link Project
Correspondence to: Feng Chen, MD, PhD, Section of Radiology, Department of Medical Diagnostic Sciences, Faculty of Medicine, University of Leuven, Herestraat 49, bus 7003, 3000 Leuven, Belgium. chenfengbe@yahoo.com.cn
Telephone: +32-16-330165 Fax: +32-16-343765
Received: October 11, 2010 Revised: March 28, 2011
Accepted: April 4, 2011
Published online: April 28, 2011

Abstract

Dr. Feng Chen is a chief medical doctor and the vice chairman of the Department of Radiology in Zhong Da Hospital at Southeast University, Nanjing, China and a senior researcher in the Department of Radiology at the Catholic University of Leuven, Belgium. His main areas of interest are translational imaging research including stroke, tumor angiogenesis, assessment of therapeutic response in solid tumors, and magnetic resonance contrast media. Dr. Feng Chen has published 44 scientific papers in peer-reviewed international journals. He and his colleagues have developed an imaging platform which includes animal models, animal preparations and multiparametric magnetic resonance imaging (MRI) protocols for translational animal imaging research using clinical machines. His MRI findings on rodent stroke are considered to "serve as a model for future laboratory investigations of treatment of acute stroke and unify the approaches developed for clinical studies". He and his colleagues have introduced a novel liver tumor model in rodents, in which a series of studies concerning the antitumor activity of vascular disrupting agents have been successively conducted and assessed by *in vivo* MRI, especially by diffusion weighted imaging as an imaging biomarker. His goal is to provide valuable references for clinical practice and to contribute to the translation of animal imaging research into patient applications.

Figure 1 Feng Chen, MD, PhD, Section of Radiology, Department of Medical Diagnostic Sciences, Faculty of Medicine, University of Leuven, Herestraat 49, bus 7003, 3000 Leuven, Belgium.

Key words: Animal study; Contrast agent; Magnetic resonance imaging; Therapeutic assessment; Translational research; Tumor angiogenesis; Tumor therapy; Vascular disrupting agent

Peer reviewer: Roberto Grassi, MD, Full Professor of Radiology, Department " Magrassi-Lanzara " Institute of Radiology, Second University of Naples, Piazza Miraglia, Naples, 80138, Italy

Chen F. Feng Chen's work on translational and clinical imaging. *World J Radiol* 2011; 3(4): 120-124 Available from: URL: http://www.wjgnet.com/1949-8470/full/v3/i4/120.htm DOI: http://dx.doi.org/10.4329/wjr.v3.i4.120

INTRODUCTION AND EDUCATIONAL EXPERIENCE

Dr. Feng Chen is a chief medical doctor and the vice chairman of the Department of Radiology in Zhong Da Hospital at Southeast University, Nanjing, China. Currently, he is also a senior researcher in the Department of Radiology at the Catholic University of Leuven, Belgium (Figure 1). He obtained his Bachelor's degree in Medicine in 1984 and Master's degree in Radiology in 1987 from Nanjing Railway Medical College (known as Medical School of Southeast University since 2000), China. He was employed as a radiologist in Zhong Da Hospital of Southeast University from 1987 to 2001. He was awarded a Chinese Overseas Scholarship to support his clinical magnetic resonance imaging (MRI) research at Leeds University in the UK as a visiting scholar from 1997 to 1998. He obtained his PhD degree from the Catholic University of Leuven in 2007. Since then he has been employed at the University of Leuven.

Dr. Feng Chen has published 44 scientific papers in peer-reviewed international journals. He has accepted several invitations to be a panel expert at international cancer conferences, to speak at international meetings, and to write reviews or chapters on small animal imaging and oncology imaging using clinical MR scanners. Throughout his academic career, he has been supported by a series of awards including the Chinese Scholarship Council; National Natural Science Foundation of China; EAR-ECR Research and Education Fund Fellowship Grant, European Congress of Radiology 2000, and European Union Asia-Link Program. He was also the silver prize winner of the QUIZ on Asian-Oceanian Seminars on Abdominal Radiology in 1997 and the silver prize winner of the QUIZ on Diagnostic and Interventional Radiology in 1999.

ACADEMIC STRATEGY AND GOALS

As a radiologist with more than 15 years work experience, Dr. Chen is well aware of the vital role of preclinical imaging research in studying the mechanism of human pathologies and in finding a solution for problems encountered in daily clinical practice. Therefore, over the last 9 years Dr. Chen's main work has been focused on translational imaging research[1-15]. Since clinical MR scanners are available to most institutions conducting animal experiments, he and his colleagues have developed a platform which includes animal models, animal preparations and a multiparametric MRI protocol for translational animal imaging research using clinical machines[16]. Based on this imaging platform, a number of animal models such as the modified photothrombotic stroke model[1], implanted liver tumor model[4,17] and reperfused partial liver infarction model in rodents[11] have been characterized, and the therapeutic efficacy of some novel thrombolytic and anticancer agents have been monitored and evaluated[9,12,18]. Dr. Chen is also pursuing the further investigation of ischemic diseases and tumor angiogenesis imaging, and exploring novel specific imaging and biological markers for the noninvasive assessment of pathological processes. The goal is to provide valuable references for clinical practice and to contribute to the translation of animal imaging research into patient applications.

ACADEMIC ACHIEVEMENTS

MRI studies in rodent stroke

During the 5-year period of his PhD program, Dr. Chen systematically studied a model of photochemically-induced thrombosis (PIT) of proximal middle cerebral artery occlusion with MRI using a 1.5 Tesla clinical scanner[1-3,7,8,19]. With this model, the therapeutic effects of a novel anti-stroke agent, microplasmin (μPli) has been monitored and evaluated with MRI, and compared with the approved thrombolytic agent, tissue plasminogen activator (tPA)[9]. The results indicated that μPli with superior safety may be a potential alternative to tPA for the treatment of focal ischemic stroke.

The main findings of this series of studies included: (1) An ischemic penumbra defined with diffusion and perfusion mismatch using MRI has been approved in this PIT stroke model, which is used as an inclusion criterion before treatment[6,9]; (2) A delayed perfusion phenomenon has been observed for the first time in a stroke animal model by MR perfusion imaging, which plays an important role in maintaining perfusion to the "penumbra" region after stroke onset[3,8]; and (3) The evidence of μPli in the treatment of the stroke model has been documented with noninvasive multiparametric MRI[9,20].

The findings of Dr. Chen and his colleagues "demonstrate the ability to identify the ischemic and putatively infarcted regions before therapy, to institute therapy in a model that compares thrombolytic agents, and to document the response and complication rates. These findings serve as a model for future laboratory investigations of the treatment of acute stroke and unify the approaches developed for clinical studies" as stated in an Editorial on Dr. Chen and his colleague's article which appeared in an issue of *Radiology*[21].

Imaging assessment of therapeutic effects in oncology

Dr. Chen's research activities and contribution in this field are mainly associated with the following work:

Novel liver implanted tumor models in rodents were developed and characterized using comprehensive MRI techniques which included morphologic, functional, and metabolic information[4,17]. These models provided an upgraded research platform for the preclinical assessment of diagnostic and therapeutic strategies as indicated by the consequent outcomes listed below.

Diffusion weighted imaging (DWI) has emerged as a unique and powerful non-invasive MRI technique. Its value as an imaging biomarker has been investigated extensively

in imaging-based diagnosis in a variety of translational applications including cerebral ischemia and solid tumors using small animals. Through technical adaptation and optimization, Dr. Chen and his colleagues have been able to perform clinically relevant animal studies with conclusions based on DWI quantification using a clinical magnet[5,22].

MRI monitoring and evaluation of experimental hepatic rhabdomyosarcoma treated with a vascular disrupting agent (VDA) has been conducted in a series of studies[12-15,18]. The results demonstrate that clinical MRI allows monitoring of VDA-related vascular shutdown and the discrimination between viable tissue and necrotic tumor tissue. However, a single dose of VDA seems insufficient for tumor eradication due to evident peripheral residue and recurrence[23]. Therefore, VDA combined with other therapeutic strategies, such as antiangiogenics, have been proposed and are undergoing investigation, and are believed to be more easily translated into patient practice because of the clinically relevant experimental set-up.

Investigation and application of tissue specific MR contrast agents

Necrosis-avid contrast agents (NACAs) have thus far been discovered and developed by Prof. Ni in the Catholic University of Leuven, Belgium as necrosis-targeting markers for MRI identification of non-viable tissue[24]. During recent years, Dr. Chen has been actively involved in the investigation of NACAs[25,26] and their application in acute myocardial infarction[27], tissue viability assessment, and therapeutic evaluation after interventional therapies[28].

Dr. Chen also compared the effects of two superparamagnetic iron oxide (SPIO) contrast agents, ferumoxides and SHU-555A, in MRI of liver and spleen in the early phase of their clinical application[29], which provided valuable information for best practice in patients.

Computed tomography gastrography for diagnosis of gastric carcinoma

Gastric carcinoma is one of the leading causes of death in East Asia. Dr Chen was awarded an EAR-ECR Fellowship Grant in this field by the Research and Education Fund during the European Congress of Radiology 2000 in Vienna. In this study, two- and three-dimensional display techniques after spiral computed tomography (CT) scanning were cross-referenced. The role of the combined CT technique was compared with that of upper gastrointestinal series, fiberoptic gastroscopy and histopathology in the detection, Borrmann's classification, and staging of gastric carcinoma[30]. Based on the work described above, Dr. Chen, together with two colleagues, edited a book entitled "Virtual Endoscopy and Related 3D in Clinical Medicine"[31]. Dr. Chen also systematically introduced the diagnostic test, the receiver operative characteristic curve (ROC)[32] approach in diagnostic radiology in China.

Imaging study on relationship between anomalous junction of pancreaticobiliary duct and diseases of biliary tract and pancreas

Dr. Chen systematically investigated and reported, for the first time, the occurrence of anomalous junction of the pancreaticobiliary duct (AJPBD) based on cholangiopancreatography in a Chinese population. The results showed that AJPBD is a possible risk factor for biliary duct and pancreatic diseases. A new complex pattern of AJPBD was proposed and a novel technique for magnetic resonance pancreatography after oral juice stimulation was developed. Dr. Chen's study findings have been listed as one of the most important advances in abdominal radiology in China[33].

PERSPECTIVE

Medical imaging is a rapidly growing field in medicine. Small animal imaging has becoming a major player in an increasing number of animal experiments in which MRI has been a favorite choice for *in vivo* monitoring due to its advantages which include excellent resolution and innocuousness[34]. As one of his research interests, Dr. Chen's work will focus on the novel anti-tumor strategies involving the application of VDA assessed by *in vivo* imaging techniques. Antivascular tumor therapies with VDAs are a promising approach in oncologic research and have been conducted in a number of studies[5,12,14,18]. However, rapid tumor re-growth from a residual viable rim after treatment with a VDA compromises the therapeutic efficacy of these agents[23]. Several approaches have been suggested to solve this problem including biological and targeted radiotherapy methods. For instance, tumor rebound after VDA treatment is reported to be associated with the acute mobilization of bone marrow (BM)-derived circulating endothelial progenitor cells (EPCs) induced by VDA, which contributes to the responsive tumor neoangiogenesis. The combined use of antiangiogenics with VDA may inhibit the mobilization of EPCs so that tumor recurrence may be prevented or reduced[35]. However, critical controversy exists in the literature regarding this theory and the consequent role of EPCs in tumor growth[36]. Therefore, exploration of this scientific issue may allow better insight into the mechanism of tumor recurrence, and lead to new anti-tumor strategies and promote imaging research.

ACKNOWLEDGMENTS

I would like to thank all of my colleagues and friends in Southeast University at Nanjing China, St. James University Hospitals at Leeds UK and Catholic University of Leuven Belgium for their collaborations to my work and support of my career.

REFERENCES

1 **Chen F**, Suzuki Y, Nagai N, Peeters R, Coenegrachts K, Coudyzer W, Marchal G, Ni Y. Visualization of stroke with clinical MR imagers in rats: a feasibility study. *Radiology* 2004; **233**: 905-911

2 **Chen F**, Suzuki Y, Nagai N, Peeters R, Sun X, Coudyzer W, Marchal G, Ni Y. Rat cerebral ischemia induced with photochemical occlusion of proximal middle cerebral artery: a

stroke model for MR imaging research. *MAGMA* 2004; **17**: 103-108
3 **Chen F**, Suzuki Y, Nagai N, Peeters R, Marchal G, Ni Y. Dynamic susceptibility contrast-enhanced perfusion MR imaging at 1.5 T predicts final infarct size in a rat stroke model. *J Neurosci Methods* 2005; **141**: 55-60
4 **Chen F**, Sun X, De Keyzer F, Yu J, Peeters R, Coudyzer W, Vandecaveye V, Landuyt W, Bosmans H, Van Hecke P, Marchal G, Ni Y. Liver tumor model with implanted rhabdomyosarcoma in rats: MR imaging, microangiography, and histopathologic analysis. *Radiology* 2006; **239**: 554-562
5 **Chen F**, De Keyzer F, Wang H, Vandecaveye V, Landuyt W, Bosmans H, Hermans R, Marchal G, Ni Y. Diffusion weighted imaging in small rodents using clinical MRI scanners. *Methods* 2007; **43**: 12-20
6 **Chen F**, Liu Q, Wang H, Suzuki Y, Nagai N, Yu J, Marchal G, Ni Y. Comparing two methods for assessment of perfusion-diffusion mismatch in a rodent model of ischaemic stroke: a pilot study. *Br J Radiol* 2008; **81**: 192-198
7 **Chen F**, Suzuki Y, Nagai N, Jin L, Yu J, Wang H, Marchal G, Ni Y. Rodent stroke induced by photochemical occlusion of proximal middle cerebral artery: evolution monitored with MR imaging and histopathology. *Eur J Radiol* 2007; **63**: 68-75
8 **Chen F**, Suzuki Y, Nagai N, Sun X, Coudyzer W, Yu J, Marchal G, Ni Y. Delayed perfusion phenomenon in a rat stroke model at 1.5 T MR: an imaging sign parallel to spontaneous reperfusion and ischemic penumbra? *Eur J Radiol* 2007; **61**: 70-78
9 **Chen F**, Suzuki Y, Nagai N, Sun X, Wang H, Yu J, Marchal G, Ni Y. Microplasmin and tissue plasminogen activator: comparison of therapeutic effects in rat stroke model at multiparametric MR imaging. *Radiology* 2007; **244**: 429-438
10 **De Keyzer F**, Vandecaveye V, Thoeny H, Chen F, Ni Y, Marchal G, Hermans R, Nuyts S, Landuyt W, Bosmans H. Dynamic contrast-enhanced and diffusion-weighted MRI for early detection of tumoral changes in single-dose and fractionated radiotherapy: evaluation in a rat rhabdomyosarcoma model. *Eur Radiol* 2009; **19**: 2663-2671
11 **Wu X**, Wang H, Chen F, Jin L, Li J, Feng Y, DeKeyzer F, Yu J, Marchal G, Ni Y. Rat model of reperfused partial liver infarction: characterization with multiparametric magnetic resonance imaging, microangiography, and histomorphology. *Acta Radiol* 2009; **50**: 276-287
12 **Wang H**, Sun X, Chen F, De Keyzer F, Yu J, Landuyt W, Vandecaveye V, Peeters R, Bosmans H, Hermans R, Marchal G, Ni Y. Treatment of rodent liver tumor with combretastatin a4 phosphate: noninvasive therapeutic evaluation using multiparametric magnetic resonance imaging in correlation with microangiography and histology. *Invest Radiol* 2009; **44**: 44-53
13 **Thoeny HC**, De Keyzer F, Chen F, Ni Y, Landuyt W, Verbeken EK, Bosmans H, Marchal G, Hermans R. Diffusion-weighted MR imaging in monitoring the effect of a vascular targeting agent on rhabdomyosarcoma in rats. *Radiology* 2005; **234**: 756-764
14 **Thoeny HC**, De Keyzer F, Vandecaveye V, Chen F, Sun X, Bosmans H, Hermans R, Verbeken EK, Boesch C, Marchal G, Landuyt W, Ni Y. Effect of vascular targeting agent in rat tumor model: dynamic contrast-enhanced versus diffusion-weighted MR imaging. *Radiology* 2005; **237**: 492-499
15 **Thoeny HC**, De Keyzer F, Chen F, Vandecaveye V, Verbeken EK, Ahmed B, Sun X, Ni Y, Bosmans H, Hermans R, van Oosterom A, Marchal G, Landuyt W. Diffusion-weighted magnetic resonance imaging allows noninvasive in vivo monitoring of the effects of combretastatin a-4 phosphate after repeated administration. *Neoplasia* 2005; **7**: 779-787
16 **Chen F**, De Keyzer F, Ni Y. Cancer Models - Multiparametric Applications of Clinical MRI in Rodent Hepatic Tumor Model. In: Schröder L, Faber C, editors. In vivo NMR imaging: methods and protocols. New York: Humana Press, 2011; In press
17 **Wang H**, Van de Putte M, Chen F, De Keyzer F, Jin L, Yu J, Marchal G, de Witte P, Ni Y. Murine liver implantation of radiation-induced fibrosarcoma: characterization with MR imaging, microangiography and histopathology. *Eur Radiol* 2008; **18**: 1422-1430
18 **Wang H**, Li J, Chen F, De Keyzer F, Yu J, Feng Y, Nuyts J, Marchal G, Ni Y. Morphological, functional and metabolic imaging biomarkers: assessment of vascular-disrupting effect on rodent liver tumours. *Eur Radiol* 2010; **20**: 2013-2026
19 **Chen F**, Marchal G, Ni Y. Rodent models and magnetic resonance imaging: diagnostic and therapeutic utilities for stroke. *Int J Model Ident Contr* 2010; **9**: 275-287
20 **Suzuki Y**, Chen F, Ni Y, Marchal G, Collen D, Nagai N. Microplasmin reduces ischemic brain damage and improves neurological function in a rat stroke model monitored with MRI. *Stroke* 2004; **35**: 2402-2406
21 **Hackney DB**. Does MR imaging improve precision in stroke thrombolysis trials? *Radiology* 2007; **244**: 323-324
22 **Sun X**, Wang H, Chen F, De Keyzer F, Yu J, Jiang Y, Feng Y, Li J, Marchal G, Ni Y. Diffusion-weighted MRI of hepatic tumor in rats: comparison between in vivo and postmortem imaging acquisitions. *J Magn Reson Imaging* 2009; **29**: 621-628
23 **Tozer GM**, Kanthou C, Baguley BC. Disrupting tumour blood vessels. *Nat Rev Cancer* 2005; **5**: 423-435
24 **Ni Y**, Bormans G, Chen F, Verbruggen A, Marchal G. Necrosis avid contrast agents: functional similarity versus structural diversity. *Invest Radiol* 2005; **40**: 526-535
25 **Van de Putte M**, Wang H, Chen F, de Witte PA, Ni Y. Hypericin as a marker for determination of tissue viability after intratumoral ethanol injection in a murine liver tumor model. *Acad Radiol* 2008; **15**: 107-113
26 **Ni Y**, Huyghe D, Verbeke K, de Witte PA, Nuyts J, Mortelmans L, Chen F, Marchal G, Verbruggen AM, Bormans GM. First preclinical evaluation of mono-[123I]iodohypericin as a necrosis-avid tracer agent. *Eur J Nucl Med Mol Imaging* 2006; **33**: 595-601
27 **Jin J**, Teng G, Feng Y, Wu Y, Jin Q, Wang Y, Wang Z, Lu Q, Jiang Y, Wang S, Chen F, Marchal G, Ni Y. Magnetic resonance imaging of acute reperfused myocardial infarction: intraindividual comparison of ECIII-60 and Gd-DTPA in a swine model. *Cardiovasc Intervent Radiol* 2007; **30**: 248-256
28 **Ni Y**, Chen F, Mulier S, Sun X, Yu J, Landuyt W, Marchal G, Verbruggen A. Magnetic resonance imaging after radiofrequency ablation in a rodent model of liver tumor: tissue characterization using a novel necrosis-avid contrast agent. *Eur Radiol* 2006; **16**: 1031-1040
29 **Chen F**, Ward J, Robinson PJ. MR imaging of the liver and spleen: a comparison of the effects on signal intensity of two superparamagnetic iron oxide agents. *Magn Reson Imaging* 1999; **17**: 549-556
30 **Chen F**, Ni YC, Zheng KE, Ju SH, Sun J, Ou XL, Xu MH, Zhang H, Marchal G. Spiral CT in gastric carcinoma: comparison with barium study, fiberoptic gastroscopy and histopathology. *World J Gastroenterol* 2003; **9**: 1404-1408
31 **Yang XJ**, Chen F, Han P. Virtual Endoscopy and Related 3D Imaging in Clinical Medicine. Beijing: People's Medical Publishing House, 2000
32 **Ward J**, Chen F, Guthrie JA, Wilson D, Lodge JP, Wyatt JI, Robinson PJ. Hepatic lesion detection after superparamagnetic iron oxide enhancement: comparison of five T2-weighted sequences at 1.0 T by using alternative-free response receiver operating characteristic analysis. *Radiology* 2000; **214**: 159-166
33 **Xie J**. Progress of abdominal radiology in recent 50 years in China. *Zhonghua Fangshexue Zazhi* 1999; **33** (Suppl): 23-27

34 **Brockmann MA**, Kemmling A, Groden C. Current issues and perspectives in small rodent magnetic resonance imaging using clinical MRI scanners. *Methods* 2007; **43**: 79-87
35 **Shaked Y**, Ciarrocchi A, Franco M, Lee CR, Man S, Cheung AM, Hicklin DJ, Chaplin D, Foster FS, Benezra R, Kerbel RS. Therapy-induced acute recruitment of circulating endothelial progenitor cells to tumors. *Science* 2006; **313**: 1785-1787
36 **Purhonen S**, Palm J, Rossi D, Kaskenpää N, Rajantie I, Ylä-Herttuala S, Alitalo K, Weissman IL, Salven P. Bone marrow-derived circulating endothelial precursors do not contribute to vascular endothelium and are not needed for tumor growth. *Proc Natl Acad Sci USA* 2008; **105**: 6620-6625

S- Editor Cheng JX **L- Editor** Webster JR **E- Editor** Zheng XM

World Journal of Radiology

Online Submissions: http://www.wjgnet.com/1949-8470office
wjr@wjgnet.com
www.wjgnet.com

World J Radiol 2011 April 28; 3(4): I
ISSN 1949-8470 (online)

Acknowledgments to reviewers of *World Journal of Radiology*

Many reviewers have contributed their expertise and time to the peer review, a critical process to ensure the quality of *World Journal of Radiology*. The editors and authors of the articles submitted to the journal are grateful to the following reviewers for evaluating the articles (including those published in this issue and those rejected for this issue) during the last editing time period.

Kubilay Aydin, MD, Professor, Istanbul University, Istanbul Faculty of Medicine, Department of Radiology, Neuroradiology Division Capa, Istanbul, Turkey

Abhijit P Datir, MB BS, MD, FRCR, DMRE, Division of Interventional Radiology, Jackson Memorial Hospital, 1611 NW 12th Avenue, West Wing 279, Miami, FL 33136, United States

Adnan Kabaalioglu, MD, Professor, Akdeniz University Hospital, 07059, Antalya, Turkey

Chan Kyo Kim, MD, Assistant Professor, Department of Radiology, Samsung Medical Center, Sungkyunkwan University School of Medicine, 50 Ilwon-dong, Kangnam-gu, Seoul 135-710, South Korea

Edson Marchiori, MD, PhD, Full Professor of Radiology, Department of Radiology, Fluminense Federal University, Rua Thomaz Cameron, 438, Valparaiso, CEP 25685, 120, Petrópolis, Rio de Janeiro, Brazil

Roberto Miraglia, MD, Department of Diagnostic and Interventional Radiology, Mediterranean Institute for Transplantation and Advanced Specialized Therapies (IsMeTT), Via Tricomi 1, Palermo, 90100, Italy. Adjunct Associate Professor of Radiology, University of Pittsburgh, United States

Nathalie Lassau, MD, PhD, Imaging Department, Ultrasonography Unit and UPRES EA 40-40, Institut Gustave Roussy,rue Camille-Desmoulins, 94805 Villejuif, France

Ahmed A Shokeir, MD, PhD, FEBU, Professor, Urology Department, Urology and Nephrology Center, Mansoura University, Mansoura 35516, Egypt

Roberto Grassi, MD, Full Professor of Radiology, Department "Magrassi-Lanzara " Institute of Radiology, Second University of Naples, Piazza Miraglia, Naples, 80138, Italy

World Journal of Radiology

Online Submissions: http://www.wjgnet.com/1949-8470office
wjr@wjgnet.com
www.wjgnet.com

World J Radiol 2011 April 28; 3(4): I
ISSN 1949-8470 (online)

Events Calendar 2011

January 23-27
Radiology at Snowbird
San Diego, Mexico

January 24-28
Neuro/ENT at the Beach
Palm Beach, FL, United States

February 28-29
MIAD 2011 - 2nd International Workshop on Medical Image Analysis and Description for Diagnosis System
Rome, Italy

February 5-6
Washington Neuroradiology Review
Arlington, VA, United States

February 12-17
MI11 - SPIE Medical Imaging 2011
Lake Buena Vista, FL, United States

February 17-18
2nd National Conference Diagnostic and Interventional Radiology 2011
London, United Kingdom

Februrary 17-18
VII National Neuroradiology Course
Lleida, Spain

February 18
Radiology in child protection
Nottingham, United Kingdom

Februrary 19-22
COMPREHENSIVE REVIEW OF MUSCULOSKELETAL MRI
Lake Buena Vista, FL, United States

March 2-5
2011 Abdominal Radiology Course
Carlsbad, CA, United States

March 3-7
European Congress of Radiology Meeting ECR 2011 Vienna, Austria

March 6-9
World Congress Thoracic Imaging - IV
Bonita Springs, FL, United States

March 14-18
9th Annual NYU Radiology Alpine Imaging Symposium at Beaver Creek
Beaver Creek, CO, United States

March 20-25
Abdominal Radiology Course 2011
Carlsbad, CA, United States

March 26-31
2011 SIR Annual Meeting
Chicago, IL, United States

March 28-April 1
University of Utah Neuroradiology 2nd Intensive Interactive Brain & Spine Imaging Conference
Salt Lake City, UT, United States

April 3-8
1st Annual Ottawa Radiology Resident Review
Ottawa, Canada

April 3-8
43rd International Diagnostic Course Davos on Diagnostic Imaging and Interventional Techniques
Davos, Switzerland

April 6-9
Image-Based Neurodiagnosis: Intensive Clinical and Radiologic Review, CAQ Preparation
Cincinnati, OH, United States

April 28-May 1
74th Annual Scientific Meeting of the Canadian Association of Radiologists CAR
Montreal, Canada

May 5-8
EMBL Conference-Sixth International Congress on Electron Tomography
Heidelberg, Germany

May 10-13
27th Iranian Congress of Radiology
Tehran, Iran

May 14-21
Radiology in Marrakech
Marrakech, Morocco

May 21-24
European Society of Gastrointestinal and Abdominal Radiology 2011 Annual Meeting
Venice, Italy

May 23-25
Sports Medicine Imaging State of the Art: A Collaborative Course for Radiologists and Sports Medicine Specialists
New York, NY, United States

May 24-26
Russian Congress of Radiology
Moscow, Russia

May 28-31
International Congress of Pediatric Radiology (IPR)
London, United Kingdom

June 4-8
58th Annual Meeting of the Society of Nuclear Medicine
San Antonio, TX, United States

June 6-8
UKRC 2011 - UK Radiological Congress
Manchester, United Kingdom

June 8-11
CIRA 2011 - Canadian Internventinal Radiology Association Meeting
Montreal, QC, Canada

June 9-10
8th ESGAR Liver Imaging Workshop
Dublin, Ireland

June 17-19
ASCI 2011 - 5th Congress of Asian Society of Cardiovascular Imaging
Hong Kong, China

June 22-25
CARS 2011 - Computer Assisted Radiology and Surgery - 25th International Congress and Exhibition Berlin, Germany

June 27-July 1
NYU Summer Radiology Symposium at The Sagamore
Lake George, NY, United States

July 18-22
Clinical Case-Based Radiology Update in Iceland
Reykjavik, Iceland

August 1-5
NYU Clinical Imaging Symposium in Santa Fe
Santa Fe, NM, United States

September 22-25
European Society of Neuroradiology (ESNR) XXXV Congress and 19th Advanced Course
Antwerp, Belgium

October 12-14
International Conference Vipimage 2011 - Computational Vision and Medical Image Processing
Algarve, Portugal

October 15-16
Essentials of Emergency and Trauma Radiology
Ottawa, Canada

October 23-29
2011 IEEE NSS - 2011 IEEE Nuclear Science Symposium and Medical Imaging Conference
Valencia, Spain

October 25-28
NYU Radiology in Scottsdale - Fall Radiology Symposium in Scottsdale
Scottsdale, AZ, United States

October 28-30
Fourth National Congress of Professionals of Radiological Techniques Florianópolis, Brazil

October 28-30
Multi-Modality Gynecological & Obstetric Imaging
Ottawa, Canada

November 3-4
9th ESGAR Liver Imaging Workshop
Taormina, Italy

November 15-19
EANM 2011 - Annual Congress of the European Association of Nuclear Medicine
Birmingham, United Kingdom

November 22-29
NSS/MIC - Nuclear Science Symposium and Medical Imaging Conference 2011 Valencia, Spain

November 26-28
8th Asia Oceaninan Congress of Neuro-Radiology Bangkok, Thailand

World Journal of Radiology

Online Submissions: http://www.wjgnet.com/1949-8470office
wjr@wjgnet.com
www.wjgnet.com

World J Radiol 2011 April 28; 3(4): I-V
ISSN 1949-8470 (online)

INSTRUCTIONS TO AUTHORS

GENERAL INFORMATION

World Journal of Radiology (*World J Radiol*, *WJR*, online ISSN 1949-8470, DOI: 10.4329), is a monthly, open-access (OA), peer-reviewed journal supported by an editorial board of 319 experts in Radiology from 40 countries.

The biggest advantage of the OA model is that it provides free, full-text articles in PDF and other formats for experts and the public without registration, which eliminates the obstacle that traditional journals possess and usually delays the speed of the propagation and communication of scientific research results. The open access model has been proven to be a true approach that may achieve the ultimate goal of the journals, i.e. the maximization of the value to the readers, authors and society.

Maximization of personal benefits

The role of academic journals is to exhibit the scientific levels of a country, a university, a center, a department, and even a scientist, and build an important bridge for communication between scientists and the public. As we all know, the significance of the publication of scientific articles lies not only in disseminating and communicating innovative scientific achievements and academic views, as well as promoting the application of scientific achievements, but also in formally recognizing the "priority" and "copyright" of innovative achievements published, as well as evaluating research performance and academic levels. So, to realize these desired attributes of *WJR* and create a well-recognized journal, the following four types of personal benefits should be maximized. The maximization of personal benefits refers to the pursuit of the maximum personal benefits in a well-considered optimal manner without violation of the laws, ethical rules and the benefits of others. (1) Maximization of the benefits of editorial board members: The primary task of editorial board members is to give a peer review of an unpublished scientific article via online office system to evaluate its innovativeness, scientific and practical values and determine whether it should be published or not. During peer review, editorial board members can also obtain cutting-edge information in that field at first hand. As leaders in their field, they have priority to be invited to write articles and publish commentary articles. We will put peer reviewers' names and affiliations along with the article they reviewed in the journal to acknowledge their contribution; (2) Maximization of the benefits of authors: Since *WJR* is an open-access journal, readers around the world can immediately download and read, free of charge, high-quality, peer-reviewed articles from *WJR* official website, thereby realizing the goals and significance of the communication between authors and peers as well as public reading; (3) Maximization of the benefits of readers: Readers can read or use, free of charge, high-quality peer-reviewed articles without any limits, and cite the arguments, viewpoints, concepts, theories, methods, results, conclusion or facts and data of pertinent literature so as to validate the innovativeness, scientific and practical values of their own research achievements, thus ensuring that their articles have novel arguments or viewpoints, solid evidence and correct conclusion; and (4) Maximization of the benefits of employees: It is an iron law that a first-class journal is unable to exist without first-class editors, and only first-class editors can create a first-class academic journal. We insist on strengthening our team cultivation and construction so that every employee, in an open, fair and transparent environment, could contribute their wisdom to edit and publish high-quality articles, thereby realizing the maximization of the personal benefits of editorial board members, authors and readers, and yielding the greatest social and economic benefits.

Aims and scope

The major task of *WJR* is to rapidly report the most recent improvement in the research of medical imaging and radiation therapy by the radiologists. *WJR* accepts papers on the following aspects related to radiology: Abdominal radiology, women health radiology, cardiovascular radiology, chest radiology, genitourinary radiology, neuroradiology, head and neck radiology, interventional radiology, musculoskeletal radiology, molecular imaging, pediatric radiology, experimental radiology, radiological technology, nuclear medicine, PACS and radiology informatics, and ultrasound. We also encourage papers that cover all other areas of radiology as well as basic research.

Columns

The columns in the issues of *WJR* will include: (1) Editorial: To introduce and comment on major advances and developments in the field; (2) Frontier: To review representative achievements, comment on the state of current research, and propose directions for future research; (3) Topic Highlight: This column consists of three formats, including (A) 10 invited review articles on a hot topic, (B) a commentary on common issues of this hot topic, and (C) a commentary on the 10 individual articles; (4) Observation: To update the development of old and new questions, highlight unsolved problems, and provide strategies on how to solve the questions; (5) Guidelines for Basic Research: To provide guidelines for basic research; (6) Guidelines for Clinical Practice: To provide guidelines for clinical diagnosis and treatment; (7) Review: To review systemically progress and unresolved problems in the field, comment on the state of current research, and make suggestions for future work; (8) Original Articles: To report innovative and original findings in radiology; (9) Brief Articles: To briefly report the novel and innovative findings in radiology; (10) Case Report: To report a rare or typical case; (11) Letters to the Editor: To discuss and make reply to the contributions published in *WJR*, or to introduce and comment on a controversial issue of general interest; (12) Book Reviews: To introduce and comment on quality monographs of radiology; and (13) Guidelines: To introduce consensuses and guidelines reached by international and national academic authorities worldwide on the research in radiology.

Name of journal

World Journal of Radiology

ISSN

ISSN 1949-8470 (online)

Indexed and Abstracted in

PubMed Central, PubMed, Digital Object Identifer, and Directory of Open Access Journals.

Published by

Baishideng Publishing Group Co., Limited.

SPECIAL STATEMENT

All articles published in this journal represent the viewpoints of the authors except where indicated otherwise.

Biostatistical editing

Statisital review is performed after peer review. We invite an expert in Biomedical Statistics from to evaluate the statistical method used in the paper, including *t*-test (group or paired comparisons), chi-squared test, Ridit, probit, logit, regression (linear, curvilinear, or stepwise), correlation, analysis of variance, analysis of covariance, *etc*. The reviewing points include: (1) Statistical methods should be described when they are used to verify the results; (2) Whether the statistical techniques are suitable or correct; (3) Only homogeneous data can be averaged. Standard deviations are preferred to standard errors. Give the number of observations and subjects (*n*). Losses in observations, such as drop-outs from the study should be reported; (4) Values such as ED50, LD50, IC50 should have their 95% confidence limits calculated and compared by weighted probit analysis (Bliss and Finney); and (5) The word 'significantly' should be replaced by its synonyms (if it indicates extent) or the *P* value (if it indicates statistical significance).

Conflict-of-interest statement

In the interests of transparency and to help reviewers assess any potential bias, *WJR* requires authors of all papers to declare any competing commercial, personal, political, intellectual, or religious interests in relation to the submitted work. Referees are also asked to indicate any potential conflict they might have reviewing a particular paper. Before submitting, authors are suggested to read "Uniform Requirements for Manuscripts Submitted to Biomedical Journals: Ethical Considerations in the Conduct and Reporting of Research: Conflicts of Interest" from International Committee of Medical Journal Editors (ICMJE), which is available at: http://www.icmje.org/ethical_4conflicts.html.

Sample wording: [Name of individual] has received fees for serving as a speaker, a consultant and an advisory board member for [names of organizations], and has received research funding from [names of organization]. [Name of individual] is an employee of [name of organization]. [Name of individual] owns stocks and shares in [name of organization]. [Name of individual] owns patent [patent identification and brief description].

Statement of informed consent

Manuscripts should contain a statement to the effect that all human studies have been reviewed by the appropriate ethics committee or it should be stated clearly in the text that all persons gave their informed consent prior to their inclusion in the study. Details that might disclose the identity of the subjects under study should be omitted. Authors should also draw attention to the Code of Ethics of the World Medical Association (Declaration of Helsinki, 1964, as revised in 2004).

Statement of human and animal rights

When reporting the results from experiments, authors should follow the highest standards and the trial should conform to Good Clinical Practice (for example, US Food and Drug Administration Good Clinical Practice in FDA-Regulated Clinical Trials; UK Medicines Research Council Guidelines for Good Clinical Practice in Clinical Trials) and/or the World Medical Association Declaration of Helsinki. Generally, we suggest authors follow the lead investigator's national standard. If doubt exists whether the research was conducted in accordance with the above standards, the authors must explain the rationale for their approach and demonstrate that the institutional review body explicitly approved the doubtful aspects of the study.

Before submitting, authors should make their study approved by the relevant research ethics committee or institutional review board. If human participants were involved, manuscripts must be accompanied by a statement that the experiments were undertaken with the understanding and appropriate informed consent of each. Any personal item or information will not be published without explicit consents from the involved patients. If experimental animals were used, the materials and methods (experimental procedures) section must clearly indicate that appropriate measures were taken to minimize pain or discomfort, and details of animal care should be provided.

SUBMISSION OF MANUSCRIPTS

Manuscripts should be typed in 1.5 line spacing and 12 pt. Book Antiqua with ample margins. Number all pages consecutively, and start each of the following sections on a new page: Title Page, Abstract, Introduction, Materials and Methods, Results, Discussion, Acknowledgements, References, Tables, Figures, and Figure Legends. Neither the editors nor the publisher are responsible for the opinions expressed by contributors. Manuscripts formally accepted for publication become the permanent property of Baishideng Publishing Group Co., Limited, and may not be reproduced by any means, in whole or in part, without the written permission of both the authors and the publisher. We reserve the right to copy-edit and put onto our website accepted manuscripts. Authors should follow the relevant guidelines for the care and use of laboratory animals of their institution or national animal welfare committee. For the sake of transparency in regard to the performance and reporting of clinical trials, we endorse the policy of the ICMJE to refuse to publish papers on clinical trial results if the trial was not recorded in a publicly-accessible registry at its outset. The only register now available, to our knowledge, is http://www.clinicaltrials.gov sponsored by the United States National Library of Medicine and we encourage all potential contributors to register with it. However, in the case that other registers become available you will be duly notified. A letter of recommendation from each author's organization should be provided with the contributed article to ensure the privacy and secrecy of research is protected.

Authors should retain one copy of the text, tables, photographs and illustrations because rejected manuscripts will not be returned to the author(s) and the editors will not be responsible for loss or damage to photographs and illustrations sustained during mailing.

Online submissions

Manuscripts should be submitted through the Online Submission System at: http://www.wjgnet.com/1949-8470office. Authors are highly recommended to consult the ONLINE INSTRUCTIONS TO AUTHORS (http://www.wjgnet.com/1949-8470/g_info_20100316162358.htm) before attempting to submit online. For assistance, authors encountering problems with the Online Submission System may send an email describing the problem to wjr@wjgnet.com, or by telephone: +86-10-85381892. If you submit your manuscript online, do not make a postal contribution. Repeated online submission for the same manuscript is strictly prohibited.

MANUSCRIPT PREPARATION

All contributions should be written in English. All articles must be submitted using word-processing software. All submissions must be typed in 1.5 line spacing and 12 pt. Book Antiqua with ample margins. Style should conform to our house format. Required information for each of the manuscript sections is as follows:

Title page

Title: Title should be less than 12 words.

Running title: A short running title of less than 6 words should be provided.

Authorship: Authorship credit should be in accordance with the standard proposed by International Committee of Medical Journal Editors, based on (1) substantial contributions to conception and design, acquisition of data, or analysis and interpretation of data; (2) drafting the article or revising it critically for important intellectual content; and (3) final approval of the version to be published. Authors should meet conditions 1, 2, and 3.

Institution: Author names should be given first, then the complete name of institution, city, province and postcode. For example, Xu-Chen Zhang, Li-Xin Mei, Department of Pathology, Chengde Medical College, Chengde 067000, Hebei Province, China. One author may be represented from two institutions, for example, George Sgourakis, Department of General, Visceral, and Transplantation Surgery, Essen 45122, Germany; George Sgourakis, 2nd Surgical

Department, Korgialenio-Benakio Red Cross Hospital, Athens 15451, Greece

Author contributions: The format of this section should be: Author contributions: Wang CL and Liang L contributed equally to this work; Wang CL, Liang L, Fu JF, Zou CC, Hong F and Wu XM designed the research; Wang CL, Zou CC, Hong F and Wu XM performed the research; Xue JZ and Lu JR contributed new reagents/analytic tools; Wang CL, Liang L and Fu JF analyzed the data; and Wang CL, Liang L and Fu JF wrote the paper.

Supportive foundations: The complete name and number of supportive foundations should be provided, e.g., Supported by National Natural Science Foundation of China, No. 30224801

Correspondence to: Only one corresponding address should be provided. Author names should be given first, then author title, affiliation, the complete name of institution, city, postcode, province, country, and email. All the letters in the email should be in lower case. A space interval should be inserted between country name and email address. For example, Montgomery Bissell, MD, Professor of Medicine, Chief, Liver Center, Gastroenterology Division, University of California, Box 0538, San Francisco, CA 94143, United States. montgomery.bissell@ucsf.edu

Telephone and fax: Telephone and fax should consist of +, country number, district number and telephone or fax number, e.g., Telephone: +86-10-85381892 Fax: +86-10-85381893

Peer reviewers: All articles received are subject to peer review. Normally, three experts are invited for each article. Decision for acceptance is made only when at least two experts recommend an article for publication. Reviewers for accepted manuscripts are acknowledged in each manuscript, and reviewers of articles which were not accepted will be acknowledged at the end of each issue. To ensure the quality of the articles published in *WJR*, reviewers of accepted manuscripts will be announced by publishing the name, title/position and institution of the reviewer in the footnote accompanying the printed article. For example, reviewers: Professor Jing-Yuan Fang, Shanghai Institute of Digestive Disease, Shanghai, Affiliated Renji Hospital, Medical Faculty, Shanghai Jiaotong University, Shanghai, China; Professor Xin-Wei Han, Department of Radiology, The First Affiliated Hospital, Zhengzhou University, Zhengzhou, Henan Province, China; and Professor Anren Kuang, Department of Nuclear Medicine, Huaxi Hospital, Sichuan University, Chengdu, Sichuan Province, China.

Abstract

There are unstructured abstracts (no more than 256 words) and structured abstracts (no more than 480). The specific requirements for structured abstracts are as follows:

An informative, structured abstracts of no more than 480 words should accompany each manuscript. Abstracts for original contributions should be structured into the following sections. AIM (no more than 20 words): Only the purpose should be included. Please write the aim as the form of "To investigate/study/…; MATERIALS AND METHODS (no more than 140 words); RESULTS (no more than 294 words): You should present *P* values where appropriate and must provide relevant data to illustrate how they were obtained, e.g. 6.92 ± 3.86 *vs* 3.61 ± 1.67, $P < 0.001$; CONCLUSION (no more than 26 words).

Key words

Please list 5-10 key words, selected mainly from *Index Medicus*, which reflect the content of the study.

Text

For articles of these sections, original articles and brief articles, the main text should be structured into the following sections: INTRODUCTION, MATERIALS AND METHODS, RESULTS and DISCUSSION, and should include appropriate Figures and Tables. Data should be presented in the main text or in Figures and Tables, but not in both. The main text format of these sections, editorial, topic highlight, case report, letters to the editors, can be found at: http://www.wjgnet.com/1949-8470/g_info_20100313183720.htm.

Illustrations

Figures should be numbered as 1, 2, 3, *etc.*, and mentioned clearly in the main text. Provide a brief title for each figure on a separate page. Detailed legends should not be provided under the figures. This part should be added into the text where the figures are applicable. Figures should be either Photoshop or Illustrator files (in tiff, eps, jpeg formats) at high-resolution. Examples can be found at: http://www.wjgnet.com/1007-9327/13/4520.pdf; http://www.wjgnet.com/1007-9327/13/4554.pdf; http://www.wjgnet.com/1007-9327/13/4891.pdf; http://www.wjgnet.com/1007-9327/13/4986.pdf; http://www.wjgnet.com/1007-9327/13/4498.pdf. Keeping all elements compiled is necessary in line-art image. Scale bars should be used rather than magnification factors, with the length of the bar defined in the legend rather than on the bar itself. File names should identify the figure and panel. Avoid layering type directly over shaded or textured areas. Please use uniform legends for the same subjects. For example: Figure 1 Pathological changes in atrophic gastritis after treatment. A: ...; B: ...; C: ...; D: ...; E: ...; F: ...; G: …*etc.* It is our principle to publish high resolution-figures for the printed and E-versions.

Tables

Three-line tables should be numbered 1, 2, 3, *etc.*, and mentioned clearly in the main text. Provide a brief title for each table. Detailed legends should not be included under tables, but rather added into the text where applicable. The information should complement, but not duplicate the text. Use one horizontal line under the title, a second under column heads, and a third below the Table, above any footnotes. Vertical and italic lines should be omitted.

Notes in tables and illustrations

Data that are not statistically significant should not be noted. $^{a}P < 0.05$, $^{b}P < 0.01$ should be noted ($P > 0.05$ should not be noted). If there are other series of *P* values, $^{c}P < 0.05$ and $^{d}P < 0.01$ are used. A third series of *P* values can be expressed as $^{e}P < 0.05$ and $^{f}P < 0.01$. Other notes in tables or under illustrations should be expressed as ^{1}F, ^{2}F, ^{3}F; or sometimes as other symbols with a superscript (Arabic numerals) in the upper left corner. In a multi-curve illustration, each curve should be labeled with ●, ○, ■, □, ▲, △, *etc.*, in a certain sequence.

Acknowledgments

Brief acknowledgments of persons who have made genuine contributions to the manuscript and who endorse the data and conclusions should be included. Authors are responsible for obtaining written permission to use any copyrighted text and/or illustrations.

REFERENCES

Coding system

The author should number the references in Arabic numerals according to the citation order in the text. Put reference numbers in square brackets in superscript at the end of citation content or after the cited author's name. For citation content which is part of the narration, the coding number and square brackets should be typeset normally. For example, "Crohn's disease (CD) is associated with increased intestinal permeability[1,2]". If references are cited directly in the text, they should be put together within the text, for example, "From references[19,22-24], we know that..."

When the authors write the references, please ensure that the order in text is the same as in the references section, and also ensure the spelling accuracy of the first author's name. Do not list the same citation twice.

PMID and DOI

Pleased provide PubMed citation numbers to the reference list, e.g. PMID and DOI, which can be found at http://www.ncbi.nlm.nih.gov/sites/entrez?db=pubmed and http://www.crossref.org/SimpleTextQuery/, respectively. The numbers will be used in E-version of this journal.

Style for journal references

Authors: the name of the first author should be typed in bold-faced letters. The family name of all authors should be typed with the initial letter capitalized, followed by their abbreviated first and middle initials. (For example, Lian-Sheng Ma is abbreviated as Ma LS, Bo-Rong Pan as Pan BR). The title of the cited article and italicized journal title (journal title should be in its abbreviated form as shown in PubMed), publication date, volume number (in black), start page, and end page [PMID: 11819634 DOI: 10.3748/wjg.13.5396].

Style for book references

Authors: the name of the first author should be typed in bold-faced letters. The surname of all authors should be typed with the initial letter capitalized, followed by their abbreviated middle and first initials. (For example, Lian-Sheng Ma is abbreviated as Ma LS, Bo-Rong Pan as Pan BR) Book title. Publication number. Publication place: Publication press, Year: start page and end page.

Format

Journals

English journal article (list all authors and include the PMID where applicable)

1 **Jung EM**, Clevert DA, Schreyer AG, Schmitt S, Rennert J, Kubale R, Feuerbach S, Jung F. Evaluation of quantitative contrast harmonic imaging to assess malignancy of liver tumors: A prospective controlled two-center study. *World J Gastroenterol* 2007; **13**: 6356-6364 [PMID: 18081224 DOI: 10.3748/wjg.13.6356]

Chinese journal article (list all authors and include the PMID where applicable)

2 **Lin GZ**, Wang XZ, Wang P, Lin J, Yang FD. Immunologic effect of Jianpi Yishen decoction in treatment of Pixu-diarrhoea. *Shijie Huaren Xiaohua Zazhi* 1999; **7**: 285-287

In press

3 **Tian D**, Araki H, Stahl E, Bergelson J, Kreitman M. Signature of balancing selection in Arabidopsis. *Proc Natl Acad Sci USA* 2006; In press

Organization as author

4 **Diabetes Prevention Program Research Group**. Hypertension, insulin, and proinsulin in participants with impaired glucose tolerance. *Hypertension* 2002; **40**: 679-686 [PMID: 12411462 PMCID:2516377 DOI:10.1161/01.HYP.0000035706.28494.09]

Both personal authors and an organization as author

5 **Vallancien G**, Emberton M, Harving N, van Moorselaar RJ; Alf-One Study Group. Sexual dysfunction in 1, 274 European men suffering from lower urinary tract symptoms. *J Urol* 2003; **169**: 2257-2261 [PMID: 12771764 DOI:10.1097/01.ju.0000067940.76090.73]

No author given

6 21st century heart solution may have a sting in the tail. *BMJ* 2002; **325**: 184 [PMID: 12142303 DOI:10.1136/bmj.325.7357.184]

Volume with supplement

7 **Geraud G**, Spierings EL, Keywood C. Tolerability and safety of frovatriptan with short- and long-term use for treatment of migraine and in comparison with sumatriptan. *Headache* 2002; **42** Suppl 2: S93-99 [PMID: 12028325 DOI:10.1046/j.1526-4610.42.s2.7.x]

Issue with no volume

8 **Banit DM**, Kaufer H, Hartford JM. Intraoperative frozen section analysis in revision total joint arthroplasty. *Clin Orthop Relat Res* 2002; (**401**): 230-238 [PMID: 12151900 DOI:10.1097/00003086-200208000-00026]

No volume or issue

9 Outreach: Bringing HIV-positive individuals into care. *HRSA Careaction* 2002; 1-6 [PMID: 12154804]

Books

Personal author(s)

10 **Sherlock S**, Dooley J. Diseases of the liver and billiary system. 9th ed. Oxford: Blackwell Sci Pub, 1993: 258-296

Chapter in a book (list all authors)

11 **Lam SK**. Academic investigator's perspectives of medical treatment for peptic ulcer. In: Swabb EA, Azabo S. Ulcer disease: investigation and basis for therapy. New York: Marcel Dekker, 1991: 431-450

Author(s) and editor(s)

12 **Breedlove GK**, Schorfheide AM. Adolescent pregnancy. 2nd ed. Wieczorek RR, editor. White Plains (NY): March of Dimes Education Services, 2001: 20-34

Conference proceedings

13 **Harnden P**, Joffe JK, Jones WG, editors. Germ cell tumours V. Proceedings of the 5th Germ cell tumours Conference; 2001 Sep 13-15; Leeds, UK. New York: Springer, 2002: 30-56

Conference paper

14 **Christensen S**, Oppacher F. An analysis of Koza's computational effort statistic for genetic programming. In: Foster JA, Lutton E, Miller J, Ryan C, Tettamanzi AG, editors. Genetic programming. EuroGP 2002: Proceedings of the 5th European Conference on Genetic Programming; 2002 Apr 3-5; Kinsdale, Ireland. Berlin: Springer, 2002: 182-191

Electronic journal (list all authors)

15 Morse SS. Factors in the emergence of infectious diseases. Emerg Infect Dis serial online, 1995-01-03, cited 1996-06-05; 1(1): 24 screens. Available from: URL: http://www.cdc.gov/ncidod/eid/index.htm

Patent (list all authors)

16 **Pagedas AC**, inventor; Ancel Surgical R&D Inc., assignee. Flexible endoscopic grasping and cutting device and positioning tool assembly. United States patent US 20020103498. 2002 Aug 1

Statistical data

Write as mean ± SD or mean ± SE.

Statistical expression

Express *t* test as *t* (in italics), *F* test as *F* (in italics), chi square test as χ^2 (in Greek), related coefficient as *r* (in italics), degree of freedom as υ (in Greek), sample number as *n* (in italics), and probability as *P* (in italics).

Units

Use SI units. For example: body mass, m (B) = 78 kg; blood pressure, p (B) = 16.2/12.3 kPa; incubation time, t (incubation) = 96 h, blood glucose concentration, c (glucose) 6.4 ± 2.1 mmol/L; blood CEA mass concentration, p (CEA) = 8.6 24.5 μg/L; CO_2 volume fraction, 50 mL/L CO_2, not 5% CO_2; likewise for 40 g/L formaldehyde, not 10% formalin; and mass fraction, 8 ng/g, *etc.* Arabic numerals such as 23, 243, 641 should be read 23 243 641.

The format for how to accurately write common units and quantums can be found at: http://www.wjgnet.com/1949-8470/g_info_20100313185816.htm.

Abbreviations

Standard abbreviations should be defined in the abstract and on first mention in the text. In general, terms should not be abbreviated unless they are used repeatedly and the abbreviation is helpful to the reader. Permissible abbreviations are listed in Units, Symbols and Abbreviations: A Guide for Biological and Medical Editors and Authors (Ed. Baron DN, 1988) published by The Royal Society of Medicine, London. Certain commonly used abbreviations, such as DNA, RNA, HIV, LD50, PCR, HBV, ECG, WBC, RBC, CT, ESR, CSF, IgG, ELISA, PBS, ATP, EDTA, mAb, can be used directly without further explanation.

Italics
Quantities: *t* time or temperature, *c* concentration, *A* area, *l* length, *m* mass, *V* volume.
Genotypes: *gyrA*, *arg* 1, *c myc*, *c fos*, *etc.*
Restriction enzymes: *Eco*RI, *Hin*dI, *Bam*HI, *Kbo* I, *Kpn* I, *etc.*
Biology: *H. pylori*, *E coli*, *etc.*

Examples for paper writing
Editorial: http://www.wjgnet.com/1949-8470/g_info_20100313182341.htm

Frontier: http://www.wjgnet.com/1949-8470/g_info_2010031318 2448.htm

Topic highlight: http://www.wjgnet.com/1949-8470/g_info_201003 13182639.htm

Observation: http://www.wjgnet.com/1949-8470/g_info_20100313 182834.htm

Guidelines for basic research: http://www.wjgnet.com/1949-8470/g_info_20100313183057.htm

Guidelines for clinical practice: http://www.wjgnet.com/1949-8470/g_info_20100313183238.htm

Review: http://www.wjgnet.com/1949-8470/g_info_20100313 183433.htm

Original articles: http://www.wjgnet.com/1949-8470/g_info_2010 0313183720.htm

Brief articles: http://www.wjgnet.com/1949-8470/g_info_201003 13184005.htm

Case report: http://www.wjgnet.com/1949-8470/g_info_20100313 184149.htm

Letters to the editor: http://www.wjgnet.com/1949-8470/g_info_20 100313184410.htm

Book reviews: http://www.wjgnet.com/1949-8470/g_info_201003 13184803.htm

Guidelines: http://www.wjgnet.com/1949-8470/g_info_20100313 185047.htm

SUBMISSION OF THE REVISED MANUSCRIPTS AFTER ACCEPTED

Please revise your article according to the revision policies of *WJR*. The revised version including manuscript and high-resolution image figures (if any) should be re-submitted or uploaded online. The author should send copyright transfer letter, and responses to the reviewers and science news to us *via* email.

Editorial Office

World Journal of Radiology
Editorial Department: Room 903, Building D,
Ocean International Center, No. 62 Dongsihuan Zhonglu,
Chaoyang District, Beijing 100025, China
E-mail: wjr@wjgnet.com
http://www.wjgnet.com
Telephone: +86-10-8538-1892
Fax: +86-10-8538-1893

Language evaluation
The language of a manuscript will be graded before it is sent for revision. (1) Grade A: priority publishing; (2) Grade B: minor language polishing; (3) Grade C: a great deal of language polishing needed; and (4) Grade D: rejected. Revised articles should reach Grade A or B.

Copyright assignment form
Please download a Copyright assignment form from http://www.wjgnet.com/1949-8470/g_info_20100313185522.htm.

Responses to reviewers
Please revise your article according to the comments/suggestions provided by the reviewers. The format for responses to the reviewers' comments can be found at: http://www.wjgnet.com/1949-8470/g_info_20100313185358.htm.

Proof of financial support
For paper supported by a foundation, authors should provide a copy of the document and serial number of the foundation.

Links to documents related to the manuscript
WJR will be initiating a platform to promote dynamic interactions between the editors, peer reviewers, readers and authors. After a manuscript is published online, links to the PDF version of the submitted manuscript, the peer-reviewers' report and the revised manuscript will be put on-line. Readers can make comments on the peer reviewer's report, authors' responses to peer reviewers, and the revised manuscript. We hope that authors will benefit from this feedback and be able to revise the manuscript accordingly in a timely manner.

Science news releases
Authors of accepted manuscripts are suggested to write a science news item to promote their articles. The news will be released rapidly at EurekAlert/AAAS (http://www.eurekalert.org). The title for news items should be less than 90 characters; the summary should be less than 75 words; and main body less than 500 words. Science news items should be lawful, ethical, and strictly based on your original content with an attractive title and interesting pictures.

Publication fee
WJR is an international, peer-reviewed, Open-Access, online journal. Articles published by this journal are distributed under the terms of the Creative Commons Attribution Non-commercial License, which permits use, distribution, and reproduction in any medium, provided the original work is properly cited, the use is non commercial and is otherwise in compliance with the license. Authors of accepted articles must pay a publication fee. The related standards are as follows. Publication fee: 1300 USD per article; Reprints fee: 350 USD per 100 reprints, including postage cost. Editorial, topic highlights, book reviews and letters to the editor are published free of charge.